

UNCLASSIFIED

AD NUMBER
AD482279
NEW LIMITATION CHANGE
TO Approved for public release, distribution unlimited
FROM Distribution authorized to U.S. Gov't. agencies and their contractors; Administrative/Operational Use; Jan 1966. Other requests shall be referred to Air Force Materials Lab., Metals & Ceramics Div., Wright-Patterson AFB, OH 45433.
AUTHORITY
AFSC/IST [WPAFB, OH] ltr dtd 21 Mar 1989

THIS PAGE IS UNCLASSIFIED

AU NO. AD482279

DDG FILE COPY

AFML-TR-65-2
Part IV, Volume II

✓ B



**TERNARY PHASE EQUILIBRIA IN TRANSITION METAL-
BORON-CARBON-SILICON-SYSTEMS**

**Part IV. Thermochemical Calculations
Volume II. Thermodynamic Interpretation
of Ternary Phase Diagrams**

**E. Rudy
Aerojet-General Corporation**

**TECHNICAL REPORT NO. AFML-TR-65-2, Part IV, Volume II
January 1966**

This document is subject to special export controls and each transmittal to foreign governments or foreign nationals may be made only with prior approval of Metals and Ceramics Division, Air Force Materials Laboratory, Wright-Patterson Air Force Base, Ohio.

**Air Force Materials Laboratory
Research and Technology Division
Air Force Systems Command
Wright-Patterson Air Force Base, Ohio**

**DDC
RECEIVED
MAY 24 1966
RECEIVED
A AP**

33245

NOTICES

When Government drawings, specifications, or other data are used for any purpose other than in connection with a definitely related Government procurement operation, the United States Government thereby incurs no responsibility nor any obligation whatsoever; and the fact that the Government may have formulated, furnished, or in any way supplied the said drawings, specifications, or other data, is not to be regarded by implication or otherwise as in any manner licensing the holder or any other person or corporation, or conveying any rights or permission to manufacture, use, or sell any patented invention that may in any way be related thereto.

ACCESSION for	
CFSTI	WINDS CHINA
DDC	EXP. DATE
U. A. 1000000	
CONFIDENTIAL	
DATE OF DEPOSIT	
DEPT.	FILE
2	

Copies of this report should not be returned to the Research and Technology Division unless return is required by security considerations, contractual obligations, or notice on a specific document.

18 AFML TR-65-2-PT-4-Vol-2
Part IV, Volume II

6 TERNARY PHASE EQUILIBRIA IN TRANSITION METAL-
BORON-CARBON-SILICON SYSTEMS.

Part IV. Thermochemical Calculations.

Volume II. Thermodynamic Interpretation
of Ternary Phase Diagrams.

9 Documentary rept.

10 E^{metal} Rudy.

15 AF 33(615)-1247

11 Jan. 66,

16 AF-7350

12 167 p.

17 735001

This document is subject to special export controls and each transmittal to foreign governments or foreign nationals may be made only with prior approval of Metals and Ceramics Division, Air Force Materials Laboratory, Wright-Patterson Air Force Base, Ohio

(400 11-2)

147-
00K

PREVIOUS PAGE WAS BLANK, THEREFORE NOT FILMED.

FOREWORD (Cont'd)

Volume III. Zr-Ta-C System
Volume IV. Ti-Zr-C, Ti-Hf-C, and Zr-Hf-C Systems
Volume V. Ti-Hf-B System
Volume VI. Zr-Hf-B System
Volume VII. Ti-Si-C, Nb-Si-C, and W-Si-C Systems

Part III. Special Experimental Techniques

Volume I. High Temperature Differential Thermal
Analysis.

Part IV. Thermochemical Calculations

Volume I. Thermodynamic Properties of Group IV,
V, and VI Binary Transition-Metal Carbides.

This technical report has been reviewed and is approved.



W. G. RAMKE
Chief, Ceramics and Graphite Branch
Metals and Ceramics Division
Air Force Materials Laboratory

ABSTRACT

The equilibrium conditions for two-phase and three-phase equilibria in ternary systems are derived from the minimum conditions for the free energy, and special solutions are discussed on model examples. The predictive capabilities of the thermodynamic approach are demonstrated on a number of refractory carbide systems, and methods for the determination of phase stabilities from experimental phase equilibrium data are outlined. The thermodynamic discussions are supplemented by a general review of recent phase diagram work on refractory transition metal-B-element systems.

NASA Scientific and Technical Information Facility

operated for the National Aeronautics and Space Administration by Documentation Incorporated

Post Office Box 33
College Park, Md. 20740

Telephone | Area Code 301
779-2121

FACILITY CONTROL NO. 33245

DATE 5/24/66

ATTACHED IS A DOCUMENT ON LOAN

FROM: NASA Scientific and Technical Information Facility

TO: Defense Documentation Center
Attn: DDC-IRC (Control Branch)
Cameron Station
Alexandria, Va. 22314

In accordance with the NASA-DOD Cooperative AD Number Assignment Agreement it is requested that an AD number be assigned to the attached report.

- As this is our only available copy the return of the document (with AD number and any applicable distribution limitations) to the address below is essential.
- This document may be retained by DDC. If retained, please indicate AD number and any applicable distribution limitations on the reproduced copy of the title page and return to the address below.

Return Address: NASA Scientific and Technical Information Facility
Attention: INPUT BRANCH
P. O. Box 33
College Park, Maryland 20740

NASA Scientific and Technical Information Facility

operated for the National Aeronautics and Space Administration by Documentation Incorporated

Post Office Box 33
College Park, Md. 20740

Telephone | Area Code 301
779-2121

FACILITY CONTROL NO. 33545

DATE 5/24/66

ATTACHED IS A DOCUMENT ON LOAN

FROM: NASA Scientific and Technical Information Facility

TO: Defense Documentation Center
Attn: DDC-IRC (Control Branch)
Cameron Station
Alexandria, Va. 22314

In accordance with the NASA-DOD Cooperative AD Number Assignment Agreement it is requested that an AD number be assigned to the attached report.

As this is our only available copy the return of the document (with AD number and any applicable distribution limitations) to the address below is essential.

This document may be retained by DDC. If retained, please indicate AD number and any applicable distribution limitations on the reproduced copy of the title page and return to the address below.

Return Address: NASA Scientific and Technical Information Facility
Attention: INPUT BRANCH
P. O. Box 33
College Park, Maryland 20740

TERNARY PHASE EQUILIBRIA IN TRANSITION METAL-
BORON-CARBON-SILICON-SYSTEMS

Part IV. Thermochemical Calculations

Volume II. Thermodynamic Interpretation
of Ternary Phase Diagrams

E. Rudy

Aerojet-General Corporation

TECHNICAL REPORT NO. AFML-TR-65-2, Part IV, Volume II

January 1966

This document is subject to special export controls and each transmittal to foreign governments or foreign nationals may be made only with prior approval of Metals and Ceramics Division, Air Force Materials Laboratory, Wright-Patterson Air Force Base, Ohio.

24 MAY 1966

Air Force Materials Laboratory
Research and Technology Division
Air Force Systems Command
Wright-Patterson Air Force Base, Ohio

11/22/45

TABLE OF CONTENTS

	PAGE
I. INTRODUCTION	1
II. THERMOCHEMISTRY OF PHASE REACTIONS IN TERNARY SYSTEMS	5
A. Two-Phase Equilibria	6
B. Three-Phase Equilibria in Ternary Systems.	14
III. DISCUSSION OF THE EQUILIBRIUM CONDITIONS ON MODEL EXAMPLES	19
A. Three-Phase Equilibria Resulting from Miscibility Gaps in Binary or Pseudo-Binary Solutions.	19
B. Three-Phase Equilibria Resulting from the Absence of Isomorphous Counter-Phases.	24
C. Binary and Pseudo-Binary Systems of Non- Isomorphous Components	24
D. Computer Approaches	47
IV. APPLICATION TO TERNARY METAL CARBON SYSTEMS.	53
A. The Tantalum-Tungsten-Carbon System.	54
1. Equilibria in the Metal-Rich Portion of the System.	73
2. The Three-Phase Equilibrium $\text{MeC}(\text{Bl}) +$ $\text{MeC}(\text{hex}) + \text{Me}_2\text{C}(\text{hex})$	80
3. The Three-Phase Equilibrium $\text{WC} + \text{MeC}_{1-x}(\text{Bl}) + \text{C}$	86
B. Back-Calculations of Thermodynamic Quantities From Experimental Phase Diagram Data.	98
1. The Two-Phase Equilibrium $(\text{W}, \text{Cr})-$ $(\text{W}, \text{Cr})_2\text{C}$	100
2. Three-Phase Equilibrium $(\text{W}, \text{Cr})_{23}\text{C}_6 -$ $(\text{W}, \text{Cr})_2\text{C} - (\text{W}, \text{Cr})$	101
3. Three-Phase Equilibrium $(\text{W}, \text{Cr})_2\text{C} +$ $+(\text{W}, \text{Cr})_{23}\text{C}_6 + (\text{W}, \text{Cr})_7\text{C}_3 (T = 1575^\circ\text{K})$	102

TABLE OF CONTENTS (Cont'd)

	PAGE
4. Three-Phase Equilibrium (Cr, W) C ₃ - -(Cr, W) ₂ C-(Cr, W) ₃ (T = 1575°K).	103
5. Three-Phase Equilibrium (Cr, W) C ₂ - -(Cr, W) ₃ C ₂ -C (T = 1863°K).	103
6. Three-Phase Equilibrium (W, Cr)C ₂ - -(W, Cr) ₂ C ₂ -C (T = 1863°K)	103
C. Discussion of the Carbon-Rich Equilibria in Uranium-Transition Metal-Carbon Systems	109
V. GENERAL DISCUSSION OF THE PHASE RELATIONSHIPS IN TERNARY SYSTEMS OF REFRACTORY TRANSITION METALS WITH B-ELEMENTS	115
A. Metal-Carbon Systems	115
B. Metal-Boron System	117
C. Refractory Ternary Systems Involving a Transition Metal and Two B-Elements	127
VI. NOTES ON THE RELATION OF PHASE DIAGRAM DATA TO APPLICATION PROBLEMS	136
VII CONCLUDING REMARKS.	142
References	143
Appendix	A-1

LIST OF ILLUSTRATIONS

FIGURE		PAGE
1	Possible Phase Relationships in Simplified Ternary System	2
2	Realistic Appearance of the Diagram Type Presented in Figure 1	3
3	Principle Appearance of the Equilibria Upon Solid Solution Formation Between the Component A and B, as well as the Intermediate Phases	4
4	Two-Phase Equilibrium in a Ternary System	7
5	Graphical Construction of the Tie Lines from the ΔF -x Curves and Effect of Temperature Upon the Distribution Equilibrium	13
6	Three-Phase Equilibrium in a Ternary System (General Case)	15
7	Three-Phase Equilibrium Resulting from a Miscibility Gap in a Pseudo-binary Solid Solution	21
8	Appearance of the Equilibria for the Case of Non-ideal Solutions, and Graphical Determination of the Tie Lines	22
9	Formation of a Three-Phase Field Due to the Absence of an Isomorphous Counterphase BC_v in the Binary System B-C	24
10	Stability Relations in a Binary System A-C	26
11a & 11b	Integral Free Energy of Disproportionation ΔF_{ZMeC_v} of a Phase Solution $(A,B)C_v$, and Corresponding Appearance of the Phase Equilibria (Diagrammatic)	32
12	Relation Between the Integral Free Energies and the Relative Atom Exchanges in Systems of Non-Isomorphous Components	36
13a & 13b	Effect of Non-Ideal Solution Behavior on the Phase Equilibria in Binary or Pseudo-binary Systems of Non-Isomorphous Components	41
14	Principal Relationships for the Stabilization of a Foreign Lattice Type β in a Binary or Pseudo-binary System	43
15	Generalized Free Enthalpy of Formation-Concentration Diagram for a Binary System at a Given Temperature and Pressure	46

LIST OF ILLUSTRATIONS (Cont'd)

FIGURE		PAGE
16	Tantalum-Carbon Phase Diagram	54
17	Tungsten-Carbon Phase Diagram	55
18	Constitution Diagram Tantalum-Tungsten-Carbon	57
19	Scheil-Schultz Reaction Diagram for the System Tantalum-Tungsten-Carbon	58
20a - 20n	Experimental Temperature Sections for the Ta-W-C System	59
	a. 1500°C	h. 2650°C
	b. 1750°C	i. 2745°C
	c. 2000°C	j. 2760°C
	d. 2190°C	k. 2835°C
	e. 2210°C	l. 3000
	f. 2300°C	m. 3200°C
	g. 2450°C	n. 3500°C
21a - 21d	Free Enthalpy of Formation-Concentration Gradients for Tantalum-Tungsten Carbide Solid Solutions	69
	a. Subcarbide Solid Solutions at $(Ta, W)C_{0.37}$	
	b. Subcarbide Solid Solutions at $(Ta, W)C_{0.43}$	
	c. Subcarbide Solid Solutions at $(Ta, W)C_{0.50}$	
	d. Cubic Monocarbide Solid Solutions at $(Ta, W)C_{0.71}$	
22	Ta-W-C: Graphical Determination of the Solubility Ranges of Ta_2C and W_2C Solid Solutions.	75
23	Integral Free Enthalpy of Disproportionation of the $(Ta, W)C_{1/2}$ Phase into Mixtures of Metal and Monocarbide Solid Solution	77
24	Calculated Vertical Section (Isopleth) Across $TaC_{0.45} - WC_{0.5}$	79
25	Free Enthalpy of Formation-Concentration Gradients for the Cubic Monocarbide Solution at Compositions Close to Stoichiometry ($\epsilon = 6500$ cal/gr. -At. Metal)	83
26	Graphical Determination of the Base Point of the Three Phase Equilibrium $WC + (Ta, W)C_{1-x}(Bl) + W_2C$ at the Cubic Monocarbide Solution.	84
27	Integral Free Enthalpy of Disproportionation of the Cubic Monocarbide Solid Solution $[(Ta, W)C_{1-x}]$ into Subcarbide $[(Ta, W)C_{1/2}]$	85

LIST OF ILLUSTRATIONS (Cont'd)

FIGURE		PAGE
28	Temperature Dependence of the Maximum Tungsten Exchange in Tantalum Monocarbide	87
29	Graphical Determination of the Base Point of the Three-Phase Equilibrium $WC-(Ta,W)C_{1-x}(B1)-C$ at the B1-Solid Solution	90
30	Integral Free Energy of Disproportionation of Tungsten Monocarbide into Cubic $(Ta,W)C_{1-x}$ Carbide Solutions and Graphite	91
31	Three-Phase Equilibrium $(Ta,W)C_{1-x}(B1)+WC + C$: Temperature Dependence of the Compositions of the Base Point at the Cubic Solid Solution.	92
32a - 32f	Calculated Temperature Sections for the Ta-W-C System	93
	a. 1750°K	
	b. 2000°K	
	c. 2250°K	
	d. 2500°K	
	e. 2700°K	
	f. ~3000°K	
33	Section of the Phase Diagram Tungsten-Chromium-Carbon at 1300°C	99
34	Section of the Phase Diagram Molybdenum-Chromium-Carbon at 1300°C	99
35	System Section W-Cr-C at 1600°K, Back-Calculated with the Thermodynamic Data Derived from the Experimental Section in Figure 33.	107
36	System Section Mo-Cr-C at 1500°K, Back-Calculated with the Thermodynamic Data Derived from the Experimental Section in Figure 34	108
37	Basic Phase Distribution in the Carbon-Rich Portion of Uranium-Refractory Transition Metal-Carbon Systems	110
38	Temperature Dependence of the Graphite-Stable Ranges in Uranium-Containing Monocarbide Solutions	113
39	Free Enthalpy Changes for the Reaction $UC + 0.86 C \rightarrow UC_{1.86} (UC_2)$ (Data Calculated from Phase Diagrams U-Me-C)	114
40	Constitution Diagram Titanium-Tantalum-Carbon	118
41	Scheil-Schuitz Reaction Diagram for the Ti-Ta-C System	119

LIST OF ILLUSTRATIONS (Cont'd)

FIGURE		PAGE
42	Liquidus Projection in the Ti-Ta-C System	119
43	Constitution Diagram Zirconium-Tantalum-Carbon	120
44	Scheil-Schultz Reaction Diagram for the Zr-Ta-C System	121
45	Liquidus Projection in the Zr-Ta-C System	121
46	Constitution Diagram Hafnium-Tantalum-Carbon	122
47	Scheil-Schultz Reaction Diagram for the Hf-Ta-C System	123
48	Liquidus Projections in the Hf-Ta-C System	123
49	Maximum Solidus Temperatures for the (Ta, Hf) C_{1-x} Monocarbide Solution	124
50	Constitution Diagram Zirconium-Hafnium-Boron	125
51	Scheil-Schultz Reaction Diagram for the Zr-Hf-B System	126
52	Liquidus Projections in the Zr-Hf-B System	126
53	Constitution Diagram Titanium-Boron-Carbon	129
54	Scheil-Schultz Reaction Diagram for the Ti-B-C System	130
55	Liquidus Projection in the Ti-B-C System	131
56	Constitution Diagram Zirconium-Boron-Carbon	132
57	Scheil-Schultz Reaction Diagram for the Zr-B-C System	133
58	Liquidus Projection in the Zr-B-C System	133
59	Constitution Diagram Hafnium-Boron Carbon	134
60	Scheil-Schultz Reaction Diagram for the Hf-B-C System	135
	Liquidus Projection in the Hf-B-C System	135
62	Conjugate Diffusion Couple Consisting of Two Ternary Solutions (A,B) C_u and (A,B) C_v (Equilibration by Interstitial Atom Diffusion)	138
63	Phase Interchange in a Conjugate Ternary Diffusion for the Case, that the Interstitial Atom C is the Only Diffusing Species	139

LIST OF ILLUSTRATIONS (Cont'd)

FIGURE		PAGE
64	Equilibration by Host (A, B) Atom Diffusion in a Ternary Diffusion Couple $(A, B)C_u + (A, B)C_v$	140
65	Effect of Composition Upon the Equilibration Reactions in a Ternary Diffusion Couple $(A, B)C_u + (A, B)C_v$ (C = Interstitial Element)	141
66	Constitution Diagram Titanium-Carbon	A-4
67	Constitution Diagram Zirconium-Carbon	A-5
68	Constitution Diagram Hafnium-Carbon	A-6
69	Constitution Diagram Vanadium-Carbon	A-7
70	Constitution Diagram Niobium-Carbon	A-7
71	Constitution Diagram Tantalum-Carbon	A-8
72	Constitution Diagram Chromium-Carbon	A-9
73	Constitution Diagram Molybdenum-Carbon	A-10
74	Constitution Diagram Tungsten-Carbon	A-11
75	Constitution Diagram Titanium-Boron	A-12
76	Constitution Diagram Zirconium-Boron	A-13
77	Constitution Diagram Hafnium-Boron	A-14
78	Constitution Diagram Vanadium-Boron	A-15
79	Constitution Diagram Niobium-Boron	A-16
80	Constitution Diagram Tantalum-Boron	A-17
81	Constitution Diagram Chromium-Boron	A-18
82	Constitution Diagram Molybdenum-Boron	A-19
83	Constitution Diagram Tungsten-Boron	A-20

LIST OF TABLES

TABLE		PAGE
1	Thermodynamic Data Used in the Calculation of the Phase Equilibria in the Ta-W-C System.	67
2	Differences for the Free Enthalpies of Formation of Tantalum and Tungsten Carbides (Values in cal/gr. -At. Metal)	67
3	Disproportionation and Transformation Energies for Tantalum and Tungsten Carbides.	68
4	Equilibrium Compositions of the Phases for the Three-Phase Equilibrium Monocarbide + Metal + Subcarbide.	78
5	Partition Equilibrium Subcarbide + Monocarbide (B1): Compatible Combinations of x'_W and x''_W	82
6	Maximum Tantalum Exchange in WC (Calculated)	89
7	Summary of Thermochemical Results on Chromium Carbides, Derived from Phase Diagram Data in the W-Cr-C and Mo-Cr-C System.	105
8	Free Enthalpies of Formation of Chromium Carbides (Compiled from the Literature).	105
9	Free Enthalpies of Formation of Unstable Chromium-Carbide Lattice Types	106

I. INTRODUCTION

At the present time, strong efforts are being made to utilize the refractory properties of the semimetal compounds of the high melting transition metals in parts for service at extremely high temperatures; similarly, special techniques, such as dispersion and precipitation strengthening, are being extensively used to improve the high temperature mechanical properties of refractory alloys, and a considerable amount of research work is being devoted to the development of oxidation resistant coatings for refractory metal alloys.

Knowledge of the phase-equilibria existing in the corresponding alloy systems is, therefore, of utmost importance for advanced alloy development work. This is especially true in those instances where the intended operation temperatures are so high that non-equilibrium states cannot be maintained over significant lengths of time; consequently, the intrinsic stability of the system itself becomes one of the controlling factors.

A simple, and most direct route, to solve a specific problem would be the consultation of the equilibrium diagram for the particular alloy system; this way, however, can be followed only in exceptional cases, for extensive phase diagram data are available for only binary systems, whereas data on higher-order alloys are scarce and usually incomplete.

In view of the large number of possible combinations, which makes a timely experimental solution of the problem nearly illusoric, the question arises of how thermodynamic principles may be applied to relate the thermochemical properties of binary alloys to their phase behavior in higher order systems.

If we consider, for example, a simple ternary system of the type shown in Figure 1 where the solubilities in the boundary phases are quite restricted, a simple consideration tells us, that in order to make the combination A + BC stable with regard to AC-B, the free energy change of the reaction



$$\Delta F_R = F_B + F_{AC} - F_A - F_{BC}$$

must be greater than zero. Knowing, therefore, the free energies of the individual compounds, one could write down the free energy changes of all

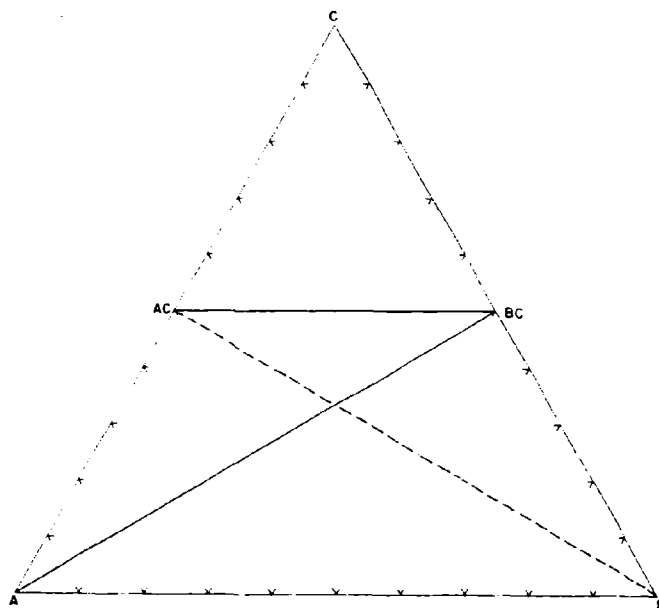


Figure 1. Possible Phase Relationships in a Simplified Ternary System

---- Metastable Equilibrium

possible combinations, and select as the stable equilibria those, for which the above condition holds. Of course, this would only hold true if no ternary compounds occur in the system, and if the range of homogeneity of the phases is so small that the corresponding free energy variations within the homogeneity fields can be neglected. Most probably, the temperature section of the system when correctly drawn, would appear as shown in Figure 2. The dark areas represent the homogeneous (single-phase) ranges of the phases, and the ternary phase field is subdivided into a number of areas where either two- or three-phases are in equilibrium.

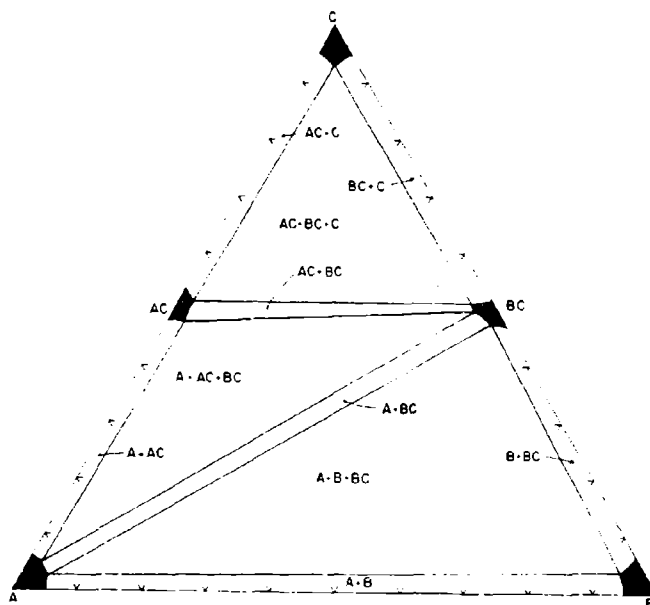


Figure 2. Realistic Appearance of the Diagram Type Presented in Figure 1.

Although this approach looks — at least on the surface — quite tempting, its predictive value is nil. First of all, we have to assume, a priori, that the homogeneity ranges of the phases will be small, and consequently accept the

risk that we might be wrong; the other possibility, of course, to establish the basic assumptions by experiment, would defeat the original purpose of the calculations. Furthermore, and this is especially true for those cases, where those ternary systems are being considered, wherein the compounds of the binary systems A-C and B-C have similar structural properties, we will have to expect extended solid solution formation between the alloy phases, which ultimately yield the conditions shown in Figure 3. Here, the elements A and B, as well as the intermediate phases AC and BC, form a complete series of solid solutions. An infinite number of composition pairs (A,B)-(A,B)C exist, which are in equilibrium with each other, and the tie lines, which connect co-existing compositions, give us the relative amount as well as the compositions of the equilibrium phases for any alloy in the two-phase field. Considering

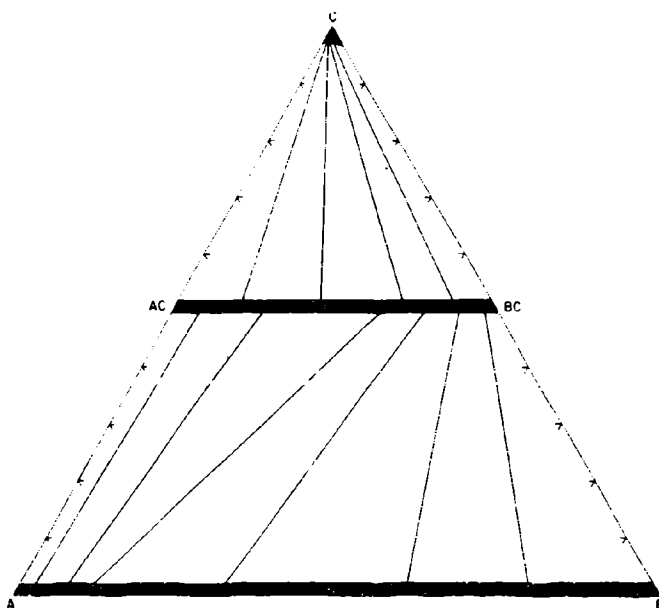


Figure 3. Principal Appearance of the Equilibria Upon Solid Solution Formation Between Two Components and the Intermediate Compounds.

this type of equilibrium from a more practical point of view, we see that the tie lines would, for example, give us the compositions of the reaction products, if alloys, from the edge system A-B, would be allowed to react with the component C.

From these considerations it becomes quite obvious, that in order to reach more definitive conclusions regarding the possible phase distribution in a given system, any reasonable thermodynamic approach would have to include the capability of quantitatively taking into account the changes introduced by extended solid solution formation, and also would have to provide us with relationships, which would principally enable us to determine the ternary homogeneity range of binary phases.

In the following sections, we shall stress briefly the basic thermodynamic approaches. After demonstrating the applicability of the equations on a few model examples, we will concentrate on the thermodynamic evaluation and interpretation of a number of recently investigated refractory alloy systems and finally discuss the capabilities and limitations of thermodynamic approaches in solving practical application problems.

II. THERMOCHEMISTRY OF PHASE REACTIONS IN TERNARY SYSTEMS

According to the phase rule, the maximum number of phases which can coexist in a three component system is five, or, with temperature and pressure fixed, three. Therefore, a temperature section of a ternary system will ordinarily be built-up by an arrangement of one-, two-, and three-phase equilibria. Four-phase reactions (four-phase temperature planes), proceeding at constant temperature, are important in the melting ranges, but seldomly

occur in the solidus regions of systems involving condensed phases. Nevertheless, the existence of four-phase temperature planes can be derived by an analysis of a series of temperature sections in the particular system⁽¹⁾. The mathematical approach, therefore, concentrates on the establishment of the conditions for the two- and three-phase equilibria at constant temperature and pressure.

A. TWO-PHASE EQUILIBRIA

In considering a two-phase field (Figure 4) in a ternary system, the total free energy of a mixture is expressible in terms of the free energies and the mole masses of the individual phases. Let G be the total free energy, and F_1 and F_2 the free energies of the coexisting phases. If phase 1 is present in a quantity v_1 moles, and phase 2 in a quantity of v_2 moles, then

$$F = v_1 F_1 + v_2 F_2 \quad (1)$$

The equilibrium state is characterized by a minimum in the value of F . Assuming constant temperature and pressure, we see that the free energies of the individual phases are concentration-dependent,

$$F_1 = f(x^1, y^1, z^1)$$

$$F_2 = f(x^2, y^2, z^2)$$

With x^1, y^1, z^1 , and x^2, y^2, z^2 denoting the compositions of phase 1 and 2, F becomes then

$$F = f(v_1, v_2, x^1, y^1, z^1, x^2, y^2, z^2)$$

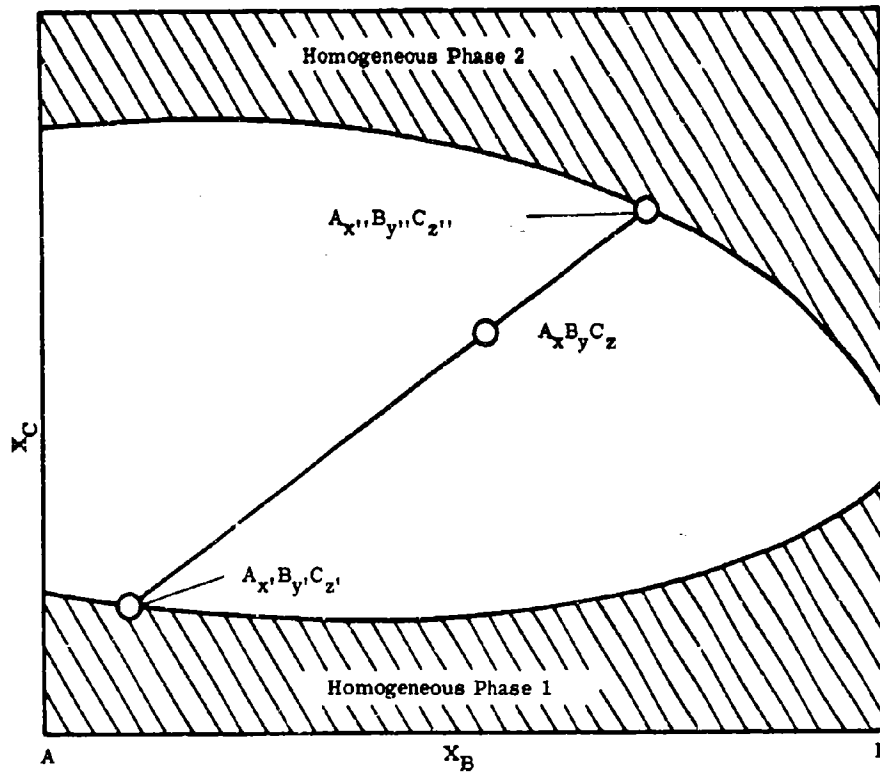


Figure 4. Two-Phase Equilibrium in a Ternary System.

The Tie Line Through the Gross Composition (xyz) Shows the Coexisting Compositions.

The relations existing between the concentration terms together with the requirement for the conservation of the atomic masses, result in the following six boundary conditions:

$$\begin{aligned}
 v_1 + v_2 &= 1 \\
 x' + y' + z' &= 1 \\
 x'' + y'' + z'' &= 1 \\
 v_1 x' + v_2 x'' &= X \\
 v_1 y' + v_2 y'' &= Y \\
 v_1 z' + v_2 z'' &= Z
 \end{aligned}$$

where X, Y, and Z stands for the gross composition of the alloy. The location of the minima is best evaluated by Lagrange's method:

$$\frac{\partial F}{\partial v_1} - \sum \frac{\partial N_k}{\partial N_1} \cdot a_k = 0$$

Proceeding in this way, we obtain eight determining equations for the six undetermined multipliers a_k , as well as v_1 and v_2 .

$$F_1 - a_1 - a_4 \cdot x' - a_5 y' - a_6 z' = 0 \quad (a)$$

$$F_2 - a_1 - a_4 \cdot x'' - a_5 y'' - a_6 z'' = 0 \quad (b)$$

$$v_1 \frac{\partial F_1}{\partial x'} - a_2 - a_4 v_1 = 0 \quad (c)$$

$$v_1 \frac{\partial F_1}{\partial y'} - a_2 - a_5 v_1 = 0 \quad (d)$$

$$v_1 \frac{\partial F_1}{\partial z'} - a_2 - a_6 v_1 = 0 \quad (e)$$

$$v_2 \frac{\partial F_2}{\partial x''} - a_3 - a_4 v_2 = 0 \quad (f)$$

$$v_2 \frac{\partial F_2}{\partial y''} - a_3 - a_5 v_2 = 0 \quad (g)$$

$$v_2 \frac{\partial F_2}{\partial z''} - a_3 - a_6 v_2 = 0 \quad (h)$$

From the last six equations, we obtain the important partial solution

$$\left[\frac{\partial F_1}{\partial x'} - \frac{\partial F_1}{\partial v_1} \right]_{T,P} = \left[\frac{\partial F_2}{\partial x''} - \frac{\partial F_2}{\partial v_1} \right]_{T,P} \quad (2a)$$

$$\left[\frac{\partial F_1}{\partial x'} - \frac{\partial F_1}{\partial z'} \right]_{T,P} = \left[\frac{\partial F_2}{\partial x''} - \frac{\partial F_2}{\partial z''} \right]_{T,P} \quad (2b)$$

$$\left[\frac{\partial F_1}{\partial y'} - \frac{\partial F_1}{\partial z'} \right]_{T,P} = \left[\frac{\partial F_2}{\partial y''} - \frac{\partial F_2}{\partial z''} \right]_{T,P} \quad (2c)$$

which, together with the boundary conditions and the remaining equations (a) and (b), can now be used to evaluate the undetermined multipliers; this ultimately yields the equilibrium conditions for the general case of the two-phase equilibrium.

Geometrically, the solution represents the manifold of all double tangent planes to the free energy surfaces of both phases, and implicitly contains the well-known thermochemical relation, that, in the equilibrium state the partial free energies of the components are the same in all coexisting phases.

We shall, however, not perform the evaluation of the general condition equations^{*}, since the arithmetic is quite involved and the applications of the resulting equations to actual ternary systems is too laborious and time-consuming in order to be of any practical help. They retain a certain usefulness in pseudo-systems of elements or compounds of equal stoichiometry and structure since for these cases the free energies of the boundary phases cancel, and the course of the tie lines in the two-phase fields becomes a function of only the solution terms⁽²⁾.

In many instances, and this applies especially to systems involving semi- or non-metals, the intermetallic compounds formed are either nearly perfect line compounds (true for most silicides and borides), or form defect solid solutions, which are characterized by a similar variation of the free energies across the homogeneous fields (carbides and nitrides). This affects the appearance of the ternary equilibria such that the boundaries of the one-phase regions are nearly straight lines; running parallel to the metal_1 - metal_2 -bases. The conditional equations can then be substantially

*A treatment of the general case for interstitial-type compounds is given in E. Rudy: Ta-W-C System (AFML-TR-65-2, Part II, Volume VIII, March 1966).

simplified since we may take the concentration term of one of the components, say z, as independent of x and y, i.e., we permit the free energy to be varied only by the relative exchange of A and B. Proceeding in this way, we have :

$$x' + y' = \text{const} = a \quad (\partial x' = -\partial y')$$

$$z' = \text{const}' = 1-a \quad (\partial z' = 0)$$

$$x'' + y'' = \text{const}'' = b \quad (\partial x'' = -\partial y'')$$

$$z'' = \text{const}'' = 1-b \quad (\partial z'' = 0)$$

Substituting into the partial solution from Lagrange's equation, we obtain the two equivalent conditions (3a) and (3b).

$$\left[\frac{\partial F_1}{\partial x'} \right]_{T,p} = \left[\frac{\partial F_2}{\partial x''} \right]_{T,p} \quad (3a)$$

$$\left[\frac{\partial F_1}{\partial y'} \right]_{T,p} = \left[\frac{\partial F_2}{\partial x''} \right]_{T,p} \quad (3b)$$

We note the formal analogy of these equations to the conditional equation for binary alloys in both cases. A tie line connects two points of equal free energy gradients; however, due to the additional degree of freedom, the single tie line in the binary system splits up into a ∞^1 multiplicity (∞^1 tangent planes with $T = \text{const}$) in the ternary case. Taking the example shown in Figure 3, it is seen that a change of the significant parameters, in our example the exchange of atoms A and B between the two solid solutions, alters the concentration and hence the free energy of both phases in the direction $A \rightleftharpoons B$, and the gradient, therefore, has to be taken along the same path.

A few simple considerations will show us the usefulness of these equations. Assume, for the sake of simplicity, ideal mixing between both solid solutions (A,B) and (A,B)C. Since we consider only changes in the partial lattice (A,B) to be significant, we base the calculations on one gram-atom of A+B in both solutions. In this way, we obtain as the free energy for the solid solution A-B,

$$F_{(A,B)} = x_A \cdot F_A + x_B \cdot F_B + RT (x_A \ln x_A + x_B \ln x_B)$$

and in a similar fashion for the free energy of the crystal solution (A,B)C

$$F_{(A,B)C} = x'_A \cdot F_{AC} + x'_B \cdot F_{BC} + RT (x'_A \ln x'_A + x'_B \ln x'_B)$$

x_A, x_B Atomic fraction of A and B in (A, B)

x'_A, x'_B Relative mole fraction of A and B in the solution (A,B)C. ($x'_A + x'_B = 1$)

Differentiation and rearrangement yields the equation

$$RT \ln \frac{x_B}{x_A} \cdot \frac{x'_A}{x'_B} = F_{BC} - F_B - (F_{AC} - F_A)$$

Substituting the more easily obtainable free energies of formation ΔF_f , for the free energies,

$$\Delta F_{fBC} = F_{BC} - F_B - F_C$$

$$\Delta F_{fAC} = F_{AC} - F_A - F_C$$

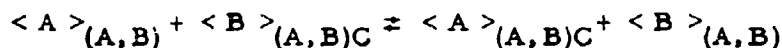
we obtain the final relationship for the tie lines of this partition equilibrium:

$$RT \ln K = \Delta F_{fBC} - \Delta F_{fAC} \quad (4)$$

The constant K abbreviates the expression

$$K = \frac{x_B}{x_A} \cdot \frac{x'_A}{x'_B}$$

and we may interpret it as the equilibrium constant of a reaction



ΔF_{fAC} and ΔF_{fBC} are the free energies of formation of the binary alloy phases AC and BC at the temperature $T(p = 1 \text{ atm})$.

From equation (4) we derive readily, that the relative distribution of A and B in the solution (A,B) and $(A,B)C$ is a function of the stabilities of the boundary phases; for equal stabilities, i.e. $\Delta F_{fBC} = \Delta F_{fAC}$, the relative concentrations of A and B in both solutions are equal. With $\Delta F_{fBC} < \Delta F_{fAC}$ (BC more stable than AC), the concentration of B in the solid solution $(A,B)C$ appears higher than in (A,B) . The reverse is true for the case $\Delta F_{fBC} > \Delta F_{fAC}$ (AC more stable than BC).

The free energy of mixing increases with increasing temperature and hence tends to equalize a given free energy difference $\Delta F_{fBC} - \Delta F_{fAC}$. For the (hypothetical) limiting case $T \rightarrow \infty$ we obtain independent of the free energy differences, equidistribution, $x_A = x'_A$ and $x_B = x'_B$.

To illustrate the method and to demonstrate the graphical solution method, we may treat the foregoing example numerically. Let, for example, the free energy of formation of the binary compound AC be -4.574 cal/mole and $\Delta G_{BC} = -2287 \text{ cal/mole}$. We want to know the equilibrium constant K as well as the tie line distribution for 500°K and 2000°K .

According to equation (4)

$$RT \ln K = \Delta F_{fBC} - \Delta F_{fAC} = 2287 \text{ cal/mole,}$$

$$K = K(500^\circ\text{K}) = 10$$

$$K = K(2000^\circ\text{K}) = 1.779$$

The knowledge of the equilibrium constants K defines for any alloy (A,B) the compositions of the products, which will be formed upon exposure to the component C. From the decreasing slope of the tie lines with increasing temperatures (Figure 5), we derive, that the reactions tend to be less selective at high temperatures, i.e., the relative distribution of the components A and B becomes less preferential.

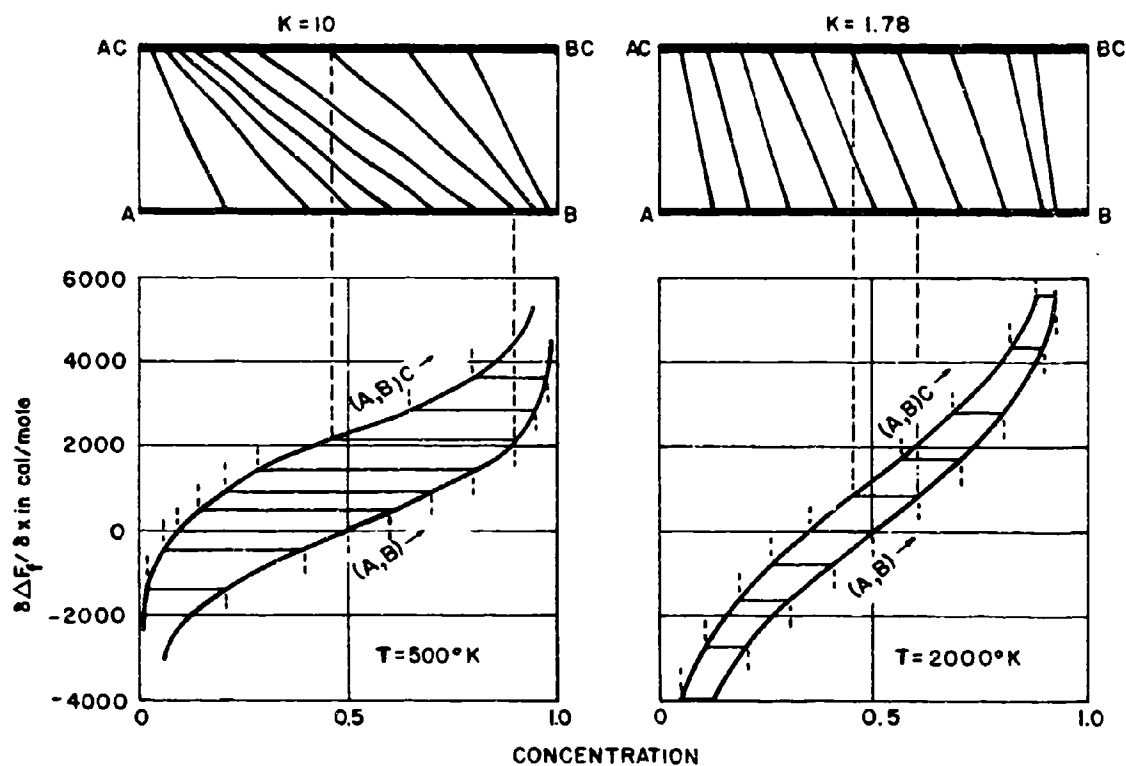


Figure 5. Graphical Construction of the Tie Lines from the ΔF -x Curves and Effect of Temperature on the Partition Equilibrium.

For direct comparison purposes, but especially in those instances, where the solutions cannot be treated as ideal, it is preferable to perform the evaluation graphically. For this purpose (equations 3a or 3b) we plot the gradients of the free energies as a function of composition; the horizontal intercepts between the curves at the chosen values x_A or x_A' immediately then yields the equilibrium compositions (Figure 5).

B. THREE-PHASE EQUILIBRIA IN TERNARY SYSTEMS (Figure 6)

The derivation of the conditional equations for the three-phase equilibrium is performed analogously to that for the two-phase equilibrium. However, in view of the bulkiness and complexity of the resulting equations, which make them of only limited use, we shall not stress the general case but rather concentrate on the simplified treatment which we will need for our subsequent discussions of actual systems. A brief review of computer approaches for the solution of the unrestricted problem will be given in a later section. We have to consider an equilibrium $A_{x'}B_{y'}C_{z'}$ - $A_{x''}B_{y''}C_{z''}$ - $A_{x'''}B_{y'''}C_{z'''}$, where z' , z'' , z''' have individually different, but otherwise constant values.

Since three phases are involved now, the total free energy of the phase mixture becomes

$$F = \nu_1 F_1 + \nu_2 F_2 + \nu_3 F_3,$$

with

$$F_1 = \phi_1(x', y', z')$$

$$F_2 = \phi_2(x'', y'', z'')$$

$$F_3 = \phi_3(x''', y''', z''')$$

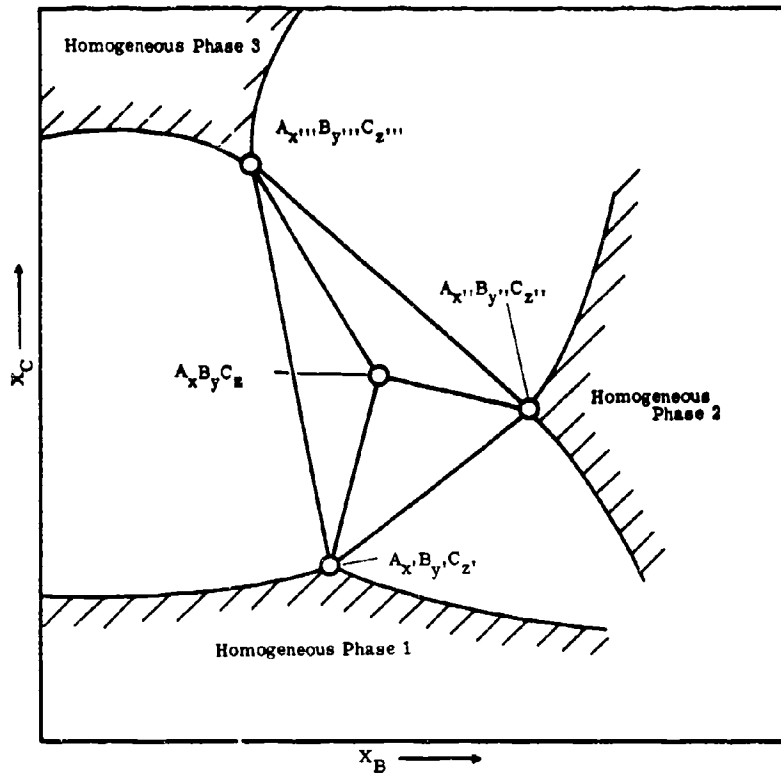


Figure 6. Three-Phase Equilibrium in a Ternary System (General Case).

Together with the boundary conditions, which results from the relations existing between the concentration terms as well as from the conservation of the atomic masses, we obtain, in the well-known manner after Lagrange to obtain the minimum, the equations:

$$F_1 - a_1 x' - a_2 (a - x') - a_3 (1 - a) - a_4 = 0 \quad (a)$$

$$F_2 - a_1 x'' - a_2 (b - x'') - a_3 (1 - b) - a_4 = 0 \quad (b)$$

$$F_3 - a_1 x''' - a_2 (c - x''') - a_3 (1 - c) - a_4 = 0 \quad (c)$$

$$v_1 \frac{\partial F_1}{\partial x'} - a_1 v_1 + a_2 v_1 = 0 \quad (d)$$

$$v_2 \frac{\partial F_2}{\partial x''} - a_1 v_2 + a_2 v_2 = 0 \quad (e)$$

$$v_3 \frac{\partial F_3}{\partial x'''} - a_1 v_3 + a_2 v_3 = 0 \quad (f)$$

with $v_1 + v_2 + v_3 = 1$

$$x' + y' = \text{const}' = a$$

$$x'' + y'' = \text{const}'' = b$$

$$x''' + y''' = \text{const}''' = c$$

From equations (d), (e), and (f) we obtain the important partial solution:

$$\left[\frac{\partial F_1}{\partial x'} \right]_{T,p} = \left[\frac{\partial F_2}{\partial x''} \right]_{T,p} = \left[\frac{\partial F_3}{\partial x'''} \right]_{T,p} = a_1 - a_2 \quad (5)$$

With this equation alone, however, the three-phase equilibrium is not yet uniquely defined. An infinite number of solutions would satisfy relation (5), and we need an additional condition in order to reduce the possible solutions to only one. For this purpose, we turn to the remaining equations and eliminate the undetermined multipliers a_1 through a_4 .

Rearrangement of equations (a), (b), and (c) yields

$$F_1 - x'(a_1 - a_2) - a_2 \cdot a - a_3 + a_3 \cdot a - a_4 = 0$$

$$F_2 - x''(a_1 - a_2) - a_2 \cdot b - a_3 + a_3 \cdot b - a_4 = 0$$

$$F_3 - x'''(a_1 - a_2) - a_2 \cdot c - a_3 + a_3 \cdot c - a_4 = 0$$

Substituting relation (5) for $a_1 - a_2$, and recalling the relation for calculating partial (\bar{F}) from the integral quantities,

$$\bar{F}_A = F + x_B \frac{\partial F}{\partial x_A}$$

we obtain

$$\bar{F}_{1B} - \bar{F}_{2B} + b(a_2 - a_3) - a(a_2 - a_3) = 0$$

$$\bar{F}_{3B} - \bar{F}_{2B} + b(a_2 - a_3) - c(a_2 - a_3) = 0$$

Elimination of a_2 and a_3 finally yields

$$\frac{\bar{F}_{1B} - \bar{F}_{2B}}{a - b} = \frac{\bar{F}_{2B} - \bar{F}_{3B}}{b - c} = \frac{\bar{F}_{1B} - \bar{F}_{3B}}{a - c} \quad (6)$$

and, due to the symmetry of the relation, the equivalent equation

$$\frac{\bar{F}_{1A} - \bar{F}_{2A}}{a - b} = \frac{\bar{F}_{2A} - \bar{F}_{3A}}{b - c} = \frac{\bar{F}_{1A} - \bar{F}_{3A}}{a - c} \quad (7)$$

The partial quantities in equation (6) and (7) are on a gram-atom basis. In practical calculations it is inconvenient to first determine the differences of the partial quantities, and then to divide by the composition factors a , b , and c in order to satisfy the conditional equations. Instead, if we base our calculations on a gram-atom of the components $A + B$, i. e., if we express the compound solutions in the form $(A, B)C_1$, we have for

$$\text{Solution 1} = (A, B)C_u$$

$$\text{Solution 2} = (A, B)C_v$$

$$\text{Solution 3} = (A, B)C_w$$

$$\bar{F}_{A(u)} = \frac{\bar{F}_{1A}}{a}; \quad u = \frac{1-a}{a}$$

$$\bar{F}_{A(v)} = \frac{\bar{F}_{2A}}{b}; \quad v = \frac{1-b}{b}$$

and

$$\bar{F}_{A(w)} = \frac{\bar{F}_{3A}}{c}; \quad w = \frac{1-c}{c}$$

Substituting in equation (7) and rearranging the terms, we obtain the conditional equation in the form:

$$(v-w) \bar{F}_{A(u)} + (w-u) \bar{F}_{A(v)} + (u-v) \bar{F}_{A(w)} = 0 \quad (8a)$$

Performing the same operation for the component B, we receive the equivalent relation

$$(v-w) \bar{F}_{B(u)} + (w-u) \bar{F}_{B(v)} + (u-v) \bar{F}_{B(w)} = 0 \quad (8b)$$

$\bar{F}_{A(u)}, \bar{F}_{A(v)}, \bar{F}_{A(w)}$... Partial free energy of A in the solutions (A,B)C_u, (A,B)C_v, and (A,B)C_w.

$\bar{F}_{B(u)}, \bar{F}_{B(v)}, \bar{F}_{B(w)}$... Partial free energy of B in the solutions (A,B)C_u, (A,B)C_v, and (A,B)C_w.

Equations (5) and (8) together now completely define the three-phase equilibrium: From all coexisting composition triples admitted by equation (5), the correct triples, i.e., the compositions of the three phases, which have the lowest free energy, are sorted out with the aid of equation (8). Equation (8) corresponds to the law of the mass action in the form of the well-known thermodynamic-relationship for the equilibrium state:

$$\sum v_i \mu_i = 0$$

where the v_i denote the mole masses of the reacting species and the μ_i are their thermodynamic potentials. The fact, that two equilibrium conditions are required reveals that the law of mass action is not sufficient to locate the three-phase equilibrium in terms of the individual equilibrium concentration of the phases.

Equation (5) and (8), will be extensively used for calculations in actual systems. For the sake of convenience, we shall refer to equation (5) as the "gradient-condition", and to equation (8), for reasons to be explained later, as the "stability-condition".

III. DISCUSSION OF THE EQUILIBRIUM CONDITIONS ON MODEL EXAMPLES

A. THREE-PHASE EQUILIBRIA RESULTING FROM MISCIBILITY GAPS IN BINARY OR PSEUDO-BINARY SOLUTIONS

This case is very frequently found in actual systems. Miscibility gaps in solid solutions may arise from large differences in the atomic sizes of the constituents, where the resulting strain energies result in positive mixing terms, and ultimately may cause the solution to separate into two distinct phases. As a first approximation, we may take account of the nonideal behavior by adding a positive enthalpy term to the ordinary mixing quantities, the later being entirely due to the entropy of mixing. The most common approach, using a parabolic form, is that originally proposed by Van Laar, and the solutions which obey this behavior are usually referred to as "regular solutions". The free energy of mixing for the regular solution is given by

$$F_{A,B}^{\text{mix}} = \epsilon \cdot x_A \cdot x_B + RT(x_A \ln x_A + x_B \ln x_B)$$

where ϵ is the so-called interaction parameter. The critical solution temperature for the regular solution is derived from the condition, that the first and second derivative must vanish at the critical point, and is given by

$$T_c = \frac{\epsilon}{2R}$$

Due to the symmetry of the terms, the critical point is located at $x = \frac{1}{2}$ and the miscibility gap by the regular solution model is symmetrical with regard to $x = \frac{1}{2}$.

A typical case for a three-phase equilibrium resulting from the formation of a miscibility gap in one of the compound solutions is shown in Figure 7. For simplicity, the same basic system layout as in the example shown in Figure 3 has been chosen.

The pseudo-binary miscibility gap is sufficiently defined by the relation

$$\left[\frac{\partial F_1}{\partial x^{II}} \right]_{x_{C_1}} = \left[\frac{\partial F_2}{\partial x^{II}} \right]_{x_{C_2}} \quad T, p = \text{const.}$$

x_{C_1}, x_{C_2}, \dots Being the composition of the terminal solid solution.

The vertex of the three-phase equilibrium at the solution (A, B) is located, according to equation (5), at that point, where the free energy gradient of the (A, B) solid solution coincides with the gradients of the solid solution

(A,B)C at the concentration points x_{C_1} and x_{C_2} . The evaluation can be done either by calculation or graphically as shown in Figure 8. To depict more

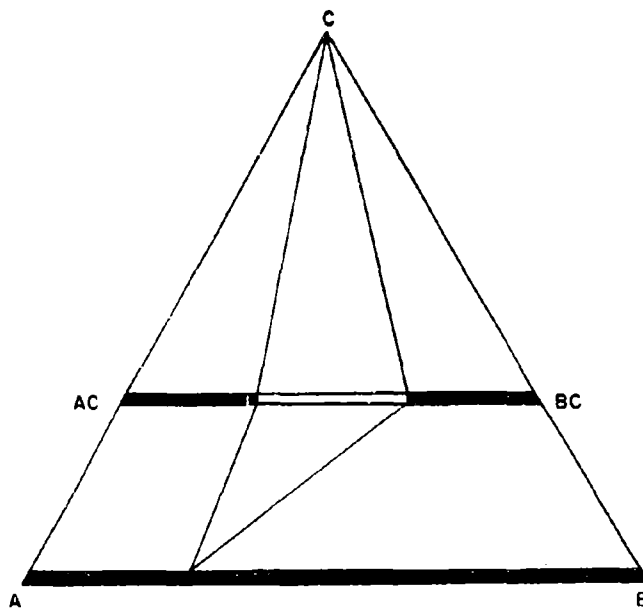


Figure 7. Three-Phase Equilibrium Resulting from a Miscibility Gap in a Pseudo-binary solid solution.

clearly the existing relations, the equilibria were drawn on a rectangular basis instead of the usual triangular one. The following data were assumed for the calculations:

$$\Delta F_{fAC} = 4574 \text{ cal/mole AC}$$

$$\Delta F_{fBC} = 2287 \text{ cal/mole BC}$$

$$\Delta T_{C_1} = 1000^\circ\text{C} (\epsilon_1 = 3960 \text{ cal/mole})$$

$$\Delta T_{C_2} = 1200^\circ\text{K} (\epsilon_2 = 4750 \text{ cal/mole})$$

The free energies of both compounds are further assumed to have the same temperature dependence so that the difference may be taken as being independent of temperature. Choosing the pure components A and B as the reference

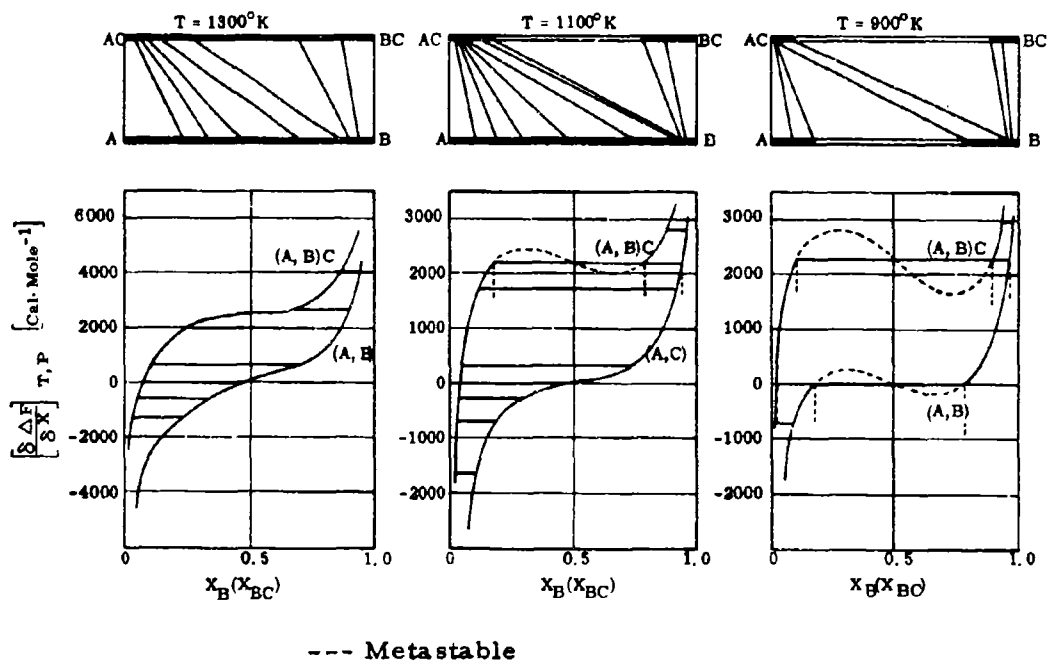


Figure 8. Appearance of the Equilibria for the Case of Nonideal Solutions, and Graphical Determination of the Tie Lines.

state, we obtain for the solid solution (A, B)

$$\Delta F_{(A,B)} = \epsilon_1 \cdot x_A^i \cdot x_B^i + RT (x_A^i \ln x_A^i + x_B^i \ln x_B^i)$$

and for the solution (A, B)C:

$$\Delta F_{(A,B)C} = x_A^{ii} \Delta F_{fAC} + x_B^{ii} \Delta F_{fAC} + \epsilon_2 \cdot x_A^{ii} \cdot x_B^{ii} + RT (x_A^{ii} \ln x_A^{ii} + x_B^{ii} \ln x_B^{ii})$$

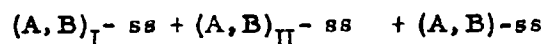
The free energy-concentration gradients become then:

$$\left[\frac{\partial \Delta F_{(A,B)}}{\partial x'_B} \right]_{T,P} = \epsilon_1 (1 - 2x'_B) + RT \ln \frac{x'_B}{1-x'_B}$$

$$\left[\frac{\partial \Delta F_{(A,B)C}}{\partial x''_B} \right]_{T,P} = \Delta F_{IBC} - \Delta F_{IAC} + \epsilon_2 (1 - 2x''_B) + RT \ln \frac{x''_B}{1-x''_B}$$

These gradients are plotted in the lower portions of Figure 8 as a function of the concentration x'_B and x''_B , respectively.

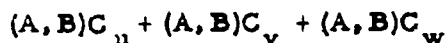
At 1300°K, both solutions are above the critical temperature, and the only heterogeneous equilibrium in existence is the two-phase equilibrium between (A, B) and (A, B) C_{1-x} . At 1100°K we notice the formation of a miscibility gap in the solution (A, B)C, with the consequent formation of a three-phase equilibrium



Finally, at 900°K both solutions exhibit miscibility gaps, and consequently, two three-phase equilibria, each of which is surrounded by three two-phase equilibria, appear. The construction of the tie lines within the two-phase fields from the gradient curves follows the same route as previously described.

Re-examining the equations, we arrive at the conclusion that for the evaluation of such three-phase equilibria, which result from the formation of miscibility gaps in binary or pseudo-binary solutions, the gradient condition is sufficient for the evaluation of the base vertex of the three-phase field.

further have an intermetallic phase AC_v which does not occur in the edge-system B-C. Due to the fact that the corresponding phase in the B-C system is missing, the solid solution $(A,B)C_v$ is ultimately terminated by a three-phase equilibrium



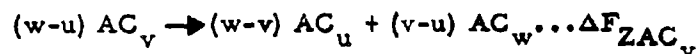
Intuitively, we are inclined to assume that the range $(A,B)_v$ will increase with increasing stability of the hypothetical phase BC_v , for we know that the solution should extend over the whole concentration range if such a compound would become stable in the binary B-C system. We therefore expect that the relative stability of the hypothetical phase BC_v , (i.e. its free energy of disproportionation into BC_u and BC_w) will be the main controlling factor for the size of the ternary range of the $(A,B)C_v$ solid solution. The general situation, shown for a binary system A-C with two phases AC_u and AC_w , and a further compound AC_v of varying stability, is depicted in Figure 10 (Case I, read BC_v instead of AC_v).

To discuss the problem mathematically, we best start out from the stability condition (8):

$$(v-w) \bar{F}_{A(u)} + (w-u) \bar{F}_{A(v)} + (v-w) \bar{F}_{A(w)} = 0$$

Basing the calculations on the components as the reference state, we may replace the free enthalpy values by the respective free enthalpies of formation, i.e. we may write $\Delta \bar{F}_{AC_u}$ in place of \bar{F}_{AC_u} without changing the form of the equation. Separation of the partial free energies into base- and concentration dependent terms yields

Where the ΔF^{mix} terms refer to the partial quantities of mixing, and the first three terms correspond to the free enthalpy change of the reaction



The quantity ΔF_{ZAC_v} may be regarded as the free enthalpy of disproportionation (ΔF_{ZAC_v}) of the phase AC_v into the neighboring phases A and AC_w . Analogously, the last three terms, containing the partial mixing quantities for the phases $(A,B)C_u$, $(A,B)C_v$, and $(A,B)C_w$, may be interpreted as the corresponding free energy changes which result from the formation of the solid solutions. The above equation may then be rewritten to

$$\Delta F_{ZAC_v} + \overline{\Delta F}_{ZAC_v}^{\text{mix}} = 0 \quad (9)$$

Due to the reciprocity of the relations, the analogous expression for the component B is obtained.

$$\Delta F_{ZBC_v} + \overline{\Delta F}_{ZBC_v}^{\text{mix}} = 0 \quad (10)$$

The three-phase equilibrium is therefore characterized by the condition that the free enthalpy of disproportionation for each of the binary compounds AC_v and BC_v are brought to balance by the corresponding partial solution terms. Knowing the solution behavior, relations (9) and (10) give us a means, to separately determine the free enthalpies of disproportionation of the phases AC_v and BC_v from experimental phase-diagram data; this allows us to assign free energy values to the hypothetical phase BC_v .

To determine the equilibrium concentrations from given thermodynamic data, we first employ the gradient condition, which yields the vertices of all possible three-phase equilibria existing across the entire concentration field. Mathematically, this procedure is equivalent to reducing the ∞^3 initially possible solutions (manifold of combinations between three concentration variables, x , x' , and x'') to a manifold of only ∞^1 [sets of interrelated triples (x, x', x'')]. These "compatible" triples of concentration terms are then inserted into equation (9) or (10); the correct composition triple is that one for which these conditions are satisfied.

In view of the transcendency of the resulting equations, which makes the arithmetic quite involved, the evaluation again is best done graphically. We will, however, not treat a model example, since the calculation techniques will be demonstrated extensively in the application section, but rather discuss a few important relations.

Relations (8) and (11) are valid for the equilibrium state; any deviation from it will result in the appearance of a finite quantity, ϕ , on the right hand side; which essentially is a measure of the relative imbalance between the disproportionation terms for the binary compounds and the mixing quantities. We may therefore generalize condition (8) and write,

$$\phi_A = \Delta F_{ZAC_v} + \overline{\Delta F}_{ZAC_v}^{\text{mix}} \quad (11)$$

$$\phi_B = \Delta F_{ZBC_v} + \overline{\Delta F}_{ZBC_v}^{\text{mix}} \quad (12)$$

and note, that at equilibrium

$$\phi(x) = 0$$

When $\phi(x)$ assumes positive values, i.e.,

$$\phi(x) > 0$$

the solution $(A,B)C_v$ is stable in respect to mechanical mixtures of $(A,B)C_u$ and $(A,B)C_w$. For the case that

$$\phi(x) < 0,$$

the solution $(A,B)C_v$ is unstable and disproportionates into mixtures of the solutions $(A,B)C_u$ and $(A,B)C_w$.

We further note, that

$$\phi_A [x_{A(u)} = 1] = \Delta F_{ZAC_v}$$

$$\phi_A [x_{A(v)} = 0] = \Delta F_{ZBC_v}$$

$$\phi_B [x_{B(u)} = 1] = \Delta F_{ZBC_v}$$

$$\phi_B [x_{B(v)} = 0] = \Delta F_{ZAC_v}$$

i.e. a perfect symmetry of the relations.

So far, our relations have dealt only with partial quantities, and we naturally expect the excess functions ϕ_A and ϕ_B to describe only the partial disproportionation quantities only. Consider now, for example, that one would be interested in knowing how much a given crystal solution, in our case the series $(A,B)C_v$ stable in respect to the neighboring phases, i.e., we would

like to know the integral free enthalpy of disproportionation of any given composition $(A, B)C_v$ into corresponding (quasi-equilibrium) mixtures of (A, B) and $(A, B)C$.

With both functions ϕ_A and ϕ_B known, the integral free enthalpy of disproportionation $\phi_i(x)$ of the crystal solution $(A, B)C_v$ would be given by:

$$\phi_{\text{int.}}(x_i) = x_{A(v)} \cdot \phi_A(x_{iA}) + x_{B(v)} \phi_B(x_{iB})$$

or, since

$$x_{B(v)} = 1 - x_{A(v)}$$

$$\phi_{\text{int.}}(x_i) = x_{A(v)} \cdot \phi_A(x_{iA}) + [1 - x_{A(v)}] \cdot \phi_B(x_{iB})$$

The concentration variables x_{iA} and x_{iB} abbreviate the sets of terms $x_{A(u)}$, $x_{A(v)}$, and $x_{A(w)}$, and $x_{B(u)}$, $x_{B(v)}$, $x_{B(w)}$, respectively; they are used to help to indicate the components to which the concentration variables refer. Thus, by agreement

$$x_{iA} = 1 - x_{iB}.$$

In order to obtain the integral function $\phi(x)$, we have to determine the interrelation between the partial functions $\phi_A(x_{iA})$ and $\phi_B(x_{iB})$. It can be shown (Appendix I) that both functions are identical, i. e.,

$$\phi_A(x_{iA}) \equiv \phi_B(x_{iB})$$

Substitution of this result into the equation for $\phi_{\text{int.}}(x_i)$, yields

$$\phi_{\text{int.}}(x_i) \equiv \phi_A(x_{iA}) \equiv \phi_B(x_{iB}) \quad (13)$$

We obtain, therefore, the important result, that the integral free energy of disproportionation of a crystal solution is equivalent to the sum of three free enthalpy of disproportionation and the partial free energy of mixing for either one of the phases participating in the equilibrium.

With these findings, we are now able to schematically list the possible reaction types (Figures 11a and 11b). Each case is found in actual systems. The case shown in Figure 11(b) is of special interest since it indicates the possibility for a ternary disproportionation of a solid solution formed between two stable, isomorphous binary phases.

As described previously, the graphical method offers the most convenient route to evaluate the equation. A closed solution for $\phi_{int.}(x_i)$, which often is useful for initial estimates of the gross behavior of the phase-relationships in a system, can be given for the case where the solutions behave ideally. For this purpose, we have to combine equations (5) with equation (8) or (11).

Expanding relation (5), we obtain ($T, p = \text{const}$)

$$\frac{\partial \Delta F_{fAC_u}}{\partial x_{A(u)}} = \Delta F_{f(AC_u)} - \Delta F_{f(BC_u)} + RT \ln \frac{x_{A(u)}}{1-x_{A(u)}}$$

$$\frac{\partial \Delta F_{fAC_v}}{\partial x_{A(v)}} = \Delta F_{f(AC_v)} - \Delta F_{f(BC_v)} + RT \ln \frac{x_{A(v)}}{1-x_{A(v)}}$$

$$\frac{\partial \Delta F_{fAC_w}}{\partial x_{A(w)}} = \Delta F_{f(AC_w)} - \Delta F_{f(BC_w)} + RT \ln \frac{x_{A(w)}}{1-x_{A(w)}}$$

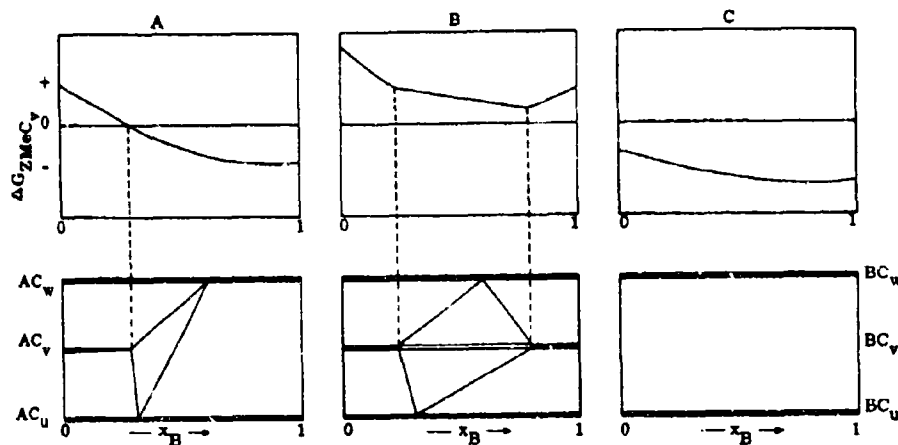


Fig. 11a

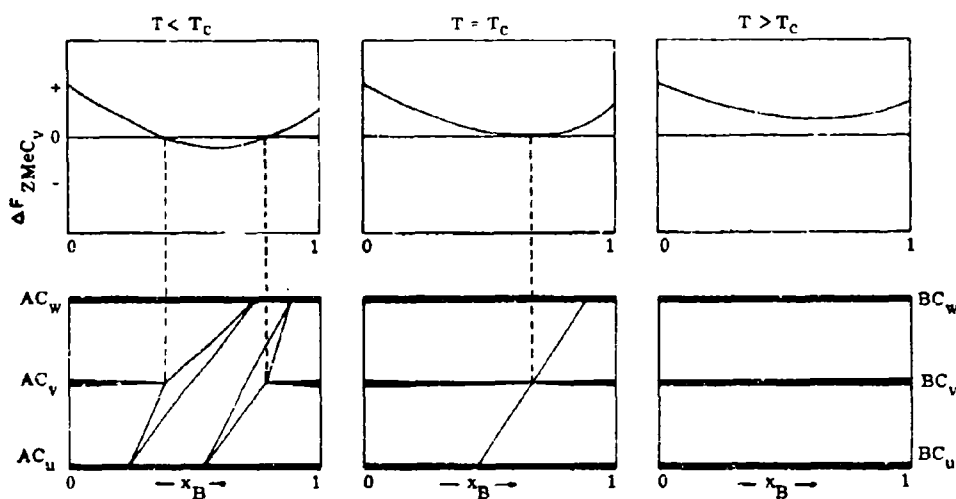


Fig. 11b

Figure 11(a) and 11(b)

Integral Free Energy of Disproportionation, ΔF_{ZMeC_v} , of a Phase Solution $(A, B)C_v$, and Corresponding Appearance of the Phase Equilibria (Diagrammatic).

Properties of the Function ΔF_{ZMeC_v} :

$$\Delta F_{ZMeC_v} [x_{B(v)} = 0] = \Delta F_{ZAC_v}$$

$$\Delta F_{ZMeC_v} [x_{B(v)} = 1] = \Delta F_{ZBC_v}$$

$\Delta F_{ZMeC_v} \geq 0$: Solution $(A, B)C_v$ Stable

$\Delta F_{ZMeC_v} \leq 0$: Solution $(A, B)C_v$ Unstable with regard to mechanic mixtures of $(A, B)C_u$ and $(A, B)C_w$

Equation (11) yields

$$\phi_A [x_{iA}] = \Delta F_{ZAC_v} + \overline{\Delta F}_{ZAC_v}^{mix}$$

$$\phi_A [x_{iA}] = \Delta F_{ZAC_v} + RT \ln \frac{x_{A(w)}^{\frac{v-u}{w-u}} \cdot x_{A(u)}^{\frac{w-v}{w-u}}}{x_{A(v)}}$$

with

$$\Delta F_{ZAC_v} = (v-u) \Delta F_{f(AC_w)} + (w-v) \Delta F_{f(AC_u)} - (w-u) \Delta F_{f(AC_v)}$$

Substitution and rearrangement of the terms yields

$$\phi_A (x_{iA}) = \phi_A [x_{A(v)}] = \Delta F_{ABC_v} - RT \ln [1 + x_{A(v)}^{K_2 - 1}]^{\frac{v-u}{w-u}} [1 + x_{A(v)}^{K_1 - 1}]^{\frac{w-v}{w-u}}$$

or, seeking ϕ as a function $x_{B(v)}$.

$$\phi_B (x_{iB}) = \phi_B [x_{B(v)}] = \Delta F_{ZAC_v} - RT \ln [1 + x_{B(v)}^{K_2' - 1}]^{\frac{u-v}{w-u}} [1 + x_{B(u)}^{K_1' - 1}]^{\frac{w-v}{w-u}}$$

The constants K_1 , K_2 , K_1' , and K_2' are defined by:

$$RT \ln K_1 = \Delta F_{f(AC_v)} - \Delta F_{f(BC_v)} - \Delta F_{f(AC_u)} + \Delta F_{f(BC_u)}$$

$$RT \ln K_2 = \Delta F_{f(AC_v)} - \Delta F_{f(BC_v)} - \Delta F_{f(AC_w)} + \Delta F_{f(BC_w)}$$

$$K_1' = \frac{1}{K_1}$$

$$K_2' = \frac{1}{K_2}$$

and u, v, w have the meaning previously allocated. We further recall that the integral function $\phi_{\text{int.}}(x)$ represented by either $\phi_A [x_{A(v)}]$ or $\phi_B [x_{B(v)}]$.

Instead of choosing the composition of the solution $(A, B)C_v$ as the independent variable, $\phi(x)$ may also be represented as a function of the concentration of the solid solutions $(A, B)C_u$, or $(A, B)C_w$. Obviously, however, the concentration points determined by $\phi(x) = 0$ then refer to the vertex of the three-phase equilibrium at that particular solution.

A further relation, which is often useful in obtaining a coarse estimate for the solubilities to be expected at high temperatures, can be obtained by seeking the limiting value of $\phi(x)$ for $T \rightarrow \infty$. Evaluation of the limit in the well-known manner after L'Hospital, yields the relations

$$x_{B(u)} [T \rightarrow \infty] = \frac{\Delta F_{ZAC_v}}{\Delta F_{ZAC_v} - \Delta F_{ZBC_u}}$$

$$x_{A(u)} [T \rightarrow \infty] = \frac{\Delta F_{ZBC_v}}{\Delta F_{ZBC_v} - \Delta F_{ZAC_u}}$$

The solutions are only meaningful, when ΔF_{ZAC_v} and ΔF_{ZBC_v} are of a different sign, i. e. one of the phases has to be unstable in the binary.

C. BINARY AND PSEUDO-BINARY SYSTEMS OF NON-ISOMORPHOUS COMPONENTS

Up to this point, we were interested only in systems where the solid solutions were formed between isostructural phases. Somewhat different conditions exist, however, if we continue with two components which differ

in their crystallographic framework. In general, temperature dependent mutual solubilities will be observed, but the two solutions will always be separated by a two-phase field of finite width. The question arises now, concerning the relations between the magnitude of the atom exchanges in the two structurally non-equivalent lattices and the energetical quantities. Furthermore, as a follow-on consideration, we will be interested in how deviations from the ideal solution will affect the overall appearance of the equilibria.

Let A and B be the constituents of the binary or pseudo-binary system. The crystal structure of A is designated with α , and that of B with β . $(A, B)_\alpha$ is then the solid solution having the α -structure, and $(A, B)_\beta$ the solution exhibiting the structural characteristics of β . We further assume that no ternary compound is formed across the concentration field, i. e., the free energies of all other phases conceivable to be formed, shall be more positive than those of $(A, B)_\alpha$, $(A, B)_\beta$, or mechanical mixtures of both.

We expect that apart from the temperature, the adaptability of the individual components to the lattice of the partner will influence the widths of the homogeneous ranges; i. e., we expect the relative atom exchanges in both lattice types to be a function of the transformation energies $\Delta F_B (\beta - \alpha)$ and $\Delta F_A (\alpha - \beta)$ for the component B and A. The free energy-concentration relationships prevailing in such a system are shown in Figure 12. In order to obtain a mathematical relation between the concentration and the free energy quantities, we start out from the well-known thermodynamic relationship that in the equilibrium state the thermodynamic potentials (partial free enthalpies) of A and B, must be the same in both solid solutions. Hence

$$\bar{F}_{A(\alpha)} = \bar{F}_{A(\beta)}$$

$$\bar{F}_{B(\alpha)} = \bar{F}_{B(\beta)}$$

Denoting the integral free enthalpy of mixing of the α -solid solution with F_{α}^{mix} , and that of β with F_{β}^{mix} , and using the stable structure as the

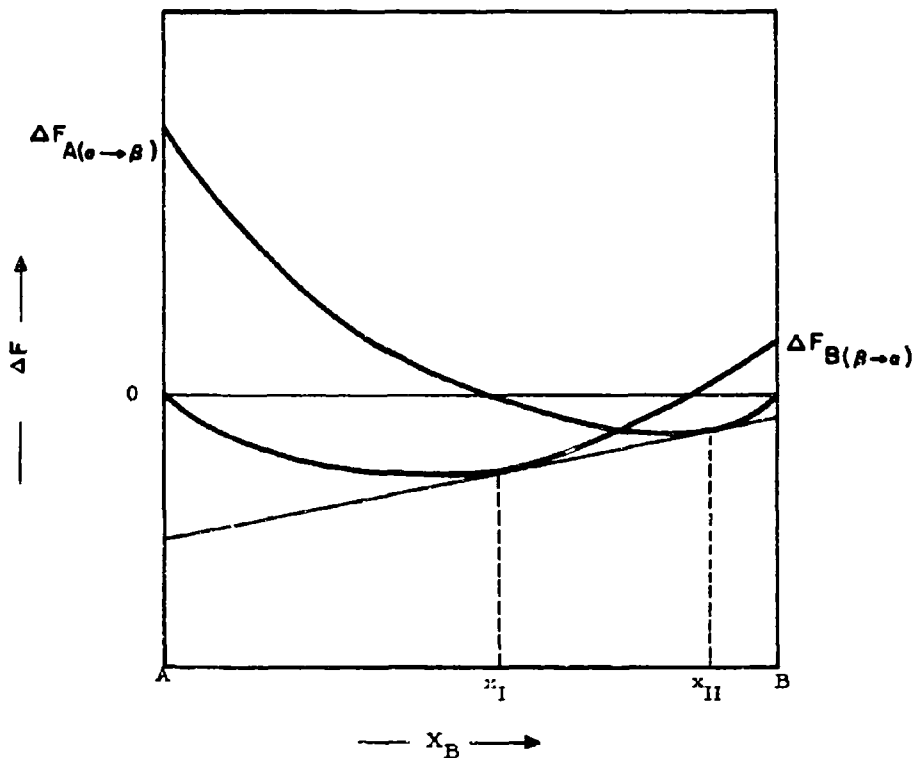


Figure 12. Relation Between the Integral Free Energies and the Relative Atom Exchanges in Systems of Non-isomorphous Components.

x_I .. Solubility Limit of the α -Solid Solution

x_{II} .. Solubility Limit of the β -Solid Solution

$\Delta F_{A(\alpha \rightarrow \beta)}$.. Free Energy Change Involved in Converting the Lattice Type of A (α) into that of B (β). (Free Energy of Transformation of A).

$\Delta F_{B(\beta \rightarrow \alpha)}$.. Free Energy of Transformation $\beta \rightarrow \alpha$ for the Component B.

reference state, we obtain

$$\bar{F}_{A(\alpha)} = \bar{F}_{A(\alpha)}^{\text{mix}}$$

$$\bar{F}_{A(\beta)} = \Delta F_{(\alpha \rightarrow \beta)} + \bar{F}_{A(\beta)}^{\text{mix}}$$

or

$$\bar{F}_{A(\alpha)}^{\text{mix}} - \bar{F}_{A(\beta)}^{\text{mix}} = \Delta F_{A(\alpha \rightarrow \beta)} \quad (12)$$

and in an analogous manner for the component B

$$\bar{F}_{B(\beta)}^{\text{mix}} - \bar{F}_{B(\alpha)}^{\text{mix}} = \Delta F_{B(\beta \rightarrow \alpha)} \quad (13)$$

If both solutions behave ideally, these expressions become, applying the well-known thermodynamic relationship for calculating partial from integral quantities,

$$\bar{F}_A = F + x_B \frac{\partial F}{\partial x_A}$$

We obtain then

$$\bar{F}_{A(\alpha)}^{\text{mix}} = RT \ln x_{A(\alpha)}$$

$$\bar{F}_{A(\beta)}^{\text{mix}} = RT \ln x_{A(\beta)}$$

$$RT \ln \frac{x_{A(\alpha)}}{x_{A(\beta)}} = \Delta F_{A(\alpha \rightarrow \beta)} \quad (14)$$

and for the component B

$$RT \ln \frac{x_{B(\beta)}}{x_{B(\alpha)}} = \Delta F_{B(\beta \rightarrow \alpha)} \quad (15)$$

With the following relations existing between the concentrations terms:

$$x_{B(\beta)} = 1 - x_{A(\beta)}$$

$$x_{B(\alpha)} = 1 - x_{A(\alpha)}$$

For the case of non-ideal solutions, the partial quantities either can be derived from known experimental data, the nonideality can be approximated by suitable mathematical expressions. Thus, for example, using the regular solution approach, we obtain the following equations:

$$\bar{F}_{A(\alpha)}^{\text{mix}} = \epsilon_{\alpha} [1 - x_{A(\alpha)}]^2 + RT \ln x_{A(\alpha)}$$

$$\bar{F}_{A(\beta)}^{\text{mix}} = \epsilon_{\beta} [1 - x_{A(\beta)}]^2 + RT \ln x_{A(\beta)}$$

$$\epsilon_{\alpha} [1 - x_{A(\alpha)}]^2 - \epsilon_{\beta} [1 - x_{A(\beta)}]^2 + RT \ln \frac{x_{A(\alpha)}}{x_{A(\beta)}} = \Delta F_{A(\alpha \rightarrow \beta)} \quad (16)$$

or, since for the majority of instances $\epsilon_{\alpha} \approx \epsilon_{\beta} = \epsilon$

$$\epsilon \cdot [x_{A(\alpha)} - x_{A(\beta)}] [x_{A(\alpha)} + x_{A(\beta)} - 2] + RT \ln \frac{x_{A(\alpha)}}{x_{A(\beta)}} = \Delta F_{A(\alpha \rightarrow \beta)}$$

Analogous expressions can be obtained for the component B.

From the foregoing equations, we derive, that the relative atom exchange in systems between non-isostructural components is principally determined by the free energy differences between the lattice types of the two partners. Since the transformation energies are positive quantities, we derive, for example, from equation (16) that with increasing $\Delta F_{A(\alpha \rightarrow \beta)}$ the

ratio $\frac{x_{A(\alpha)}}{x_{A(\beta)}}$ increases, i.e. the width of the homogeneous range of the α -phase increases, while that of β narrows down. If we consider, for example the special case, that $\Delta F_{A(\alpha \rightarrow \beta)} \gg \Delta F_{B(\beta \rightarrow \alpha)}$, the homogeneity range of the β -solution will be negligibly small.

Under these circumstances

$$\bar{F}_{B(\beta)}^{\text{mix}} \approx 0$$

and we obtain from equation (15)

$$-\bar{F}_{B(\alpha)}^{\text{mix}} = \Delta F_{B(\beta \rightarrow \alpha)}$$

For ideal solutions, this results in the simple relation:

$$RT \ln x_{B(\alpha)} = -\Delta F_{B(\beta \rightarrow \alpha)} \quad (17)$$

or, since

$$\frac{\frac{\partial \Delta F_{B(\beta \rightarrow \alpha)}}{\partial T}}{\frac{\Delta F_{B(\beta \rightarrow \alpha)}}{T}} = -\frac{1}{T^2} \frac{\partial \Delta H_{B(\beta \rightarrow \alpha)}}{\partial T}$$

in the familiar Clausius-Clapeyron-type of equation,

$$\frac{\partial \ln x}{\partial T} = \frac{\Delta H}{RT^2}$$

This relation, in the integrated form

$$\ln x = A - \frac{\Delta H}{T}$$

is commonly used to evaluate the enthalpy change ΔH from experimental solubility curves ("heats of solution").

For practical purposes, it is often convenient to have a rapid means by which the relative magnitude of both solutions can be estimated, or, for the case of narrow two-phase ranges (small free enthalpies of transformation of A and B, high temperatures), to obtain the concentration range where the two-phase equilibrium is to be expected. For this purpose, we seek the limiting expression in equation (16) and (17) for $T \rightarrow \infty$, and obtain after L'Hospital:

$$\left[\frac{x_B}{x_A} \right]_{\text{crit. conc.}} = \frac{\Delta F_{A(\alpha \rightarrow \beta)}}{\Delta F_{B(\beta \rightarrow \alpha)}}$$

i. e., the limiting concentrations of A and B are inversely proportional to their free enthalpies of transformation.

As an example, let $\Delta F_{A(\alpha \rightarrow \beta)}$ be 100 cal/gr.-At., and $\Delta F_{B(\beta \rightarrow \alpha)} = 200$ cal/gr.-At. With these values the approximate mid-point composition of the two-phase range $\alpha + \beta$ will be at

$$\frac{x_B}{x_A} = \frac{1-x_A}{x_A} = \frac{1}{2}, \text{ or } x_A = 0.55,$$

i. e., the β -range extends further than the homogeneous field of α .

In order to demonstrate the applicability of the equations discussed in this chapter and to show the possible variations in the appearance of the equilibria due to nonideal solution behavior, we shall consider one example in somewhat greater detail.

We assume two structurally different components A and B, with B transforming at T_u into a lattice type equivalent to that of A. Without seriously curtailing the generality of the results, we shall use the regular solution approach to describe the deviation from nonideal behavior, and we shall also assume that $\Delta G_{A(\alpha \rightarrow \beta)} \gg \Delta G_{B(\beta \rightarrow \alpha)}$, so that we may neglect any atom exchange in the component B. This helps us to simplify the arithmetic.

Including in equation (17) the nonideality terms, we obtain

$$\epsilon [1 - x_{B(\alpha)}]^2 + RT \ln x_{B(\alpha)} = -\Delta F_{B(\beta \rightarrow \alpha)}$$

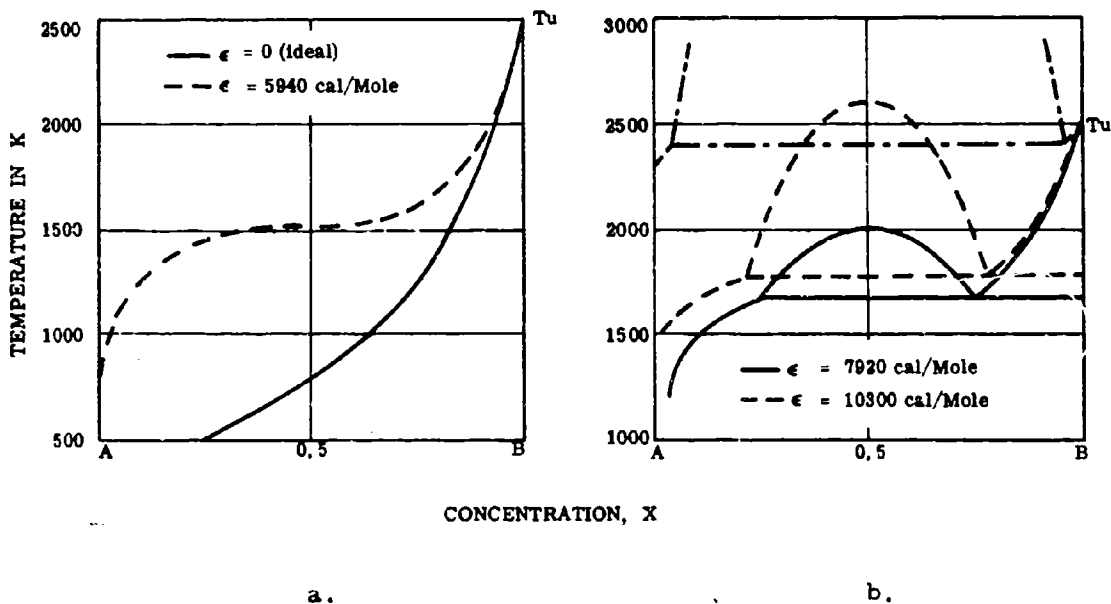


Figure 13a and 13b.

Effect of Non-ideal Solution Behavior on the Phase-Equilibria in Binary or Pseudo-Binary Systems of Non-Isomorphous Components (Regular Solutions).

Assuming, for example, $\Delta H_{B(\beta \rightarrow \alpha)} = 1500 \text{ cal/gr. -At.}$, $T_u = 2500^\circ\text{K}$, and a linear temperature dependence of the free enthalpy of transformation, we obtain, for various interaction parameters ϵ , the phase relationships shown in Figure 13a and 13b. The solubility curve for $\epsilon = 0$ (ideal solution) is shown by the solid curve in Figure 13a. For the case that $\Delta F_{B(\beta \rightarrow \alpha)}$ at the critical dissolution temperature, $T_c = \frac{\epsilon}{2R}$, is slightly more positive than the integral free enthalpy of mixing at $x = \frac{1}{2}$, we observe a strongly anomalous course of the solidus line, i. e., a strong increase of the solubility within a narrow temperature interval in the vicinity of T_c . If

$$F_{(T_c)}^{\text{mix}} > \Delta F_{B(\beta \rightarrow \alpha)} \text{ at } T = T_c, \text{ and } x = \frac{1}{2}$$

within a certain concentration range, the solution splits up into two isostructural phases, and a monotectoid reaction isotherm is introduced into the system (Figure 13b). Phenomenologically, the appearance of the monotectoid can be thought of as arising from the interaction of the miscibility gap in the α -solid solution (controlled by the nonideal solution behavior), with the solvus line of α (controlled by the free energy of transformation of $F_{B(\beta \rightarrow \alpha)}$)

Finally, we shall briefly mention an equilibrium case which is of importance in the thermodynamic evaluation of certain binary or pseudo-binary systems, and which also serves well as an introduction to a more generalized view of free energy-concentration diagrams and the energetic relationships of intermediate phases to their constituent elements. The outline shown in Figure 14 shows the principal relationships for the appearance of a foreign lattice type, β , in a system of two components A and B whose lattice types are designated with α and γ , respectively. The conditions are analogous

to those for the appearance of eutectic melt⁽²⁾ if we replace L (liquid) for β . The conditions for the non-variant ($p = \text{const}$) equilibrium, designating the stability limit of β , can easily be derived from the condition that the

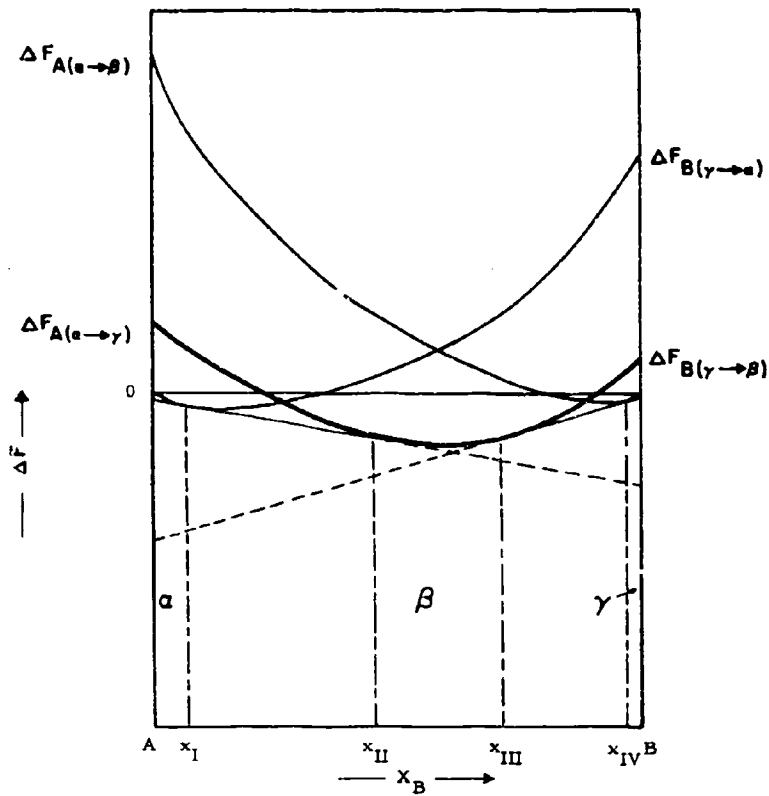


Figure 14. Principal Relationships for the Stabilization of a Foreign Lattice Type β in a Binary or Pseudo-Binary System.

Solidus Lines: Free Energy Variations Within the Homogeneous Ranges.

XI, XII and XIII, XIV: Phase Boundaries of the Solutions α , β , and γ .

chemical potentials of the components A and B must be equal in all three phases, i.e.,

$$\bar{F}_{A(\alpha)} = \bar{F}_{A(\beta)} = \bar{F}_{A(\gamma)}$$

$$\bar{F}_{B(\alpha)} = \bar{F}_{B(\beta)} = \bar{F}_{B(\gamma)}$$

The following four equations are of the type

$$\phi_i(x_\alpha, x_\beta, x_\gamma, T) \quad (i=1\dots4)$$

containing as constants the free enthalpies of transformation $\Delta F_{A(\alpha-\beta)}$, $\Delta F_{A(\alpha-\gamma)}$, $\Delta F_{B(\gamma-\alpha)}$, and $\Delta F_{B(\gamma-\beta)}$. From these equations T_0 , the temperature of the reaction isotherm, as well as the equilibrium concentrations of the three coexisting phases, can be evaluated. At temperatures above or below the reaction isotherm, the two-phase equilibria $\alpha + \beta$, $\beta + \gamma$, and $\alpha + \gamma$, are evaluated separately in the previously described manner.

Reviewing our findings and discussions in the previous sections, we note that in a number of instances hypothetical, that is, to say, in the boundary systems unstable phases enter the calculations as quantities necessary for the interpretation of the phase relationships in the combined systems. A somewhat closer examination of the conditions reveals that as a minimum requirement for the calculations, the stabilities of all binary lattice types combined have to be known.

Thus, if for example the stable lattice types of the combined binary system A-C and B-C are differentiated by $\alpha, \beta, \gamma, \delta$, and ϵ , of which, say, α, γ , and ϵ occur in A-C, and α, β , and δ in B-C, it is required that for the system A-C the thermodynamic stability of the hypothetical phases β and δ be known. Similarly, the stability of the phases γ and ϵ in the edge system

B-C have to be defined in order to be able to carry out principal predictions regarding the phase relationships likely to be found in ternary system A-B-C. These calculations, however, would still involve certain limitations, for they interpret the ternary phase-relationships only in terms of the five pre-given lattice types α , β , γ , δ , and ϵ . For greater assurance of the calculated data, the (concentration-dependent) stability of all lattice types, which conceivably may become stabilized and hence may play a role in the higher order systems, must be computed and compared with the stability of the other phase solutions. This requirement ultimately leads to the necessity of establishing more generalized, but especially more complete, free energy concentration diagrams (Figure 15), which, upon extending the relationships to include the component phases, would allow us to separate base- and concentration-dependent terms for each lattice type considered.

It is obvious, that it is principally impossible to determine thermodynamic quantities for hypothetical phases by calorimetric means; from the conventional ΔF -x diagram, therefore, only lower limits for the stability of hypothetical phases can be derived. On the other hand, by reversing the procedure, i. e., by evaluating experimentally established phase relationships (which are not necessarily restricted to solid-solid equilibria, but also may include solid-gas or solid-liquid phase equilibrium studies) with regard to the stabilities of the phases participating at the equilibria, we are able to extract stability data for hypothetical phases⁽¹⁾. Thus, by investigating a sufficiently large number of suitable sets of component combinations, we have, at least in principle, the means available to ultimately provide a reasonably complete mapping of the thermodynamic characteristics of all crystal types which are of relevance for the particular group of systems.

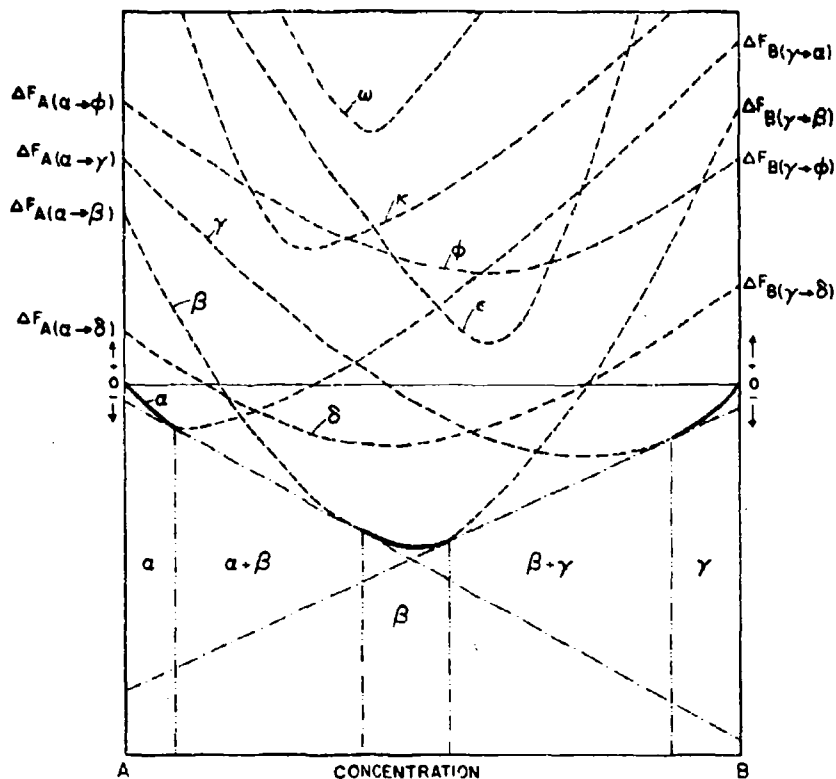


Figure 15. Generalized Free Energy of Formation - Composition Diagram for a Binary System at a Given Temperature and Pressure.

α, β, γ Stable Phases

$\delta, \epsilon, \phi, \kappa, \omega$ Unstable Phases

$\Delta F_{A(\alpha \rightarrow j)}$ Free Energy of Transformation of the Stable Lattice (α) of A into a lattice type j .

($j = \alpha, \beta, \gamma \dots w$) [$\Delta F_{A(\alpha \rightarrow \alpha)} = 0$]

$\Delta F_{B(\alpha \rightarrow j)}$ Free Energy of Transformation of the Stable Lattice (γ) of B into a Lattice Type j .

($j = \alpha, \beta, \gamma \dots w$) [$\Delta F_{B(\beta \rightarrow \beta)} = 0$]

D. COMPUTER APPROACHES

In the foregoing thermodynamic approaches for the calculation of phase equilibria, we had to preassume certain properties in order to sufficiently simplify the arithmetic to allow the equations to be solved manually. We had further restricted our discussion to cases, where two related elements A and B show a similar behavior towards the third component C.

A relative disadvantage of the simplified method lies in the fact that it does not allow a prediction of the course of the boundaries of the one-phase ranges. While this shortcoming may be negligible for systems involving quasi-line compounds, in combinations involving phases with wide, but especially markedly different homogeneous ranges in the binaries, the free energy variations due to changes in the overall stoichiometry of the phases (contents in C dependent on the A-B exchange) have to be taken into consideration in order to obtain results which more closely describe the actual behavior.

Geometrically, the general solution of the conditional equations for a two-phase equilibrium in a ternary system represents the manifold of the tangent points of all double tangent planes to the free energy surfaces in the concentration-temperature space. The solutions are, therefore, of the form

$$\phi_1(x', y', z', T) = 0$$

$$\phi_2(x'', y'', z'', T) = 0$$

The boundaries of the one-phase regions at a given temperature ($p = \text{const}$) are the intersecting curves between the surface given by the solutions

$\phi(x_1, y_1, z_1, T_0)$, and the planes resulting from the concentration relationship $x_1 + y_1 + z_1 = 1$.

For a three-phase equilibrium, the general solutions represent the tangent points of all triple tangent planes to the free energy surfaces of the three phases. The multiplicity of solutions is ∞^1 . Hence, the solutions for the equilibrium concentrations of each individual phase is of the form ($p = \text{const}$)

$$\phi_1(x_1, y_1, z_1, T) = 0$$

$$\phi_2(x_1, y_1, z_1, T) = 0$$

$$(x_1 + y_1 + z_1 = 1)$$

With $T = \text{const}$ (temperature section), the concentrations are fixed and correspond to definite triples (x_1, y_1, z_1) .

For the numerical evaluation of the unrestricted problem, the general conditional equations derived from the minimum conditions and the existing constraints after the method by Lagrange are only of limited use; the arithmetic in obtaining the equations in a form suitable for programming is quite involved and circuitous, and convergence problems are difficult to eliminate. Similar difficulties are encountered when making use of the well-known thermodynamic relationship that for the equilibrium state, the thermodynamic potentials of each component must be the same in all coexisting phases. The most direct approach for a numerical evaluation of the unrestricted problem with the aid of a computer, consists in using the original minimum requirement for the free energy, together with the existing boundary conditions.

The mathematical problem can be stated as follows: Given in a function, ϕ , which is composed of a linear combination of a series of functions ϕ_i

$$\phi = \sum_1^4 v_i \phi_i \quad (1 \leq i \leq 4)$$

The ϕ_i themselves, are functions of concentration variables x_i , y_i , z_i , as well as p and T ; the following additional constraints exist:

$$\sum v_i = 1$$

$$\sum v_i x_i = X$$

$$\sum v_i y_i = Y$$

$$\sum v_i z_i = Z$$

We easily identify ϕ as the total free energy of the heterogeneous mixture of the i phases, ϕ_i as the integral free energy of the phases i , v_i as the mass fractions, x_i , y_i , z_i as the mole fractions of the components in the phases i , p and T as pressure and temperature, and X , Y , Z as the gross composition of the phase mixture.

We are interested in cases where $p = \text{const. (1 atm)}$ and T assumes a series of discrete, but otherwise constant, values for a particular set of computations (temperature sections). According to the phase rule, and disregarding the occurrence of four-phase reaction isotherms at specific temperatures, the values of i are restricted to $1 \leq i \leq 3$, i.e., the number of co-existing phases are restricted to a maximum number of three. Thus, the problem reduces to a determination of the of the coordinates x_i^* , y_i^* , z_i^* for

for the maximum of ϕ for a series of prechosen values X, Y, Z; ϕ_1 and ϕ_2 being pregiven functions.

Actual calculations are performed in a manner that the approximate phase relationships in the system are first computed using the simplified technique previously described. This helps to limit the pregiven scanning range, x_1, y_1, z_1 , for a given set of gross-compositions (XYZ) in the calculations. After choosing a series of gross-concentration points (XYZ) from a two-phase range, the total free energy is computed for a series of combinations x_1, y_1, z_1 , and x_2, y_2, z_2 , with the density of the concentration points within the pre-determined concentration area selected to be in accord with the desired accuracy (grit spacing usually .5 atomic percent). The stable combinations ($x_1^* y_1^* z_1^*$) and ($x_2^* y_2^* z_2^*$) are those for which ϕ assumes the lowest value.

After the tie line distribution in all possible two-phase ranges has been computed, the three-phase equilibria are considered as the next step. This calculation is simplified by the fact that the compositions of two vertices from the ω^1 manifold of "compatible" three-phase combinations are already known from the calculations of the corresponding two-phase equilibria, i.e., the computer scan is limited to obtain the "compatible" composition of the third vertex. The final step in the evaluation, which sorts out the correct set of composition triple from the ω^1 manifold of solutions, consists of comparing the free energies of a series of three-phase mixtures with corresponding one- or two-phase mixtures, the stable combination being that one having the lower value. This calculation is simplified by the fact that the composition of two vertices are already known from the corresponding two-phase equilibrium, i.e., the computer scan is limited only to one phase, from which the composition of the third vertex is then obtained.

A few more words have to be said about the nature of the functions ϕ_i , the integral free energies of the homogeneous ranges in the ternary ranges.

The nature and type of function to be chosen will depend on the type of solid solution formed in the system, and hence are structure-dependent.

The free energy of mixing of substitutional types of solid solutions, where all three elements have to be regarded as equivalent can, for most purposes, be adequately approximated by the vanLaar expression,

$$\bar{F}^{\text{mix}} = \sum_{ij} \epsilon_{ij} x_i x_j + RT \sum_i x_i \ln x_i$$

where the ϵ_{ij} are the corresponding interaction parameters of the pairs $i - j$ and the x_i denote the concentrations of the components i .

For the thermodynamic description of the phases, vacancies are counted — depending on the type of lattice site involved — as equivalent to either substitutional or interstitial elements.

Ternary interstitial types of solid solutions generally can be classified into two groups. These, with a common interstitial element C,

which typically would involve systems of two metals with an interstitial element, and, on the other hand, solutions, where the two interstitial elements are distributed within the host lattice of a carrier element A. Typical cases would be systems consisting of one refractory transition metal with two interstitial elements such as Ti-C-N, Zr-C-N, Zr-O-N, etc.

A characteristic of all latter types of compounds is the fact that practically no atom exchanges between carrier and interstitial sublattice have to be taken into consideration. Thus, for example, a solution of two metal monocarbides $(A,B)C_v$ at a certain carbon defect ($v < 1$) can adequately be defined as a binary solution of (A_{x_A}, B_{x_B}) , having free energies of F_{AC_v} and F_{BC_v} at the corresponding boundary compositions. Thus

$$\phi_i = x_A \cdot F_{AC_v} + x_B \cdot F_{BC_v} + G^{\text{mix}}(x_A, x_B)$$

$$(x_A + x_B = 1)$$

To obtain the values per gram atom, the above expression would have to be divided by $1 + v$. The functions F_{AC_v} and F_{BC_v} describe the free energy variation of the phases AC_v and BC_v across their homogeneous fields in the respective binaries and are structure-dependent relations. These functions can be obtained either from experimental data, or by fitting certain pieces of experimental information such as phase boundaries, known free energy at a given composition, heat capacity data for the calculation of the temperature dependence, etc. to established thermodynamic models. Using the Schottky-Wagner theory of non-stoichiometric alloy phases⁽⁴⁾, related calculations on refractory interstitial types of compounds have especially been

performed in recent years by L. Kaufmann and co-workers⁽⁵⁾, achieving remarkable agreement between calculated and observed properties. For phases where the disordering parameters are beyond the permissible range of the simplified Schottky-Wagner theory, the thermodynamic behavior of specific crystal phases can be approximated by other suitable approaches⁽⁶⁻⁹⁾.

In conclusion to this section, it may only be mentioned, that computer calculations, using the methods described above, have been performed with considerable success on model systems and are presently being applied to the thermodynamic description of the high temperature phase relationships in ternary metal-carbon systems. A detailed review of the results, however, is beyond the scope of this report and reference may be made to the series of related reports, issued under a current Air Force program⁽¹⁰⁾.

IV. APPLICATION TO TERNARY METAL CARBON SYSTEMS

We shall demonstrate the thermodynamic approaches exclusively on ternary metal-carbon systems since the extensive experimental material available for this system class allows a close comparison between theory and experiment. We shall treat in fairly great detail the phase diagram tantalum-tungsten-carbon. The phase relationships in this system are fairly complicated, and therefore this ternary well serves to demonstrate the applicability of the thermodynamic approach.

In the sections following the discussion of the Ta-W-C system, we shall summarize the thermodynamic findings in other selected metal-carbon systems and also demonstrate the back-calculation of thermodynamic quantities from experimental phase equilibrium data. A short review of the general features

of the phase-relationships of transition metal-silicon-boron-carbon systems will conclude our excursion into the field of ternary alloys.

In the final chapter then, we shall try to relate phase diagram and thermodynamic information to practical application problems, and especially stress alloy compatibility considerations, and the significance of partition equilibria for diffusion phenomena in multi-component alloys.

A. THE TANTALUM-TUNGSTEN-CARBON SYSTEM⁽¹¹⁻¹²⁾

In the binary system tantalum-carbon (Figure 16), two intermediate phases, a subcarbide Ta_2C with hexagonal close-packed arrangement

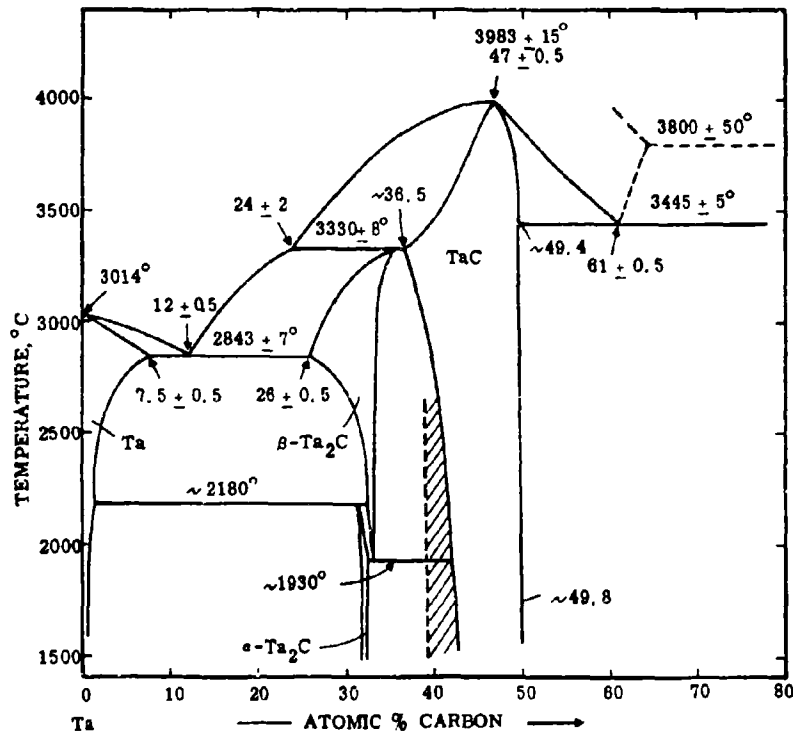


Figure 16. Tantalum-Carbon Phase Diagram.

(Shaded Area: Preferential Precipitation of Metastable ζ)

of metal atoms, and a face-centered cubic monocarbide with an extended range of carbon defect solid-solutions, are formed. Like the other subcarbides of the refractory transition metals, the carbon sublattice in Ta_2C undergoes an order-disorder type of transformation at elevated temperature. The metal host lattice is not affected by this transition.

In the tungsten-carbon system (Figure 17), the arrangement of the metal atoms in the subcarbide is the same as for Ta_2C , although the higher disordering temperature suggests differences in the degree of order in which the N carbon atoms are distributed among the $2N$ lattice sites available in the structure.

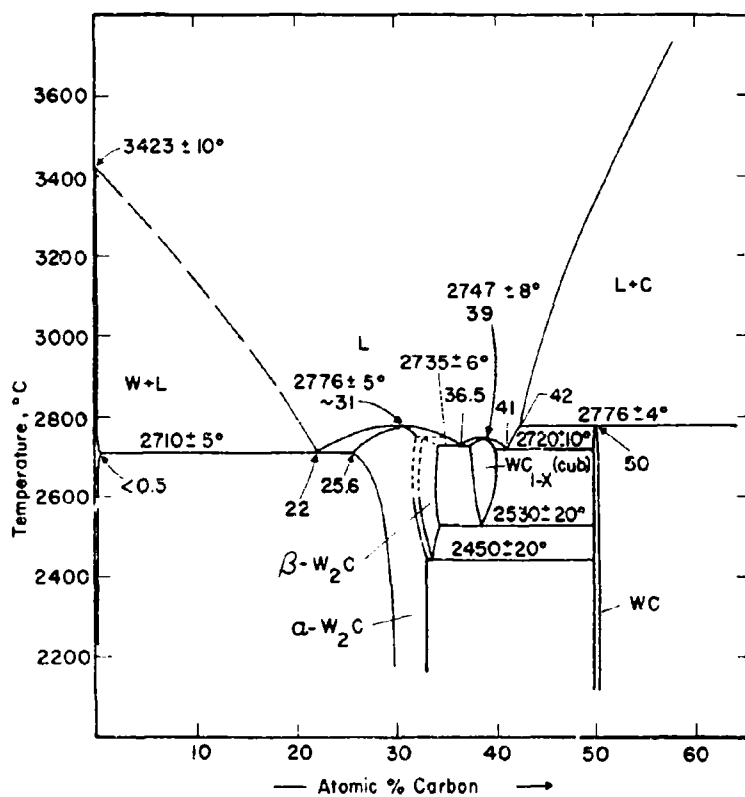


Figure 17. Tungsten-Carbon Phase Diagram.

A cubic phase, analogous to TaC, occurs as a high temperature phase at considerable substoichiometric compositions. In addition to W_2C and WC_{1-x} (B1), a monocarbide with a simple hexagonal structure and ordered distribution of carbon atoms is formed in the equiatomic concentration region.

The body-centered cubic metals form a continuous series of solid solutions (13, 14, 15).

The phase relationships in the ternary alloys system are shown in consolidated form in the ternary constitution diagram shown in Figure 18, while the interrelation of binary and ternary isothermal reactions are presented in the familiar Scheil-Schultz reaction diagram (Figure 19). For our purposes, however, it is much easier to work with the temperature sections (Figure 20a through 20n).

In examining the phase relationships, we note that the tungsten-exchange in the cubic monocarbide gradually increases with increasing temperatures, until at 2530°C, the temperature at which the cubic tungsten carbide becomes stable in the binary, a complete solid solution is formed (Figure 20h). An interesting behavior is exhibited in the metal-rich region. At lower temperatures (<2450°C), the expected solid solution between Ta_2C and W_2C is interrupted by a two-phase equilibrium B1+metal, i. e., the solid solutions of Ta_2C and W_2C are both terminated by a three-phase equilibrium in the ternary phase field. Towards higher temperatures, the ternary homogeneous ranges of the subcarbides increase and the two-phase range monocarbide + metal solution, gradually becomes narrower. Finally, at 2450°C, both three-phase equilibria merge into a single (critical) tie line. Above this temperature, the concentration space is divided into two regions where either metal + subcarbide, or subcarbide + monocarbide are in coexistence. The latter equilibria persist up to the liquidus range.

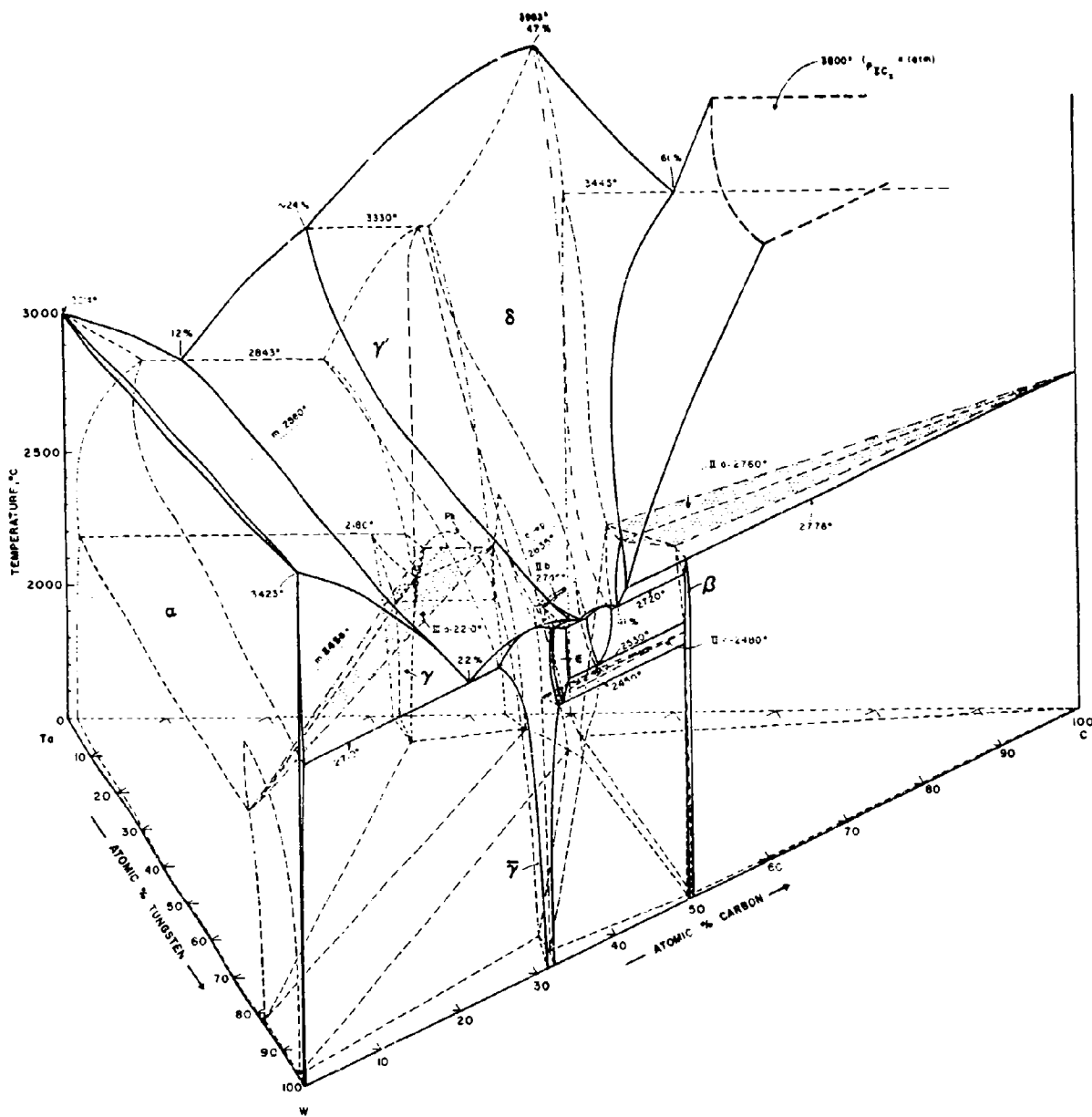


Figure 18. Constitution Diagram Tantalum-Tungsten-Carbon.

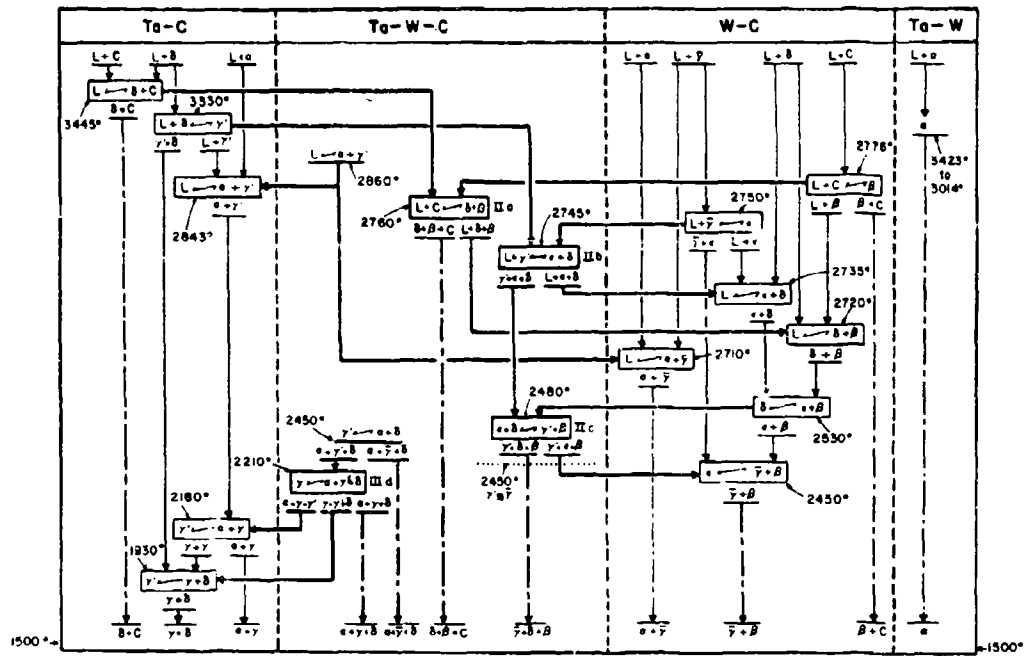


Figure 19. Scheil-Schulz Reaction Diagram for the System Tantalum-Tungsten-Carbon.

Legend of Symbols:

- a ... Body-Centered Cubic Metal Phase
- β ... Hexagonal WC Phase
- γ ... α -Ta₂C
- $\gamma', \bar{\gamma}$... β -Ta₂C and α -W₂C Solid Solutions
($\gamma \equiv \bar{\gamma}$ for $T > 2450^\circ\text{C}$)
- δ ... Face-Centered Cubic (B1) Monocarbide Phase
- ϵ ... β -W₂C Phase
- C ... Graphite

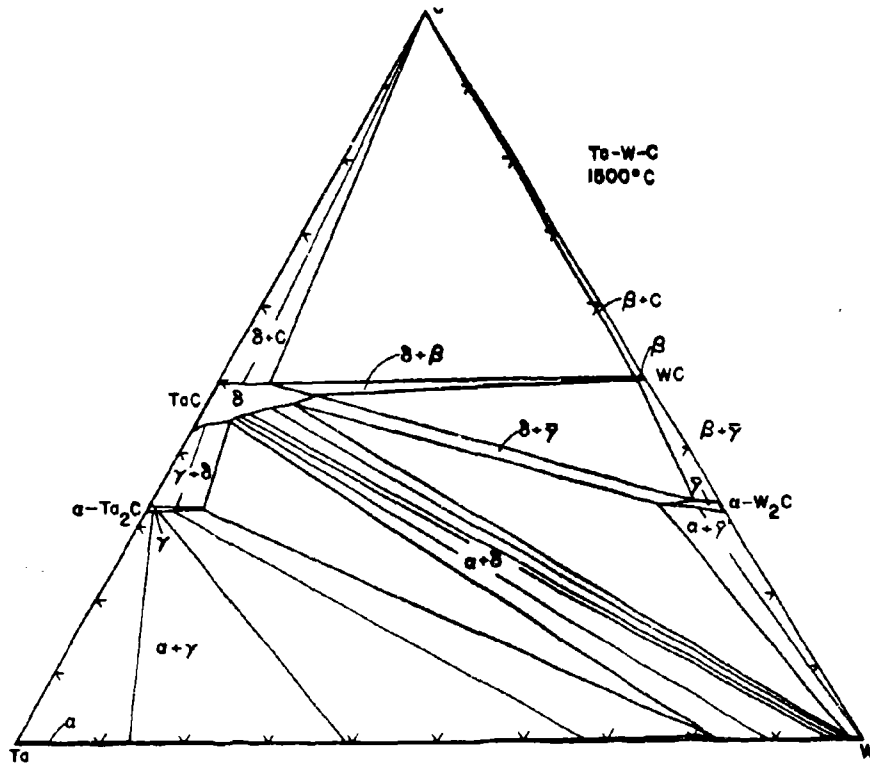


Fig. 20a

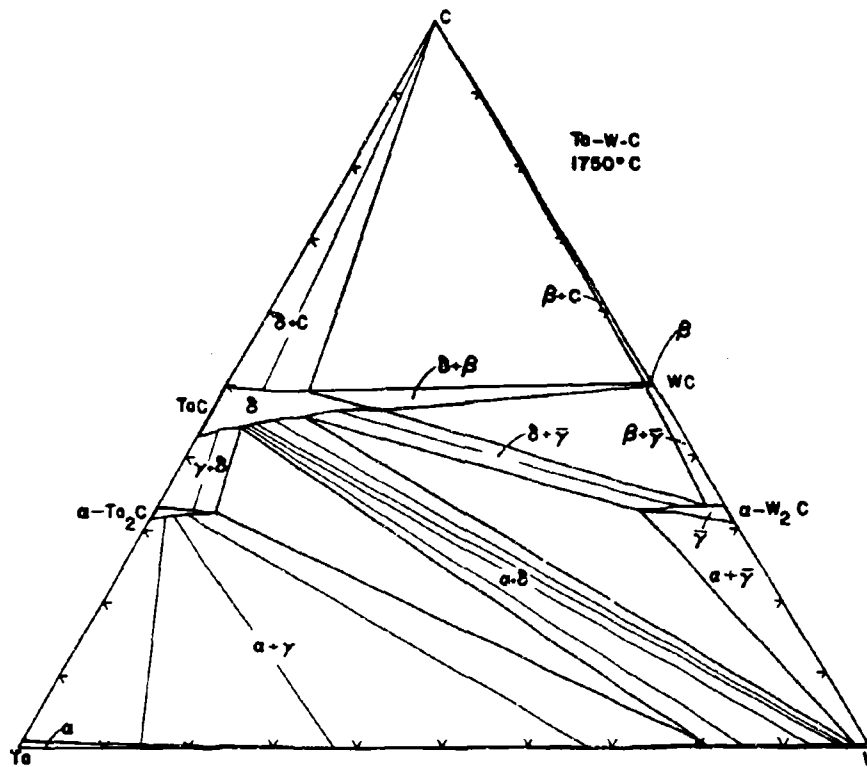


Fig. 20b

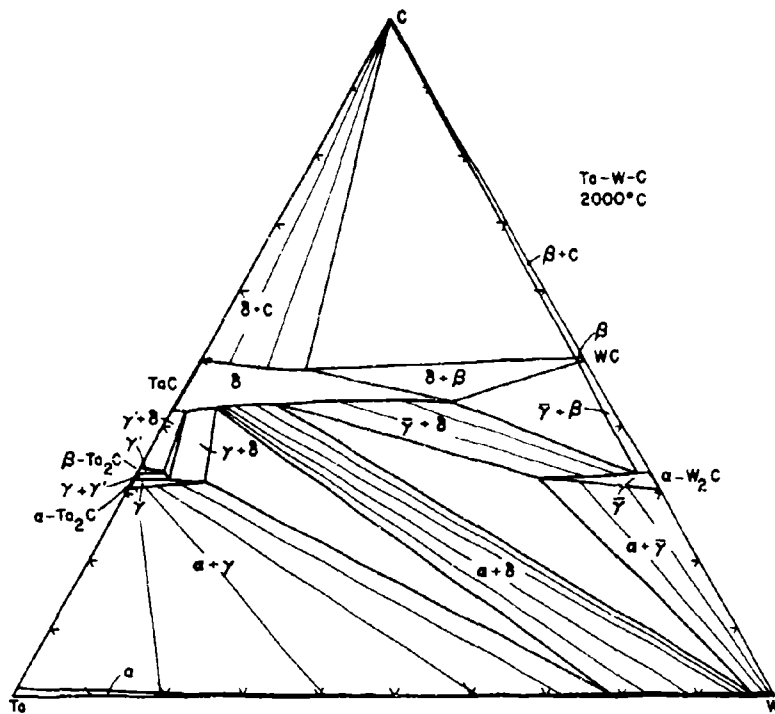


Fig. 20c

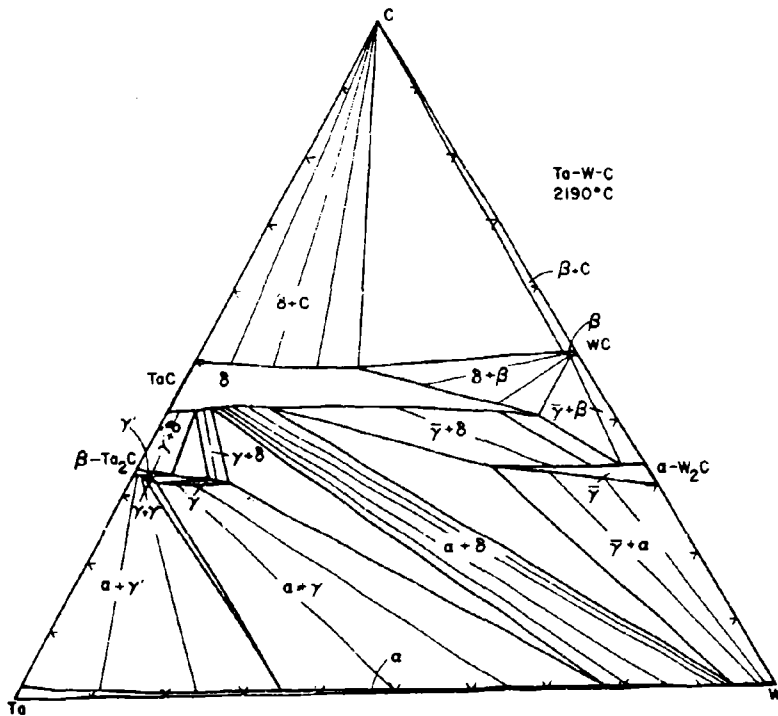


Fig. 20d

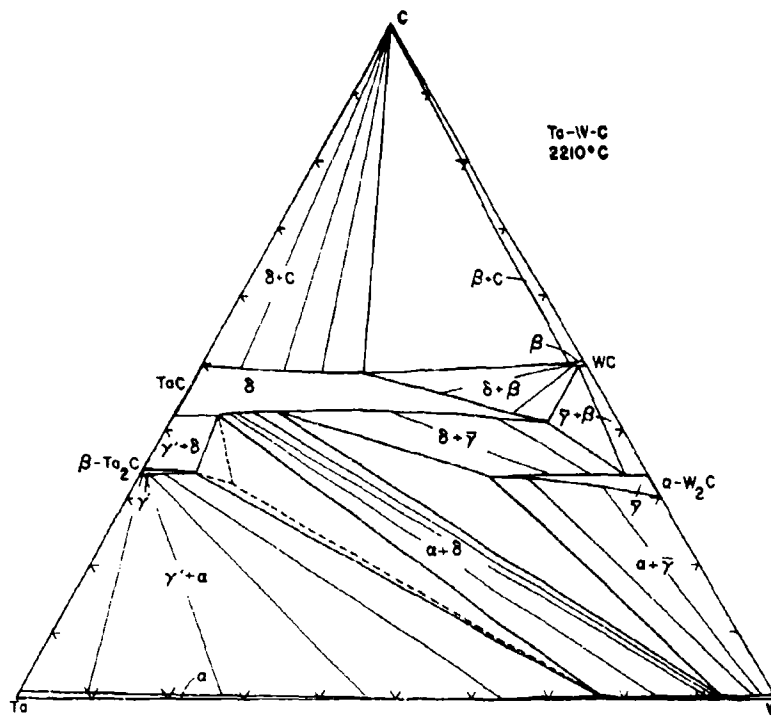


Fig. 20e

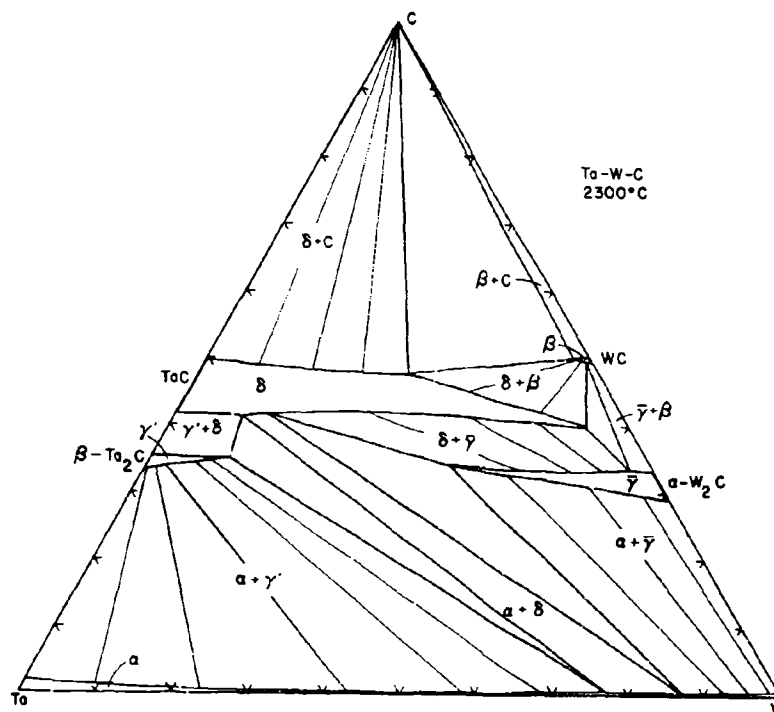


Fig. 20f

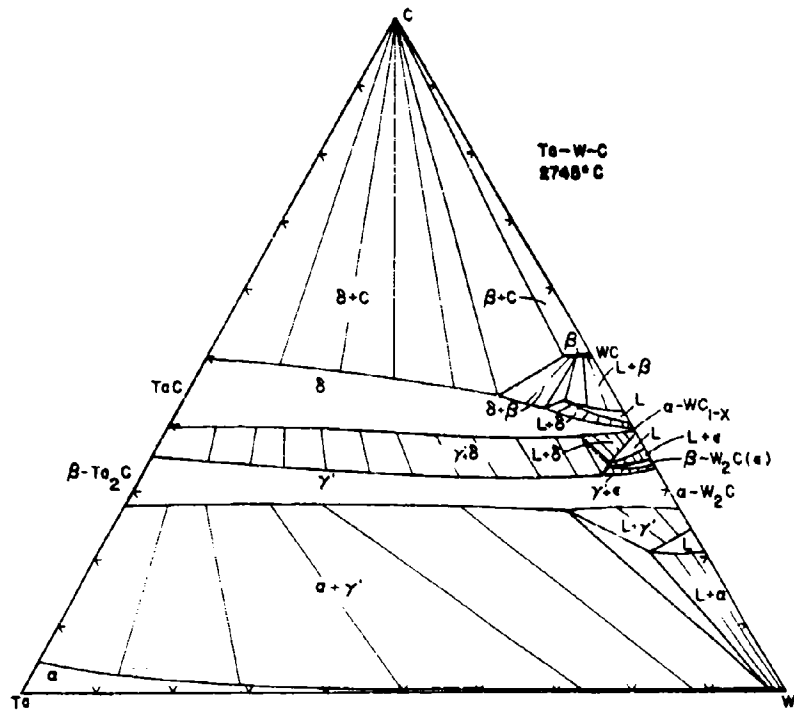


Fig. 20i

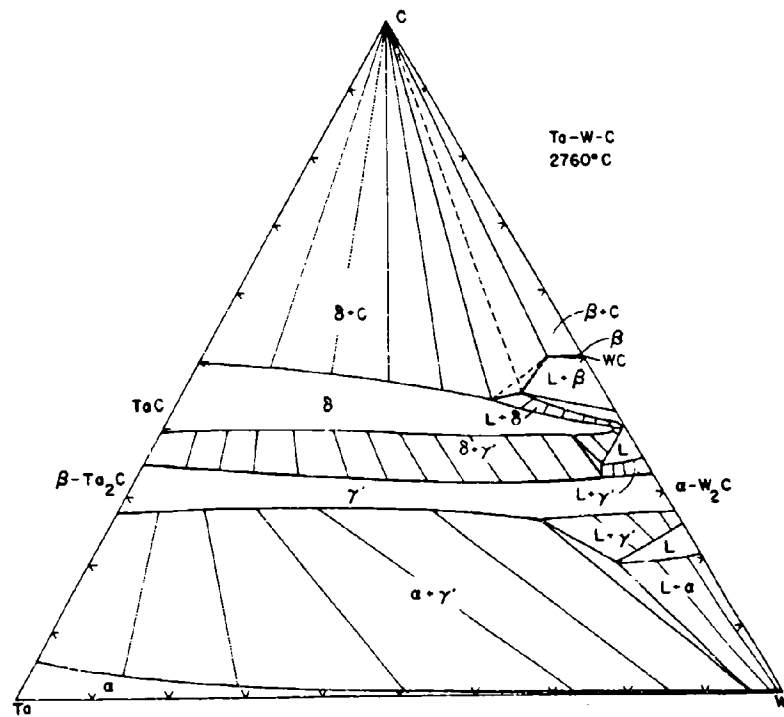


Fig. 20j

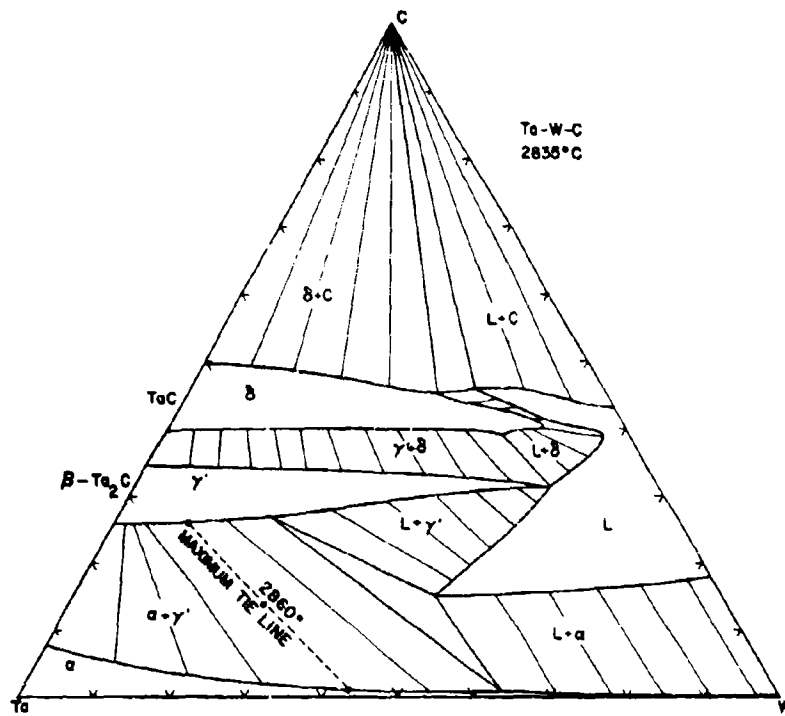


Fig. 20k

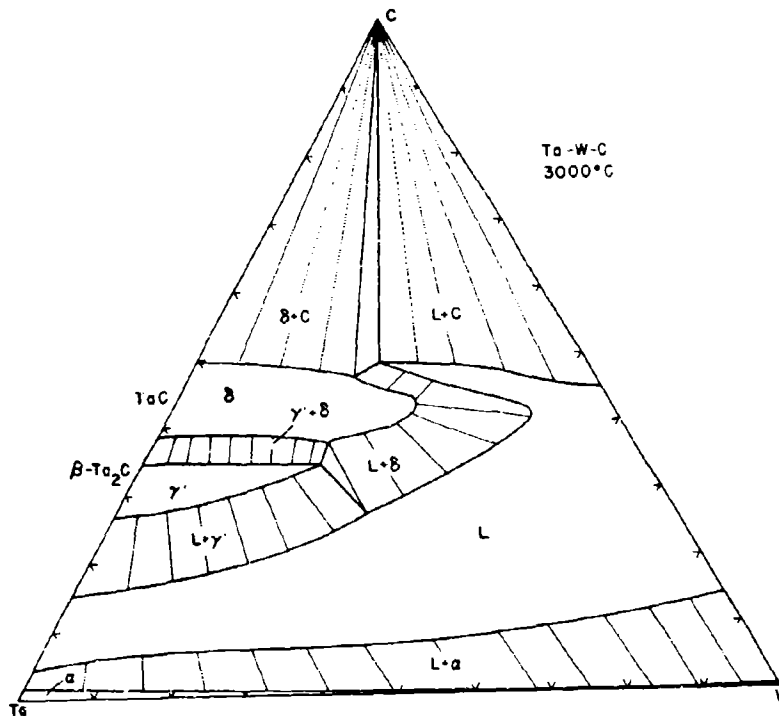


Fig. 20l

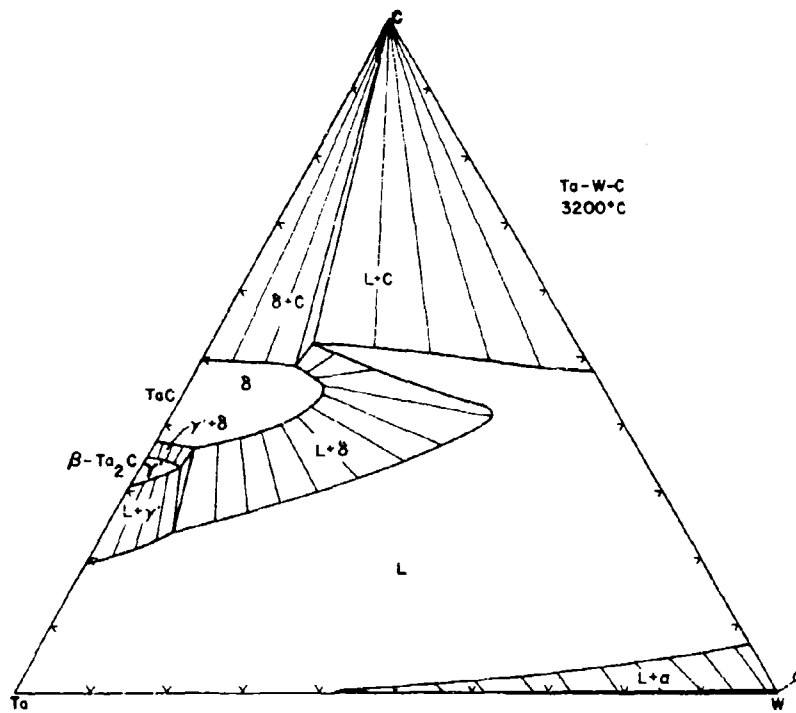


Fig.20m

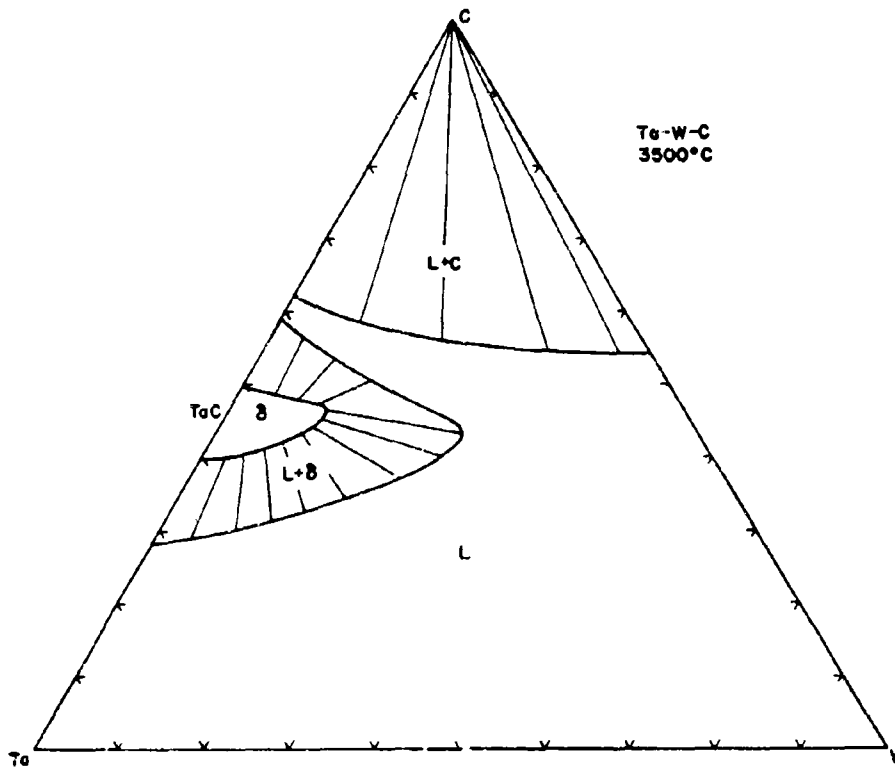


Fig. 20n

Figures 20a through 20n.

Experimental Temperature Section for the Ta-W-C System.

For the thermodynamic evaluation of the phase equilibria, the following assumptions and compromises are made:

1. The ternary homogeneity ranges originate at the binary phases and are drawn as straight lines across the ternary field.
2. Since no calorimetric data are available, the solution of the subcarbides is considered as ideal in the calculations.
3. The metal solution behaves ideally.
4. The carbon-rich boundary of the B1-phase can be described as a regular solution, having an interaction parameter of $\epsilon = + 6500$ cal/gr. -At. metal. The metal-rich boundary is described as ideal solution. These data were derived from the temperature dependence of the B1-ranges in partial systems MeC-WC⁽¹¹⁾.

The following thermodynamic data, which are based on values compiled from the literature as well as on available phase diagram information^(11,12,16,17,18), will be used in the calculations (Table 1). We further write down the free enthalpy differences, which will be useful for the calculations (Table 2 and Table 3).

The free energy gradient — concentration curves for the solid solutions formed between the various phases are

a. Metal solution

$$\left[\frac{\partial \Delta F_f(T_a, W)}{\partial x_W} \right]_{T, p} = RT \ln \frac{x_W}{1-x_W}$$

Table 1. Thermodynamic Data Used in the Calculation of the Phase Equilibria in the Ta-W-C System (Values in cal/gr. At. Metal)

Reaction	Free Enthalpy Change
$W + C \rightarrow WC$ (hex.)	$\Delta F_{fWC} = -8905 + 0.47 \cdot T$
$W + 1/2 C \rightarrow WC_{1/2}$	$\Delta F_{fWC_{1/2}} = -3,150 - 0.62 \cdot T$
$W + C \rightarrow WC$ (B1)	$\Delta F_{fWC_{1.0}} = -3745 - 0.95 \cdot T$
$W + 0.71 \cdot C \rightarrow WC_{0.71}$ (B1)	$\Delta F_{fWC_{0.71}} = -730 - 1.88 \cdot T$
$W + 0.61 \cdot C \rightarrow WC_{0.61}$ (B1)	$\Delta F_{fWC_{0.61}} = +340 - 2.08 \cdot T$
$Ta + C \rightarrow TaC$	$\Delta F_{fTaC_{1.0}} = -35,300 - 1.80T \log T + 6.48 \cdot T$
$Ta + 0.71C \rightarrow TaC_{0.71}$ (B1)	$\Delta F_{fTaC_{0.71}} = -26,200 - 1.20 \cdot T$
$Ta + 0.50C \rightarrow TaC_{1/2}$	$\Delta F_{fTaC_{1/2}} = -19,680 - 1.19 \cdot T$

Table 2. Differences in the Free Enthalpies of Formation of Tantalum and Tungsten Carbides.

(Values in cal/gr.-At. Metal)

$$\begin{aligned}
 & \left. \begin{aligned}
 \Delta F_{fTaC_{0.37}} - \Delta F_{fWC_{0.37}} \text{ (hex)} &= -11,080 \\
 \Delta F_{fTaC_{0.43}} - \Delta F_{fWC_{0.43}} \text{ (hex)} &= -14,100
 \end{aligned} \right\} \approx \text{const.} \\
 & \Delta F_{fTaC_{0.50}} - \Delta F_{fWC_{0.50}} \text{ (hex)} = -16,530 - 0.57 \cdot T \\
 & \Delta F_{fWC_{0.71}} - \Delta F_{fTaC_{0.71}} \text{ (B1)} = 25,500 - 0.68T \\
 & \Delta F_{fWC} - \Delta F_{fTaC} \text{ (B1)} = 30,700 - 0.95 \cdot T \\
 & \Delta F_{fWC} - \Delta F_{fTaC} \text{ (WC-type)} = -14,000 + 0.47 \cdot T
 \end{aligned}$$

Table 3. Disproportionation and Transformation Energies for Tantalum and Tungsten Carbides.

(Values in cal/gr. -At. Metal)

Reaction	Free Enthalpy Change
$WC^{(hex)} \rightarrow WC_{1-x}(B1) + xC \ (x \approx 0)$	$\Delta F_{ZWC} = 5160 - 1.42 \cdot T$
$WC_{1-x}(B1) \rightarrow (1-2x)WC^{(hex)} + 2xWC_{1/2}$	$\Delta F_{ZWC_{1-x}}^{(cub)} = -4790 + 1.71 \cdot T$ ($0.08 < x \leq 0.35$)
$WC_{1/2} \rightarrow 0.70 WC_{0.71}(B1) + 0.30 W$	$\Delta F_{ZWC_{1/2}} = 2635 - 0.71 \cdot T$
$TaC_{1/2} \rightarrow 0.70 TaC_{0.71} + 0.30 Ta$	$\Delta F_{ZTaC_{1/2}} = 1420 + 0.40 \cdot T$
$TaC(B1) \rightarrow TaC(WC\text{-type})$	$\Delta F_R = > 12,000 \text{ cal.}$

- b. Subcarbide Solid Solution (calculated for $y = 0.37, 0.43, \text{ and } 0.50$).

$$\left[\frac{\partial \Delta F_{f(Ta, W)C_y}}{\partial x^I W} \right]_{T, p} = \Delta F_{fWC_y} - \Delta F_{fTaC_y} + RT \ln \frac{x^I W}{1-x^I W}$$

- c. Monocarbide (B1) Solid Solution (Calculated for $(1-x) = 0.71$)

$$\left[\frac{\partial \Delta F_{f(Ta, W)C_{1-x}}}{\partial x^{II} W} \right]_{T, p} = \Delta F_{fWC_{1-x}} - \Delta F_{fTaC_{1-x}} + RT \ln \frac{x^{II} W}{1-x^{II} W}$$

These gradients are plotted as a function of the tungsten-exchange in Figures 21a through 21d.

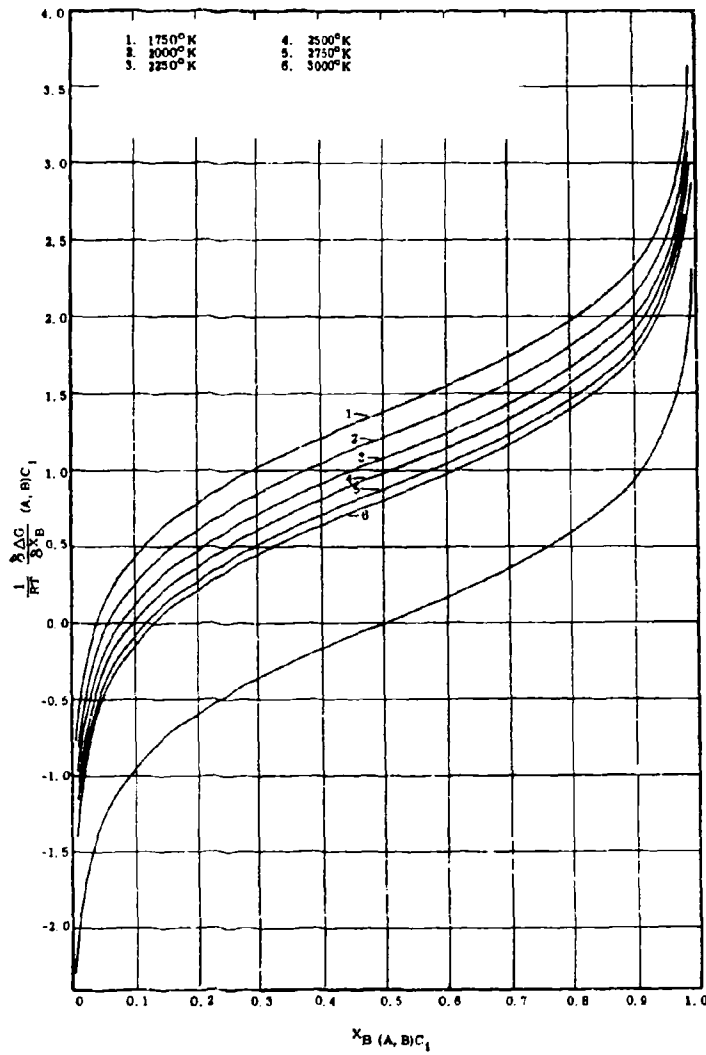


Figure 21a. Subcarbide Solid Solution at $(Ta, W)C_{0.37}$

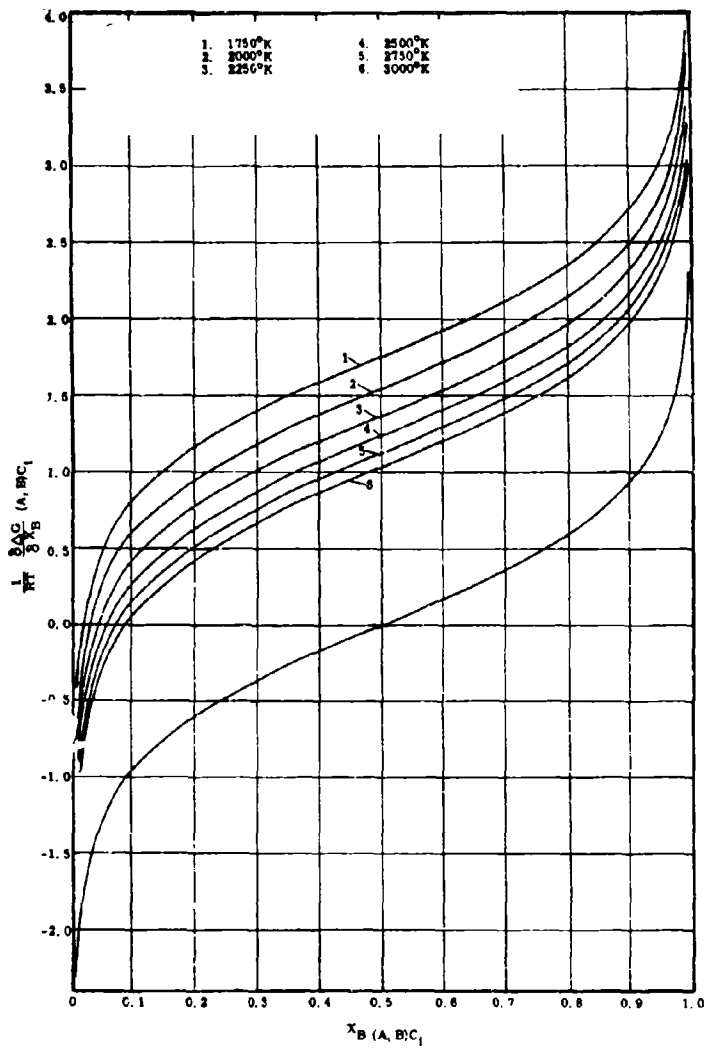


Figure 21b. Subcarbide Solid Solution at $(Ta, W)C_{0.43}$.

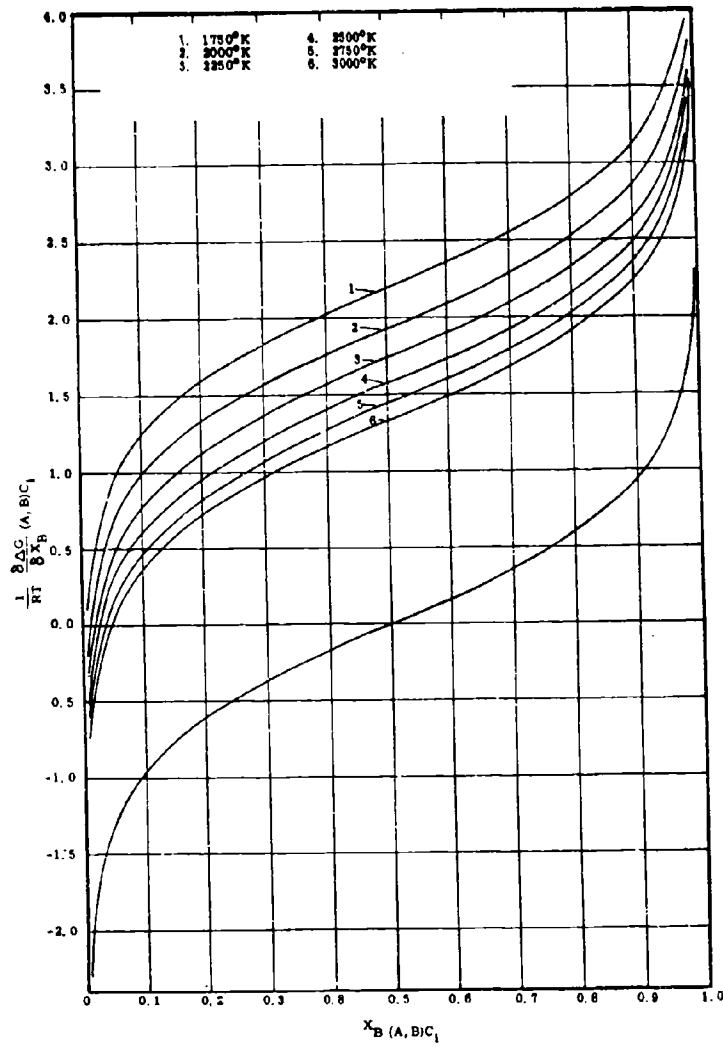


Figure 21c. Subcarbide Solid Solution at $(\text{Ta, W})\text{C}_{0.50}$.

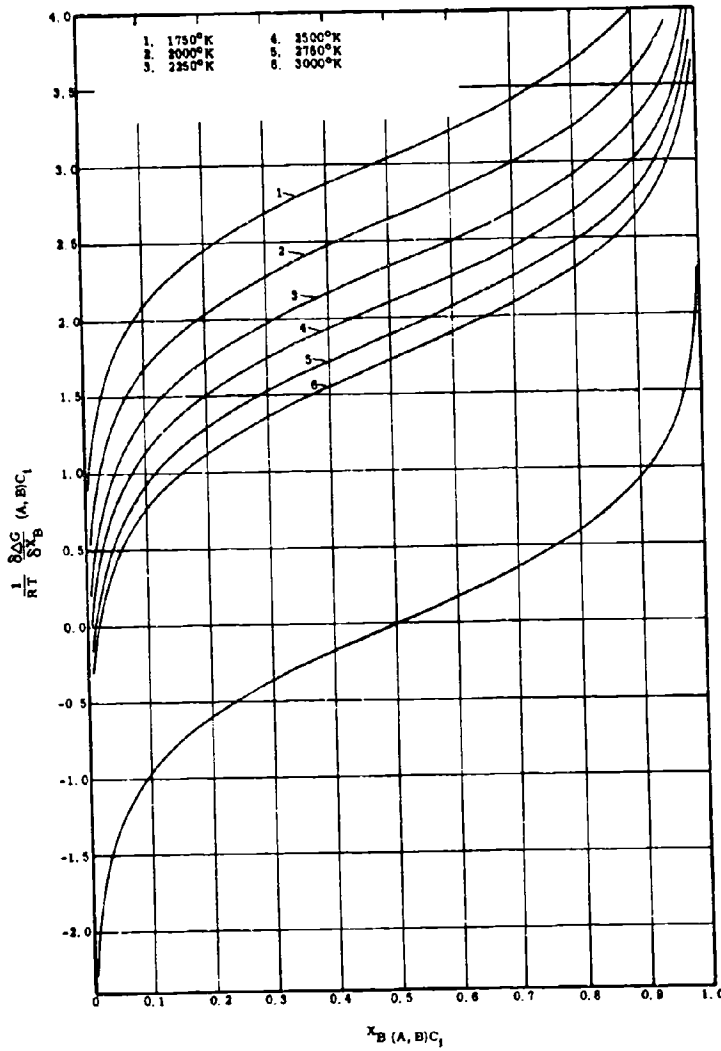


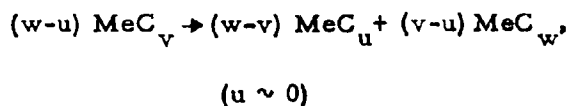
Figure 21d. Cubic Monocarbide Solid Solution at $(Ta, W)C_{0.71}$.

Figures 21a through 21d. Free Enthalpy of Formation-Concentration Gradients for Tantalum-Tungsten Carbide Solutions.

Lower Single Curves: Gradients for (Ta, W) .

1. Equilibria in the Metal-Rich Portion of the System

In view of the anomalous behavior of the subcarbide solid solution, our initial interest concentrates on the evaluation of the stability of the $(Ta, W)_2C$ solid solution and mechanical mixtures of metal plus monocarbide solid solution. Stability conditions (8a), rewritten for the disproportionation of the subcarbide (MeC_v) into monocarbide (MeC_w) and metal (MeC_u) solid solution according to



becomes ($\epsilon_{MeC_w} = 6500$)

$$-\Delta F_{ZTaC_v} = \frac{v}{w} (1-x''_{Ta})^2 + RT \ln \frac{x''_{Ta} \cdot x_{Ta}^{\frac{w-v}{w}}}{x'_{Ta}}$$

and

$$-\Delta F_{ZW C_v} = \frac{v}{w} (1-x''_W)^2 + RT \ln \frac{x''_W \cdot x_W^{\frac{w-v}{w}}}{x'_W}$$

x, x', x'' Mole fraction exchange of A or B in the metal, subcarbide, and monocarbide solid solution.

Although, A and B, strictly speaking, are not constants, their variation is not critical, and we assume for the average stoichiometries of the subcarbide and the monocarbide solid solution

$$v = 0.43 \quad (\sim 30 \text{ At. \% C})$$

and

$$w = 0.71 \quad (\sim 41.5 \text{ At. \% C})$$

With these values, we obtain for the stability condition

$$-\Delta F_{ZTaC_{0.43}} = 0.606 \cdot \epsilon (1-x''_{Ta})^2 + RT \ln \frac{x''_{Ta}{}^{0.606} \cdot x_{Ta}{}^{0.394}}{x'_{Ta}} = R(x'_{Ta})$$

and

$$-\Delta F_{ZWC_{0.43}} = 0.606 \cdot \epsilon (1-x''_W)^2 + RT \ln \frac{x''_W{}^{0.606} \cdot x_W{}^{0.394}}{x'_W} = R'(x'_W)$$

Compatible triples of x_{Ta} , x'_{Ta} , and x''_{Ta} are obtained from the free energy gradient curves in Figures 21b and 21d and are used to calculate the function $R(x'_{Ta})$ (Figure 22). Composition x''_{Ta} is determined by the condition that at equilibrium, $R(x'_{Ta})$ has to assume the value $-\Delta F_{ZTaC_{0.43}}$, i.e., we obtain x''_{Ta} as the intersection points between the function $R(x'_{Ta})$ and the lines $R_1(x'_{Ta}) = -\Delta F_{ZTaC_{0.43}}$. Performing this graphical evaluation (Figure 22), we obtain two intersection points for all temperatures below 2700°K; these indicate, that at these temperatures medium compositions of the $(Ta, W)_2C$ solid solution are unstable in respect to metal + monocarbide mixtures.

In view of the reciprocity of the relations (equation 11), it is obvious that the same result could have been achieved by plotting $R'(x'_W)$ as a function of x'_W and intersecting these curves with the lines given in $R'_1(x'_W) = -\Delta F_{ZWC_{0.43}}$.

We have previously found (equations 10, 11, and 12), that the functions $\phi_A(x_A)$ and $\phi_B(x_B)$,

$$\phi_A(x_A) = \Delta F_{ZAC_v} + \Delta F_{ZAC_v}^{mix}$$

$$\phi_B(x_B) = \Delta F_{ZBC_v} + \Delta F_{ZBC_v}^{mix}$$

are identical, and are a measure of the integral free enthalpy of disproportionation of the solution $(A, B)C_v$ into mixtures of $(A, B)C_u$ and $(A, B)C_w$.

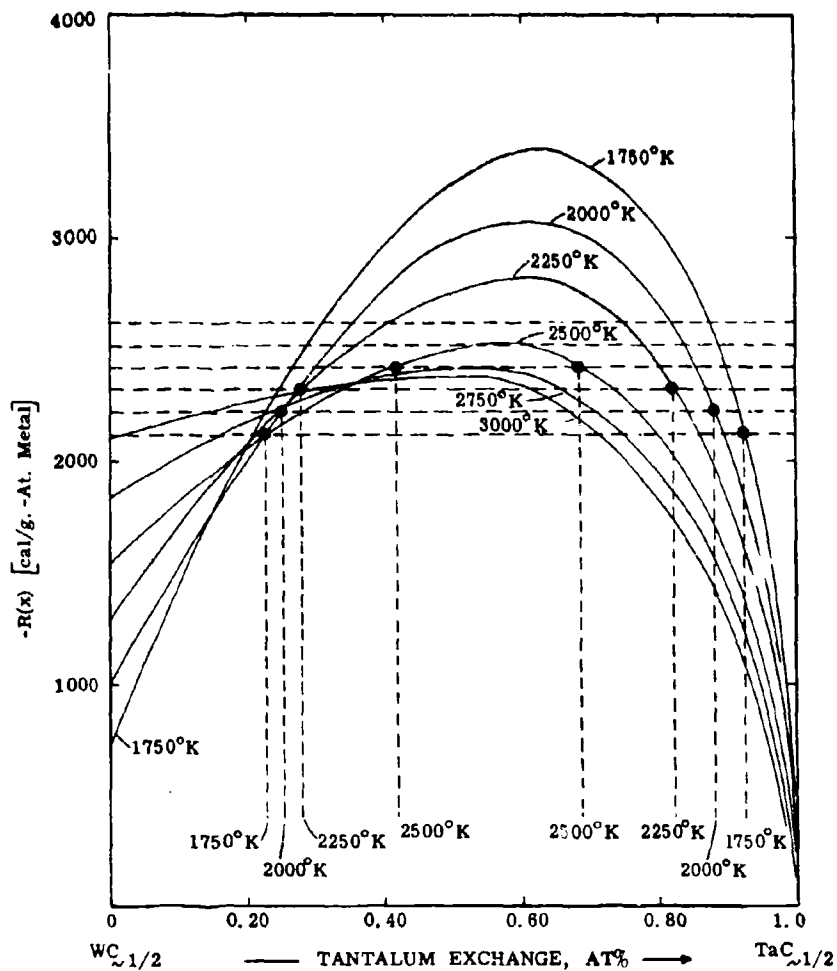
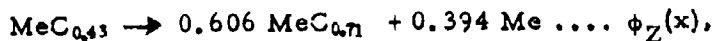


Figure 22. Ta-W-C: Graphical Determination of the Solubility Ranges of the Ta_2C and W_2C Solid Solutions.

Since $\Delta F_{ZAC_v}^{mix} = R(x'_{Ta})$, we obtain as the free enthalpy of disproportionation, $\phi_Z(x)$, of the subcarbide phase into mixtures of metal and monocarbide solid solutions according to:



$$\text{Me} = (\text{Ta}, \text{W})$$

$$\phi_A(x'_{\text{Ta}}) = \Delta F_{\text{ZTaC}_{0.43}} + R(x'_{\text{A}})$$

$$\phi_B(x'_{\text{W}}) = \Delta F_{\text{ZW}_{0.43}} + R'(x'_{\text{W}})$$

$$\phi_Z(x) \equiv \phi_A(x'_{\text{Ta}}) \equiv \phi_B(x'_{\text{W}})$$

The resulting plot of $\phi(x)$ as a function of x'_{Ta} is shown in Figure 23.

For the sake of clarity, we note that

$$\phi_Z(x'_{\text{Ta}}=0) = \Delta F_{\text{ZW}_{0.43}}$$

$$\phi_Z(x'_{\text{Ta}}=1) = \Delta F_{\text{ZTaC}_{0.43}}$$

As long as $\phi(x)$ is positive, the subcarbide solid solution is stable. $\phi'(x) = 0$ yields the maximum solid solubility limits at the given temperature; for $\phi(x) < 0$, the alloys are either two- or three-phases, i.e., single phased subcarbide alloys are unstable.

For all temperatures below 2700°K, $\phi(x)$ passes the zero line twice, and is negative between the intersection points; as a consequence, subcarbide alloys lying within this concentration range are unstable and disproportionate. Above 2700°K, $\phi_Z(x)$ remains positive over the entire range of metal-exchange, i.e., solid solution formation between W_2C and Ta_2C above 2700°K is complete.

With x'_{Ta} at $\phi_Z(x) = 0$ known, the equilibrium compositions of the phases coexisting with the terminal Me_2C compositions

at the respective temperatures can simply be read off from the corresponding free energy gradient-concentration curves.

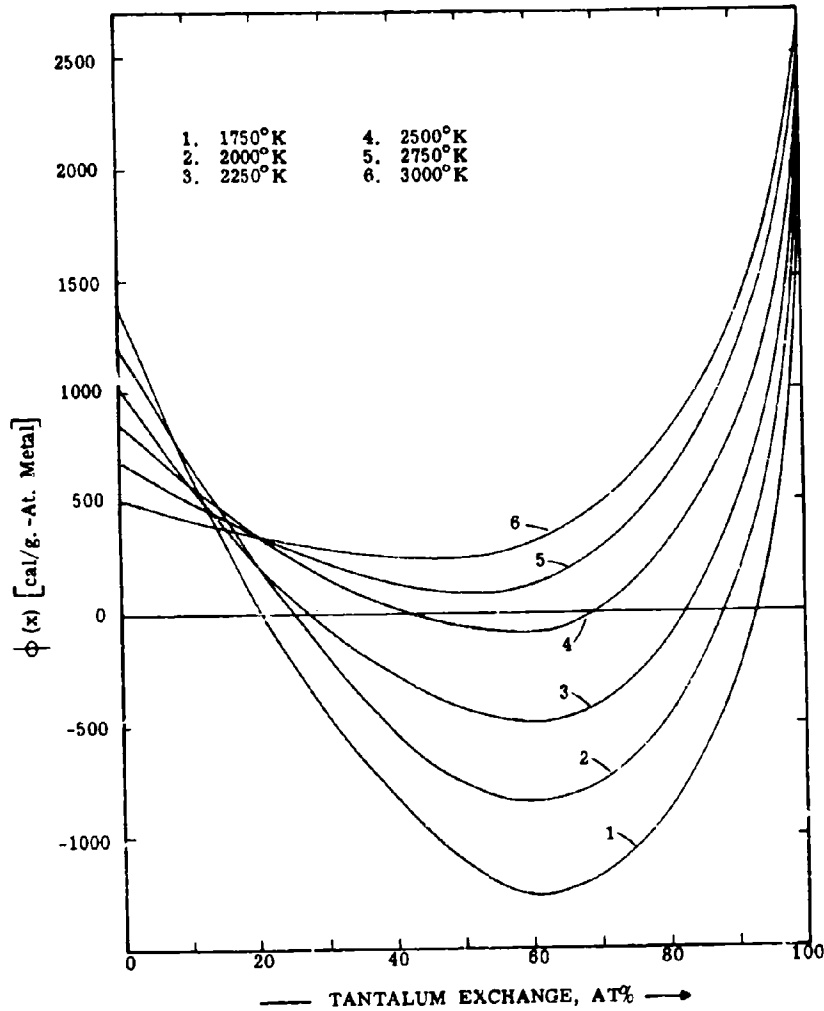


Figure 23. Integral Free Enthalpy of Disproportionation of the $(Ta, W)C_{1/2}$ Phase into Mixtures of Metal and Monocarbide Solid Solution.

$\phi_Z(x) > 0$: Subcarbide Solution Stable.

$\phi_Z(x) < 0$: Subcarbide Solution Unstable in Respect to Mixtures of Metal and Monocarbide Solutions.

We find (Table 4):

Table 4. Equilibrium Compositions of the Phases for the Three-Phase Equilibria: Monocarbide + Metal + Subcarbide

Temperature, °K	Ta-Rich Three-Phase Equilibrium			W-Rich Three-Phase Equilibrium		
	x_W	x'_W	x''_W	x_W	x'_W	x''_W
1750	0.815	0.07	0.005	0.995	0.79	0.165
200	0.825	0.12	0.010	0.992	0.75	0.195
225	0.83	0.17	0.025	0.985	0.68	0.19
2500	0.85	0.25	0.045	0.97	0.58	0.17
2700	0.91	0.38	0.10	0.91	0.38	0.10

The compositions of the two three-phase equilibria coincide at 2700°K and represent the critical tie line for the quasibinary eutectoid reaction



In contrast to the true binary reaction, the ternary reaction is of the second order, and the composition x_c , x'_c , and x''_c in terms of the above equation of reaction are defined only for the critical temperature; for $T < T_c$, two three-phase equilibria, which are separated by a two-phase field, are formed, and the equilibrium concentrations are temperature-dependent (Figure 24).

With the three-phase equilibrium in the metal-rich region of the Ta-W-C system fixed, the basic phase distribution in this concentration area of the system is defined. The end-points of the tie lines

for any given gross-composition within the five two-phase fields can be read off directly from the gradient concentration curves (Figures 21a through 21d).

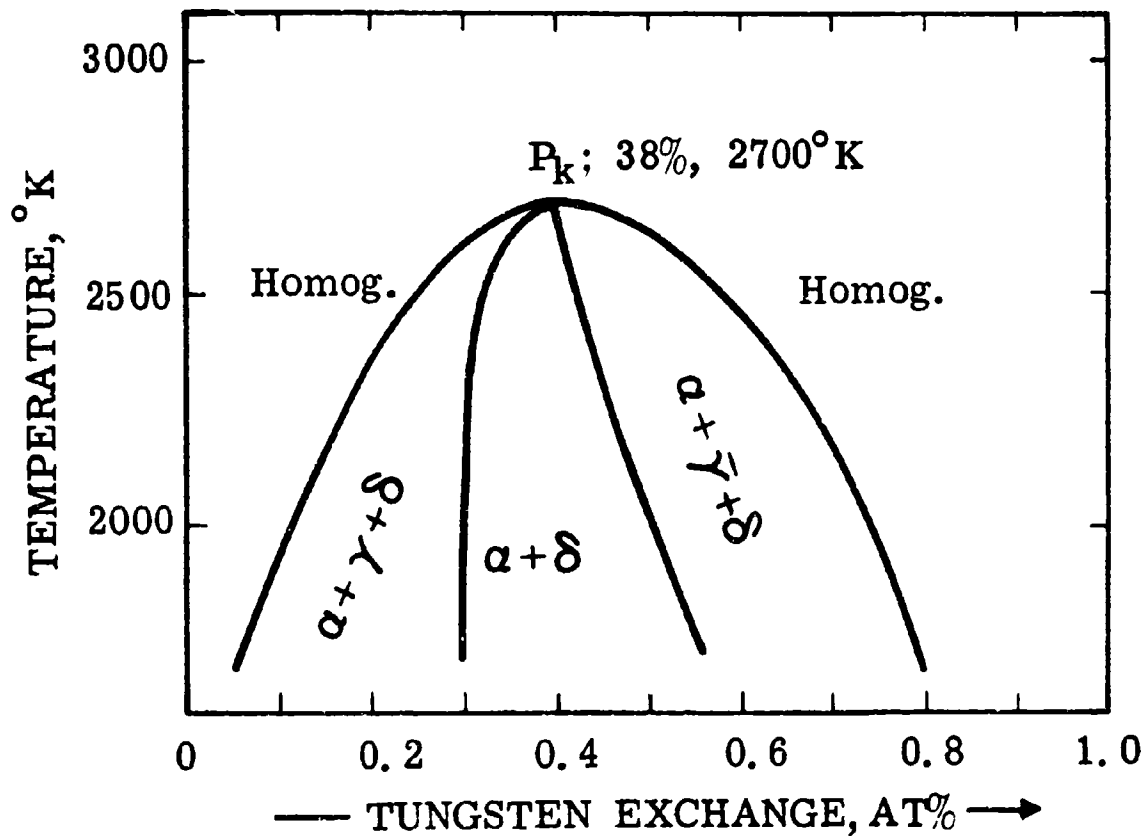


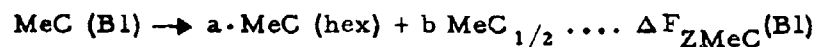
Figure 24. Calculated Vertical Section (Isopleth) Across $TaC_{0.45} - WC_{0.45}$

Note origination of two three-phase equilibria at the critical point P_K .

2. The Three-Phase Equilibrium MeC(B1) + MeC(hex)
+ Me₂C (hex)

The next three-phase equilibrium to be considered concerns the disproportionation of the cubic monocarbide phase into subcarbide and tungsten monocarbide solutions. The solution will give us the homogeneity range of the carbide solid solution as a function of temperature, and define the terminal compositions of the restraining three-phase field at the subcarbide and the tungsten monocarbide solid solution.

The overall reaction can be written as



Since the stoichiometry of the cubic monocarbide, and hence a and b varies with the metal exchange, we first have to determine by an iteration process the tungsten exchange in the monocarbide solution, in order to pick the right parameters a and b, and then determine from the (concentration-dependent) binary free enthalpies of disproportionation of the cubic monocarbide an average expression, which accounts for this concentration variation. Performing this calculation, we obtain as the average free enthalpy of disproportionation for the cubic tungsten carbide

$$\Delta F_{Z\text{WC}_{1-x}} = -4790 + 1.71 \cdot T \text{ cal/gr. -At. Tungsten}$$

It is noted, that the value must be in accordance with the binary stability limit of this phase at 2530°C. The temperature, (T_c), at which the cubic tungsten carbide becomes stable in the binary system is characterized by

$$\Delta F_{ZWC_{1-x}} = 0,$$

Hence, from the above equation,

$$T_c = \frac{4790}{1.71} = 2800^\circ\text{K} = 2530^\circ\text{C}$$

The stoichiometry factors a and b, obtained from the iteration approach, are listed below:

T (°K)	a	b
1750	0.15	0.85
2000	0.26	0.74
2250	0.45	0.55
2500	0.61	0.39
2750	0.70	0.30
3000	0.71	0.29

The overall expression describing the ternary disproportionation of the cubic tungsten monocarbide is given by [$\epsilon_{(B1)} = 6500 \text{ cal/gr. -At. Metal}$]:

$$-\Delta F_{ZWC_{1-x}} = \epsilon_{(B1)}(1-x'_W)^2 + RT \ln \frac{x''_W \cdot x''_W}{x'_W}$$

x_W, x'_W, x''_W : Tungsten exchanges in the subcarbide, cubic monocarbide and hexagonal monocarbide solid solution.

The relatively high transformation energy of the B1-tantalum monocarbide into a WC-type of lattice causes the terminal tie line of the two-phase field, B1 + WC-ss, to terminate close to the binary WC; hence, since $x''_W \approx 1$, we

neglect the corresponding solution term, obtaining the simplified equation

$$-\Delta F_{ZWC_{1-x}} = \epsilon_{(B1)} (1-x'_W)^2 + RT \ln \frac{x_W^a}{x'_W} = R'(x)$$

From the gradient curves (Figures 21c and 25), we obtain the following compatible concentrations x_W for a series of chosen values for x'_W (Table 5).

Table 5. Partition Equilibrium Subcarbide + Monocarbide (B1):
Compatible Combinations of x'_W and x_W .

x'_W	x_W				
	1750°K	2000°K	2250°K	2500°K	2750°K
0.05	0.84	0.73	0.635	0.535	0.475
0.10	0.91	0.84	0.76	0.695	0.625
0.20	0.93	0.895	0.84	0.80	0.745
0.30	0.945	0.91	0.88	0.84	0.80
0.40	0.95	0.925	0.895	0.87	0.835
0.50	0.955	0.93	0.905	0.895	0.85
0.60	0.955	0.935	0.915	0.90	0.865
0.70	0.96	0.94	0.925	0.915	0.890
0.80	0.965	0.95	0.94	0.93	0.915
0.90	0.98	0.97	0.965	0.96	0.95

The function $R'(x)$, computed with the values of x'_W and x_W listed in Table 5, are illustrated in Figure 26. The equilibrium concentration x'_W for the various temperatures T_i are the abscissa corresponding to the functional values $R''(x) = -\Delta F_{ZWC_{1-x}}(T_i)$.

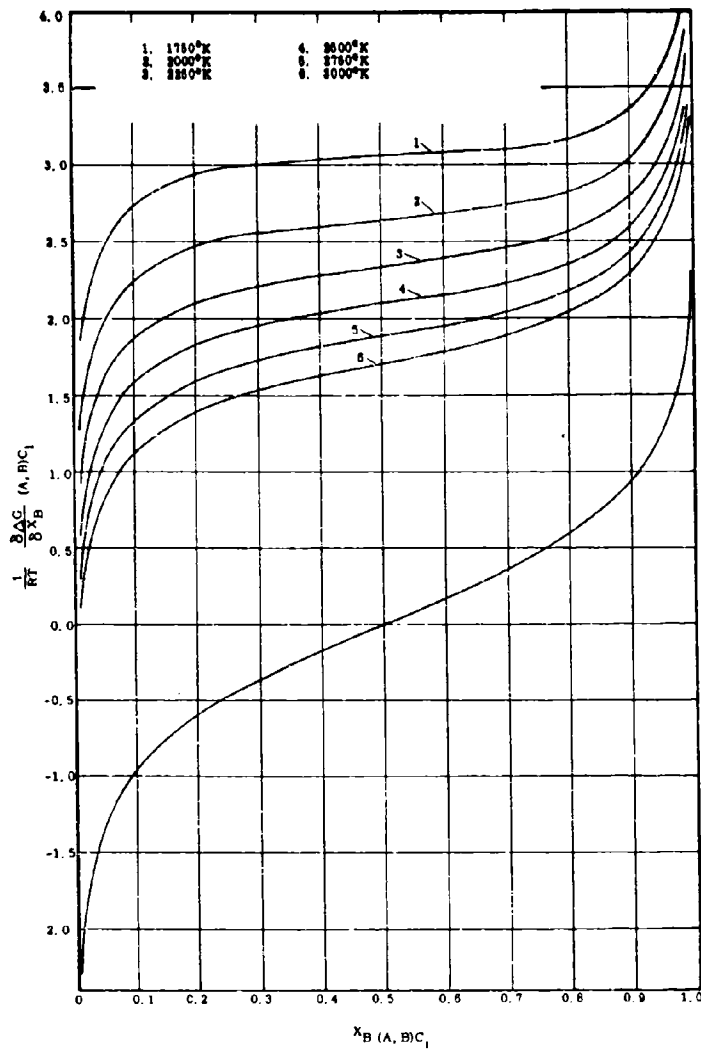


Figure 25. Free Enthalpy of Formation-Concentration Gradients for the Cubic Monocarbide Solution $(Ta, W)C_1$ at Compositions Close to Stoichiometry ($\epsilon = 6500^x$ cal/gr. -At. Metal).

Lower Single Curve: Gradient Curve for (Ta, W) .

More illustrative for the physical problem than the function $R'(x)$ are the expressions describing the integral free energies of disproportionation, which, for the present case, are a measure of the stability of the cubic solution against decomposition into the hexagonal

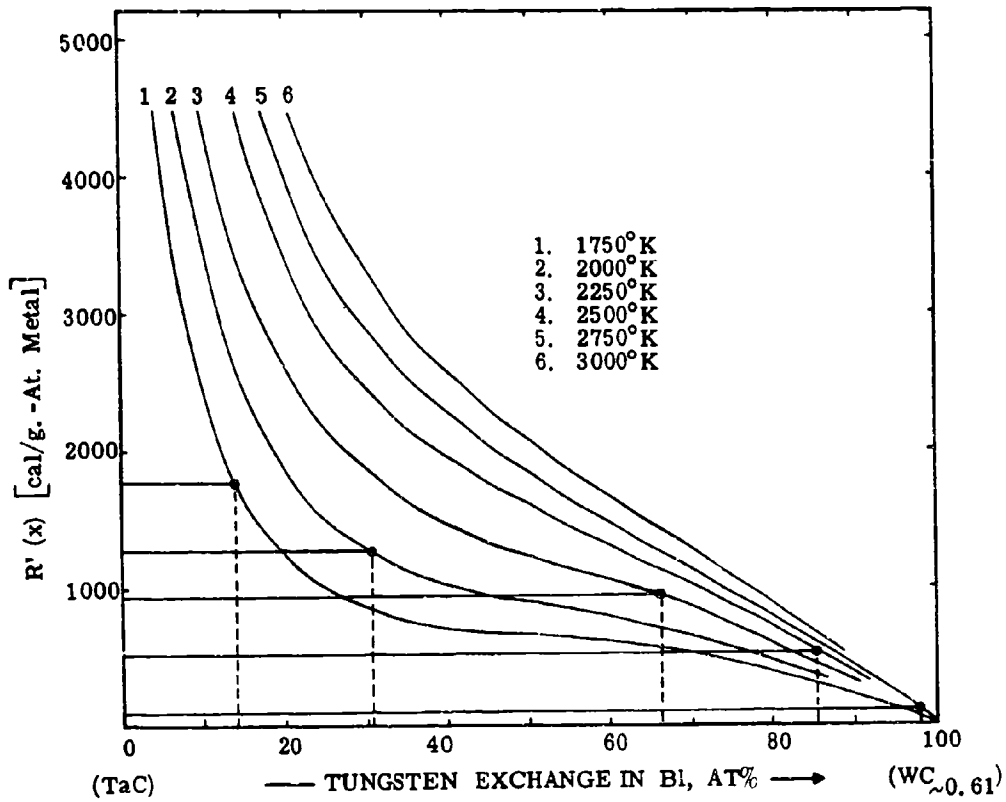


Figure 26. Graphical Determination of the Base Point of the Three-Phase Equilibrium $WC + (Ta, W) C_{1-x}(Bl) + W_2C$ at the Cubic Monocarbide Solution.

Note: The concentrations correspond to the maximum tungsten exchange in the cubic phase at the corresponding temperature.

tungsten monocarbide and tungsten-rich subcarbide solid solution. As outlined in preceding sections, this function is given by

$$\phi(x'_W) = \Delta F_{ZWC_{1-x}} + R'(x)$$

and is plotted, with x'_W as independent variable, in Figure 27.

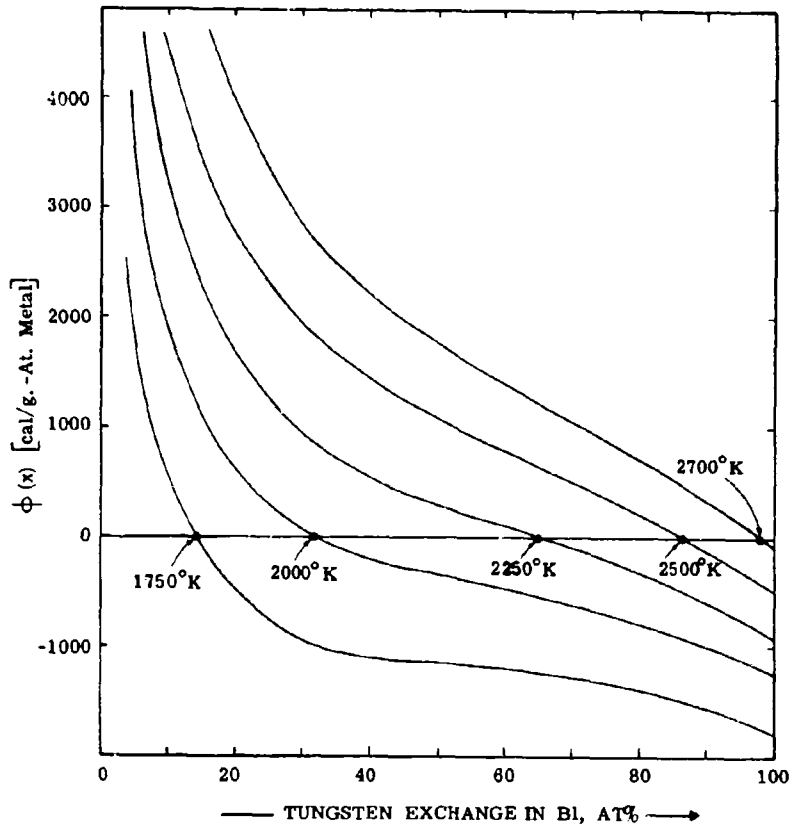


Figure 27. Integral Free Enthalpy of Disproportionation of the Cubic Monocarbide Solid Solution $[(Ta, W)C_{1-x}]$ into Subcarbide $[(Ta, W)C_{1/2}]$ and Tungsten Monocarbide.

For

$$\phi(x'_W) > 0$$

the monocarbide solid solution is stable, whereas for

$$\phi(x'_W) < 0$$

it becomes unstable in respect to phase mixtures consisting either of $\text{Me}_2\text{C} + \text{WC}$, or $\text{MeC}_{1-x} + \text{Me}_2\text{C} + \text{WC}$. The maximum tungsten exchange in the monocarbide solid solutions is given by $\phi(x'_W) = 0$, and hence is obtained from the intersection of $\phi(x'_W)$ with the abscissa $\phi(x') = 0$.

We further note that the intersection point of $\phi(x'_W)$ with the ordinate, i. e. the value of the function $\phi(x'_W)$ at $x'_W = 0$, corresponds to the free enthalpy of transformation of the cubic tantalum monocarbide into a phase exhibiting the structural characteristics of WC; according to the data presented in Table (1), this intersection point would occur at $\phi'(x'_W) \approx 12,000$ cal. A simple hexagonal tantalum monocarbide is therefore of comparatively low stability.

The functional value of $\phi(x'_W)$ at $x'_W = 1$ represents the free enthalpy of disproportionation of the binary cubic tungsten carbide into hexagonal WC and W_2C , and is negative (WC_{1-x} unstable) at temperatures below 2800°K . Above this temperature, the function $\phi(x'_W)$ does not cross the abscissa at any composition i. e., the cubic solid solution includes the tungsten-carbon binary.

The theoretical findings, as shown for the maximum tungsten exchange in the cubic solid solution, are in excellent agreement with the experimental findings (Figure 28).

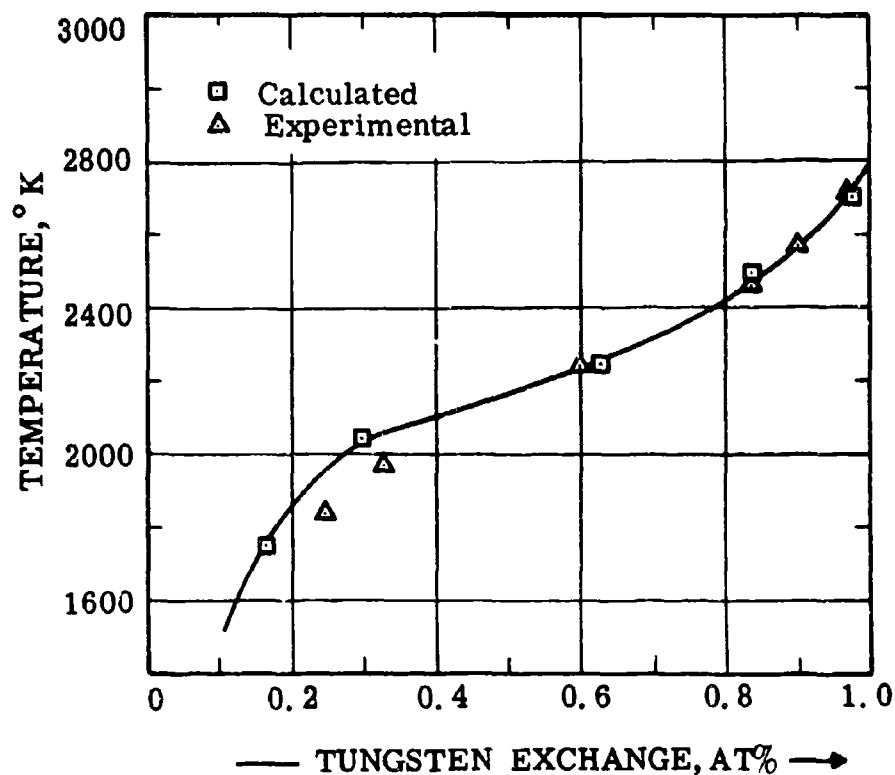
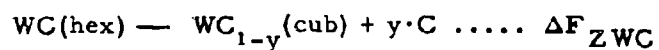


Figure 28. Temperature Dependence of the Maximum Tungsten Exchange in Tantalum Monocarbide.

3. The Three-Phase Equilibrium $WC + MeC_{1-x}(B1) + C$

The last equilibrium to be considered concerns the equilibrium existing between tungsten monocarbide, cubic monocarbide solid solution, and graphite; the overall reaction can be represented by



Since this equilibrium involves the carbon-richest compositions of the cubic monocarbide phase, the value of y will be small. Furthermore, the metal solubilities in graphite are negligible, so that we may consider it as pure graphite in our calculations.

Stability condition (8), rewritten for the present case becomes ($W = \infty$):

$$-\Delta F_{ZWC} = \epsilon_{(Bl)} (1-x_W)^2 - \epsilon_{WC} (1-x'_W)^2 + RT \ln \frac{x_W}{x'_W}$$

x_W ... tungsten exchange in the cubic solution

x'_W ... tungsten exchange in the hexagonal WC

Since y in WC_{1-x} is small, ΔF_{ZWC} corresponds, in a close approximation, to the free enthalpy of transformation of the hexagonal (stable modification of WC) into a face-centered cubic (Bl) modification of WC, for whose stability we have found (Table 2)

$$\Delta F_{ZWC} = 5160 - 1.42 \cdot T \text{ cal/gr. -At. Tungsten.}$$

Compatible couples of x_W and x'_W could be obtained from the gradient-concentration curves for the cubic and the hexagonal solid solution; however, since we know (Equation 12 and 14) that the tantalum exchange in the hexagonal WC will be governed mainly by the transformation energy of TaC (cub \rightarrow hex.); the latter is a fairly large positive quantity ($\sim +12,000$ cal/gr. -At. Ta) as compared to ΔF_{ZWC} , we expect the relative

exchange of Ta in WC to be very small. The calculation yields the following solubilities as a function of temperature (Table 6). We, therefore, disregard the solution term for the tungsten monocarbide phase, and obtain

$$-\Delta F_{ZWC} = \epsilon_{(B1)} (1-x_W)^2 + RT \ln x_W = R''(x)$$

Table 6. Maximum Tantalum Exchange in WC (Calculated)

Temperature °K	Tantalum Exchange in WC, Atomic Percent
1750	3.5
2000	4.6
2250	5.9
2500	6.6
2750	6.2
3000	5.0

The resulting plot of $R''(x)$ versus the tungsten exchange is shown in Figure 29. The vertex of the three-phase equilibrium $MeC_{1-x}(B1) + MeC(hex) + C$ at the cubic solid solution for various temperatures, T_i , is determined, as described before, by seeking the intersection points with the lines $R''(x) = -\Delta F_{ZWC}(T_i)$. The integral function

$$\phi(x_W) = \Delta F_{ZWC} + R''(x),$$

which compares the thermodynamic stability of cubic monocarbide solid solutions with that of mechanical mixtures consisting of WC and graphite, is presented in Figure 30.

In analogy to the considerations for the previously treated equilibria, the cubic solution is stable as long as

$$\phi(x) > 0,$$

and disproportionates into tungsten monocarbide and graphite for the case that $\phi(x) < 0$. The vertex of the three-phase equilibrium is determined by $\phi(x) = 0$.

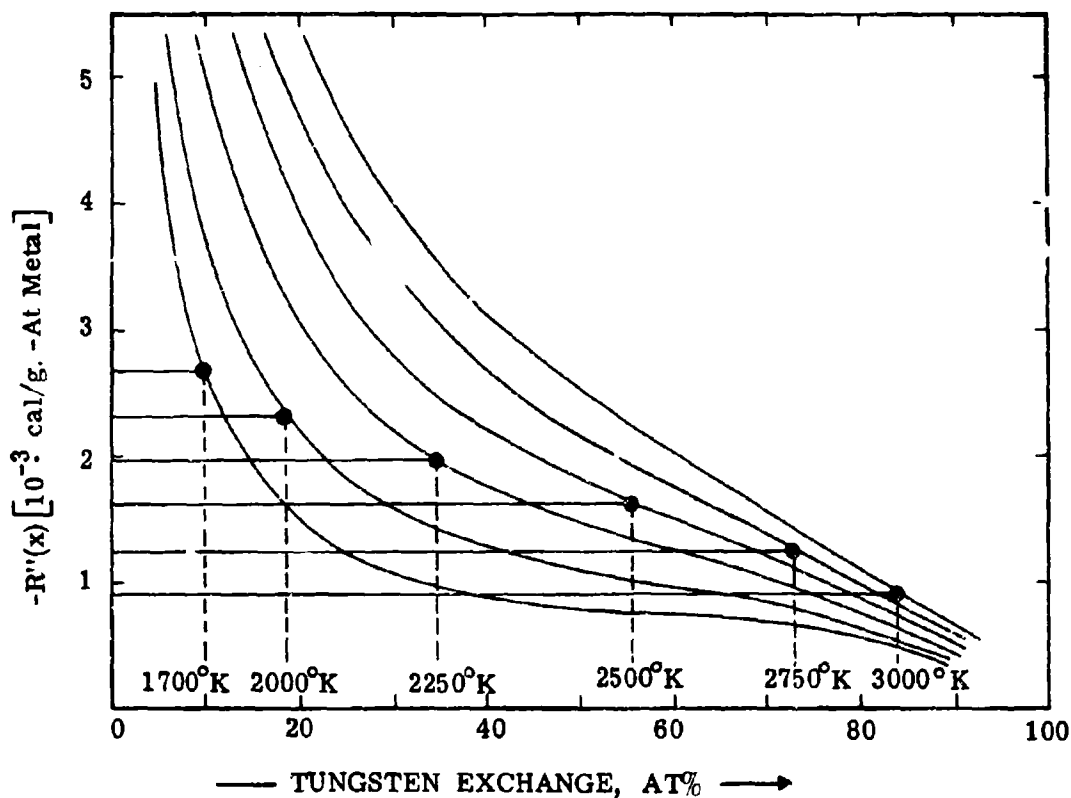


Figure 29. Graphical Determination of the Base Point of the Three-Phase Equilibrium WC-(Ta, W)C_{1-x}(B1)-C at the B1-Solid Solution.

Comparing the base points of the three-phase equilibria
 $\text{MeC}_{1-x}(\text{cub}) + \text{MeC}(\text{hex}) + \text{C}(x_{\text{W(I)}})$ and $\text{Me}_2\text{C}(\text{hex}) + \text{MeC}(\text{hex}) + \text{MeC}_{1-x}(\text{cub})$
 $(x_{\text{W(II)}})$ at the cubic solid solution, we find — as it should be —

$$x_{\text{W(II)}} > x_{\text{W(I)}}$$

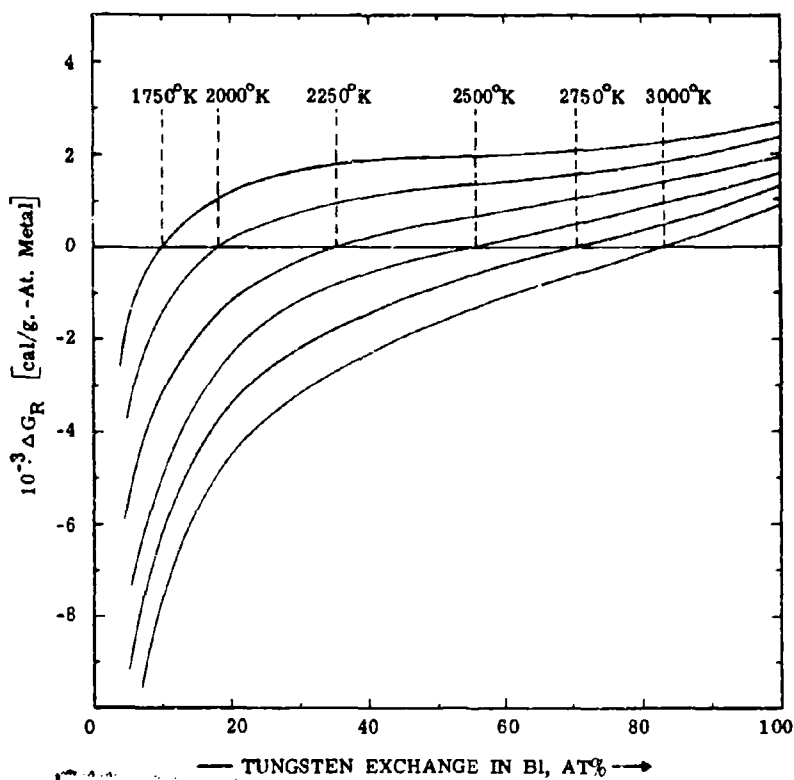


Figure 30. Integral Free Enthalpy of Disproportionation of Tungsten Monocarbide into the Cubic $(\text{Ta}, \text{W})\text{C}_{1-x}$ Carbide Solutions and Graphite.

These results take account of the previously reported discrepancies of the tungsten carbide solubility in tantalum monocarbide⁽¹⁹⁾, showing it, within certain limits, to be dependent upon the carbon concentration of the alloys. Hence, one would suspect that in view of the existing carbon defect in the cubic monocarbide solution, solubility data collected on alloys along the stoichiometric line TaC-WC actually refer to the concentrations of the ternary equilibrium involving graphite. This is evidenced by a comparison of previous literature data⁽¹⁹⁾ with the present findings and calculations (Figure 31).

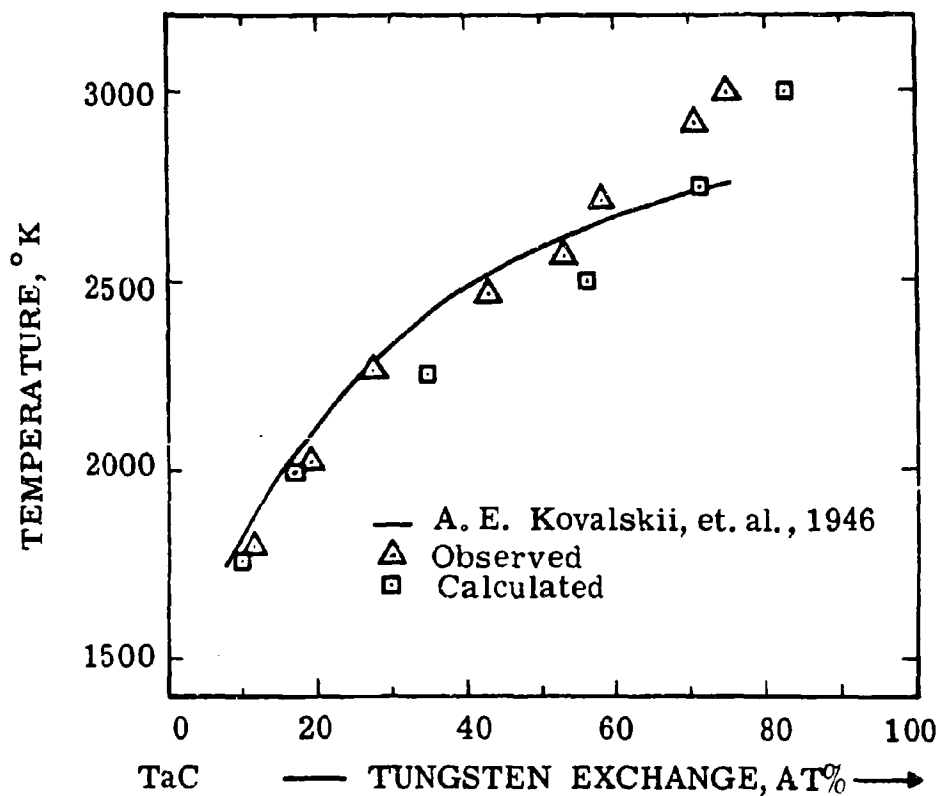


Figure 31. Three-Phase Equilibrium $(Ta, W)C_{1-x}(B1) + WC + C$: Temperature Dependence of the Composition of the Base Point at the Cubic Solid Solution.

The phase diagram data calculated in the previous sections can now be used to assemble sections of the phase diagram for the chosen temperatures. First, the ternary phase field, at a given temperature, is subdivided by the known compositions of the vertices for the three-phase equilibria. The concentrations of the (arbitrarily chosen number) of tie lines in the resulting two-phase fields are then determined from the free energy-gradient curves and incorporated into the diagrams (Figures 32a through 32f.

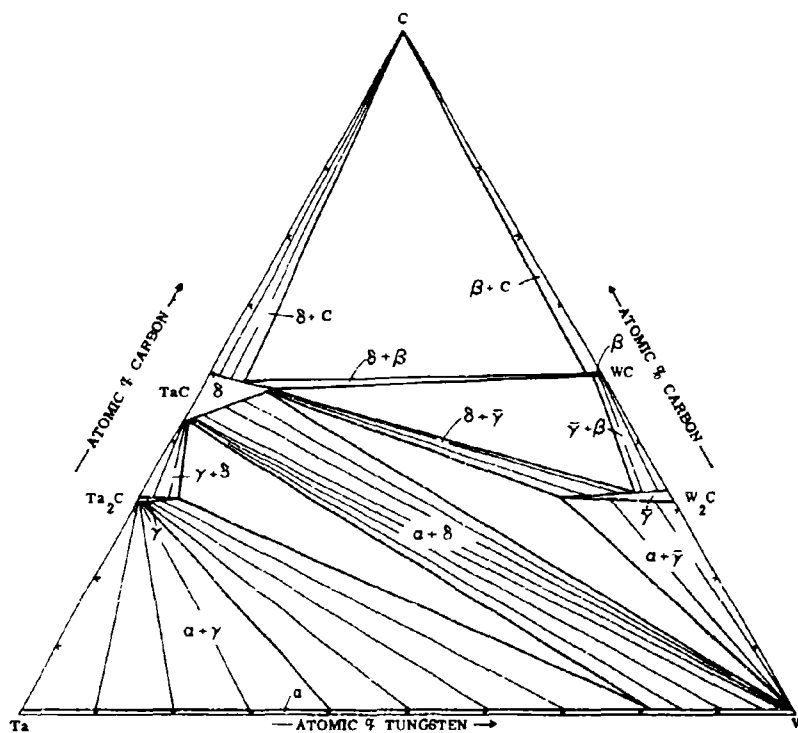


Figure 32a. 1750°C

Although the approximation of the boundaries of the one-phase ranges by straight lines is admittedly crude, the calculation was able to reproduce the actual conditions remarkably well, and also yielded

the correct temperature dependence of the equilibria. In fact, the calculated tie line distributions in the various two-phase ranges probably supersede the experimental data in accuracy. The reason for this has to be sought in the

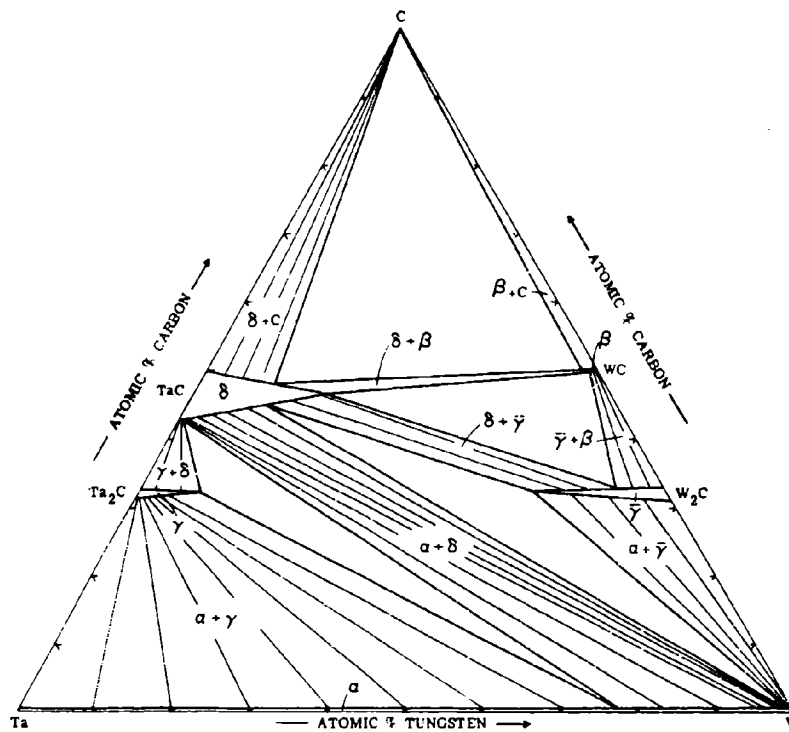


Figure 32b. 2000°K

fact that while the entire set of tie line compositions, calculated for a given temperature, are functionally interrelated, each individual experimental tie line independently carries the average experimental error. The scatter of the individual experimental equilibrium compositions is therefore expected to be more pronounced.

Due to the lack of thermochemical data, the phase equilibrium changes introduced by the α - β - Me_2C order-disorder reactions were not specifically regarded in the calculations. However, since their overall effect upon the phase behavior is only secondary, this neglect does not affect the general validity of the thermodynamic treatment.

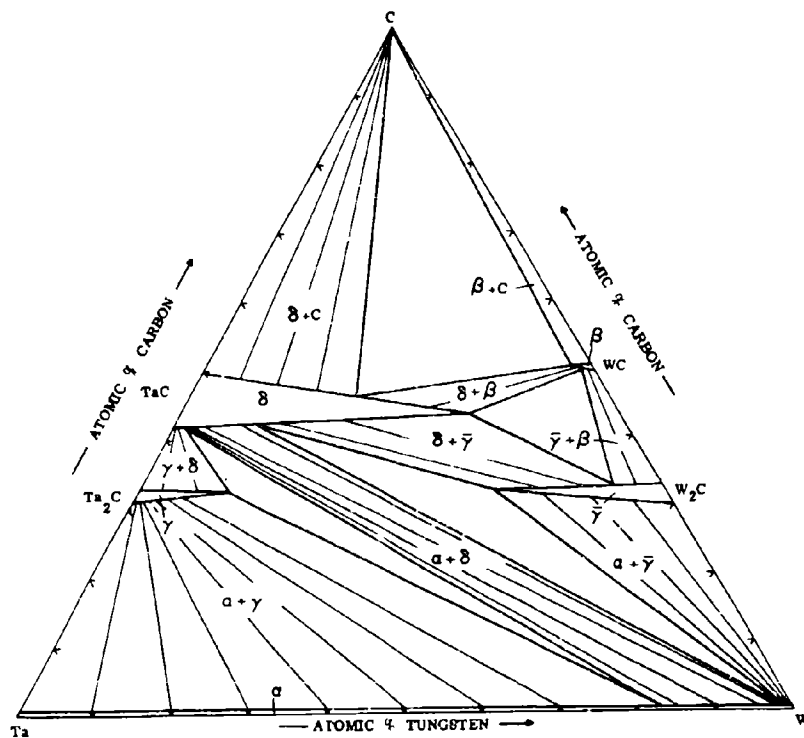


Figure 32c.

2250°K.

The results of the preceding phase equilibrium calculations would be capable of further improvement using the present solution as the zero approximation in an iterative approach, or by refining the compositions — as indicated in a previous section — by computational

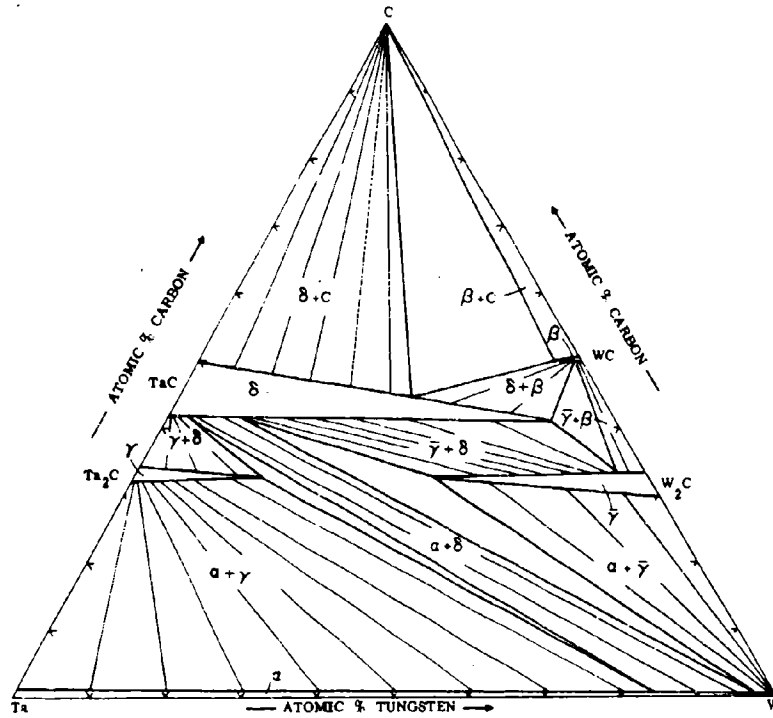


Figure 32d. 2500°K.

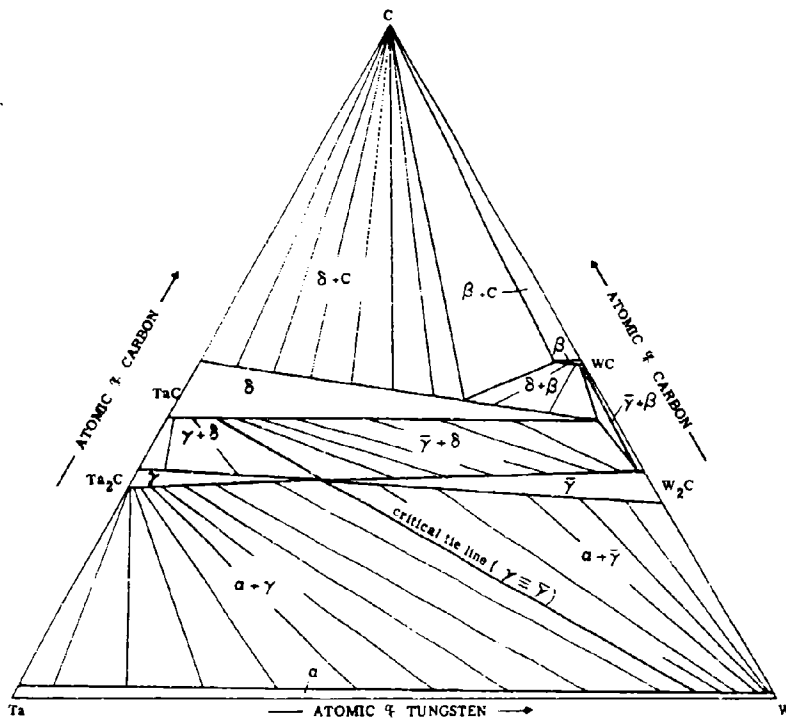


Figure 32e. 2700°K.

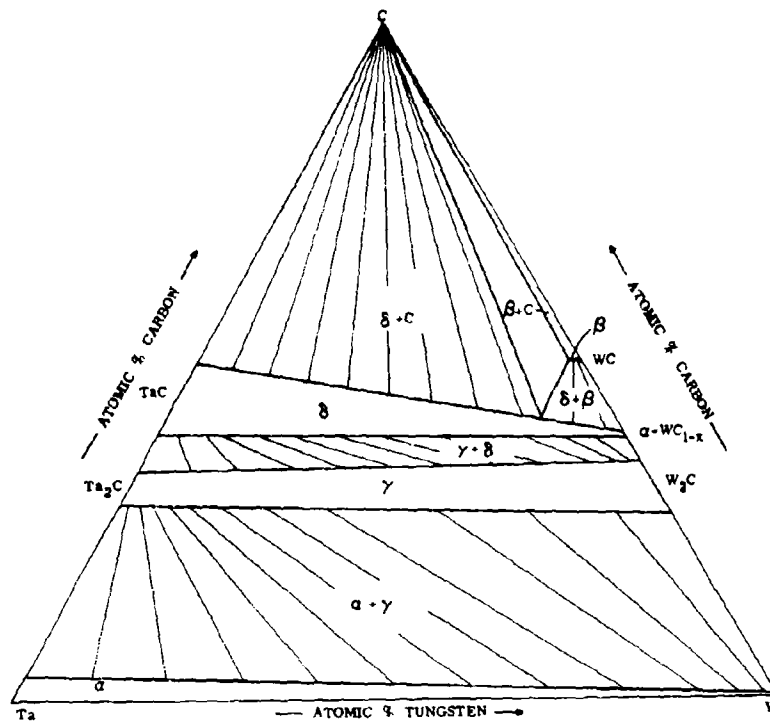


Figure 32f. $\sim 3000^{\circ}\text{K}$

Figures 32a through 32f.

Calculated Temperature Sections for the Ta-W-C System.

methods. Due to the lack of high precision thermodynamic data, however, the latter approaches would essentially become reduced to a data fit to the experiment. With present experimental means, the certainty to which high temperature phase-equilibrium data is rarely better than ± 2 atomic percent, hence the net gain in accuracy and reliability may appear as negligible. The value of an exact numerical solution of the unrestricted problem has to be, therefore,—at least for the time being—considered more as principal rather than factual.

B. BACK-CALCULATIONS OF THERMODYNAMIC QUANTITIES FROM EXPERIMENTAL PHASE DIAGRAM DATA.

Following our considerations on the tantalum-tungsten-carbon system where we were concerned mainly with the computation of the phase relationships from available thermochemical data, we shall now try the opposite way, namely to demonstrate the applicability of the thermodynamic method to extract thermochemical information from available phase diagram data. Apart from the fact that phase diagrams provide us with a convenient source to derive thermodynamic quantities for hypothetical phases, which are not accessible by calorimetric means, the need for such calculations often may arise if pertinent data for the calculation of a specific system are not available.

We choose the recently established phase diagrams Mo-Cr-C and W-Cr-C⁽¹⁶⁾ as examples for the calculations. Temperature sections for both ternary systems are shown in Figures 33 and 34. We consider the W-Cr-C system first.

Tungsten and chromium form a nearly symmetrical miscibility gap at temperatures below 1500°C. Cr_{23}C_6 exchanges at the equilibrium temperature approximately 23 atomic percent tungsten, and the hexagonal $(\text{W,Cr})_2\text{C}$ phase extends to a chromium exchange of 87 atomic percent. The equilibrium $\text{WC-Cr}_3\text{C}_2$ is stable only below approximately 1500°C and is replaced by an equilibrium $(\text{W,Cr})_2\text{C-C}$ at higher temperatures. As an approximation to the actual behavior, the vanLaar expression for regular solutions will be used throughout the calculations. The interaction parameter for the

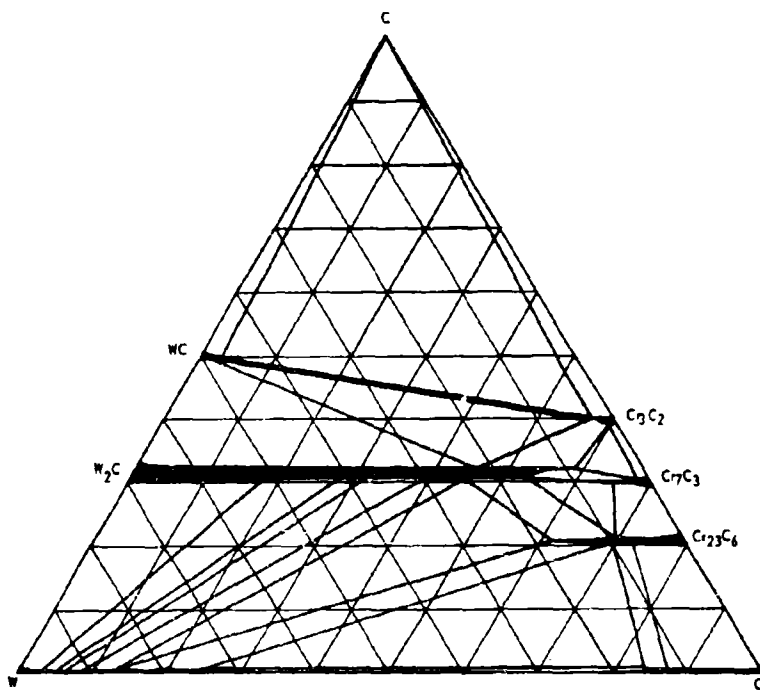


Figure 33. Section of the Phase Diagram Tungsten-Chromium-Carbon at 1300°C.

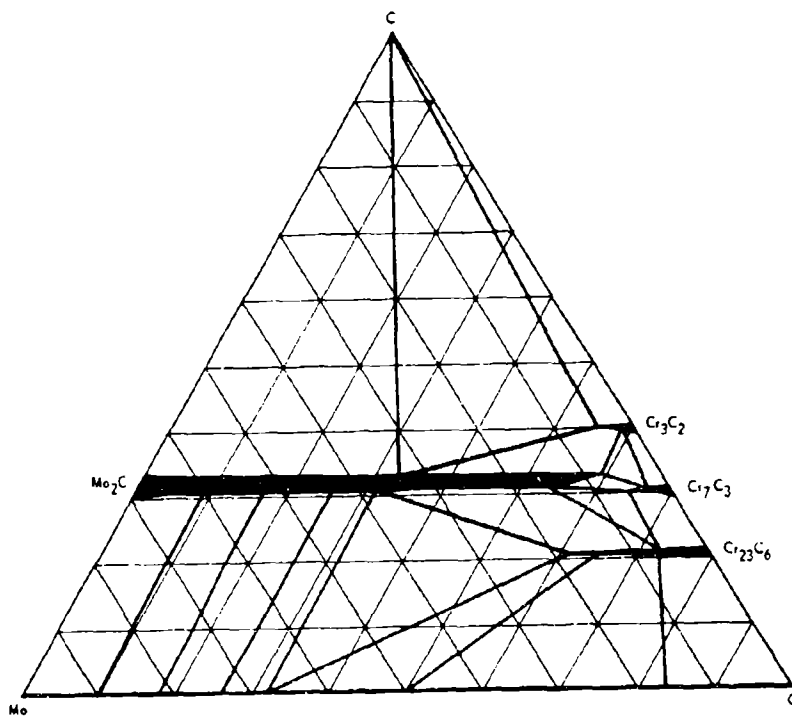


Figure 34. Section of the System Molybdenum-Chromium-Carbon at 1300°C.

system W-Cr is derived from the critical point with the aid of the relation

$$T_c = \frac{\epsilon}{2R}$$

With the experimental value of $T_c = 1770^\circ\text{K}$, ϵ becomes 7010 cal/gr. -At. metal. The corresponding interaction parameters for the carbide solid solutions were derived from considerations regarding the relative atomic sizes, the melting points of the phases, as well as the tie line distributions in the two-phase fields.

1. The Two-Phase Equilibrium (W,Cr)-(W,Cr)₂C.

Conditional equation (3) applied to both solutions yields

$$\Delta F_{f(\text{Cr}, \text{W})} = 7010 x_{\text{Cr}}(1-x_{\text{Cr}}) + RT [x_{\text{Cr}} \ln x_{\text{Cr}} + (1-x_{\text{Cr}}) \ln (1-x_{\text{Cr}})]$$

and

$$\Delta F_{f(\text{Cr}, \text{W})\text{C}_{1/2}} = x'_{\text{Cr}} \Delta F_{f, \text{CrC}_{1/2}} - (1-x'_{\text{Cr}}) \Delta F_{f\text{WC}_{1/2}} + 4000 x'_{\text{Cr}} (1-x'_{\text{Cr}}) + RT [x'_{\text{Cr}} \ln x'_{\text{Cr}} + (1-x'_{\text{Cr}}) \ln (1-x'_{\text{Cr}})]$$

$$\left[\frac{\partial \Delta F_{f(\text{Cr}, \text{W})}}{\partial x_{\text{Cr}}} \right]_{T, P} = 7010 (1-2x_{\text{Cr}}) + RT \ln \frac{x_{\text{Cr}}}{1-x_{\text{Cr}}}$$

$$\left[\frac{\partial \Delta F_{f(\text{Cr}, \text{W})\text{C}_{1/2}}}{\partial x'_{\text{Cr}}} \right]_{T, P} = \Delta F_{f, \text{CrC}_{1/2}} - \Delta F_{f\text{WC}_{1/2}} + 4000 (1-2x'_{\text{Cr}}) + RT \ln \frac{x'_{\text{Cr}}}{1-x'_{\text{Cr}}}$$

$$\Delta F_{f\text{CrC}_{1/2}} - \Delta F_{f\text{WC}_{1/2}} = 7010 (1-2x_{\text{Cr}}) - 4000 (1-2x'_{\text{Cr}}) + RT \ln \frac{x_{\text{Cr}}}{1-x_{\text{Cr}}} \cdot \frac{1-x'_{\text{Cr}}}{x'_{\text{Cr}}}$$

$\Delta F_{fCrC_{1/2}}$ = Free enthalpy of formation of $CrC_{1/2}$ with a structure analogous to that of W_2C .

$\Delta F_{fWC_{1/2}}$ = Free enthalpy of formation of $WC_{1/2}$.

x_{Cr} , x'_{Cr} = Mole fraction chromium exchange in W and $WC_{1/2}$, respectively.

This difference in the free enthalpies of formation for the subcarbides can now be evaluated from the end points x_{Cr} and x'_{Cr} of the experimental tie lines at the two solutions (Figure 33).

Performing the calculation, we obtain as the mean value and standard deviation:

$$\Delta F_{fCrC_{1/2}} - \Delta F_{fWC_{1/2}} = -1500 \pm 500 \text{ cal/gr. -At. Metal (T = 1575°K).}$$

2. Three-Phase Equilibrium $(W,Cr)_{23}C_6$ - $(W,Cr)_2C$ - (W,Cr) .

Stability condition (8), rewritten for this equilibrium

($u = 0$, $v = 0.266$, $w = 0.436$) becomes:

$$-\Delta F_{ZCrC_{0.266}} = 0.39\epsilon_1(1-x_{Cr})^2 + 0.61\epsilon_3(1-x''_{Cr})^2 - \epsilon_2(1-x'_{Cr})^2 + RT \ln \frac{x''_{Cr}^{0.61} \cdot x_{Cr}^{0.39}}{x'_{Cr}}$$

$\epsilon_1, \epsilon_2, \epsilon_3$.. Interaction parameters for the solutions (W,Cr) , $(W,Cr)C_{6/23}$ and $(W,Cr)C_{1/2}$. (70.0, 4000, and 4000 cal/gr. -At Metal)

$x_{Cr}, x'_{Cr}, x''_{Cr}$.. Mole fraction chromium exchange in tungsten and the solutions (Cr,W) , $(Cr,W)_{23}C_6$ and $(Cr,W)C_{1/2}$

Inserting the experimental points from the phase diagram, i.e. $x_{Cr} = 0.13$,

$x'_{Cr} = 0.77$, and $x''_{Cr} = 0.65$, we obtain the free enthalpy of disproportionation of

$\text{CrC}_{6/23}$ into a hypothetical $\text{CrC}_{1/2}$ and chromium:

$$\Delta F_{\text{ZCrC}_{6/23}} = 970 \text{ cal/gr. -At Cr (T = 1575°K).}$$

Substituting tungsten for chromium in the above equation, and inserting the equivalent concentration $x_{\text{W}}^i = 1 - x_{\text{Cr}}^i$, we obtain for the free enthalpy of disproportionation of a hypothetical $\text{WC}_{6/23}$ into tungsten and $\text{WC}_{1/2}$:

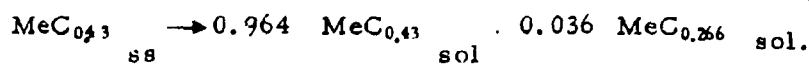
$$\Delta F_{\text{ZWC}_{6/23}} = -1790 \text{ cal/gr. -At. W, (T = 1575°K)}$$

i. e. a phase W_{23}C_6 is unstable with regard to a mechanical mixture of W_2C and W.

Analogous expressions are now written down for all other three-phase equilibria in the system, and the free enthalpies of disproportionation for the corresponding phases evaluated.

3. Three-Phase Equilibrium $(\text{W,Cr})_2\text{C} + (\text{W,Cr})_{23}\text{C}_6 + (\text{W,Cr})_7\text{C}_3$
(T = 1575°K).

The corresponding reaction is ($u = 0.266$, $v = 0.43$,
 $w = 0.436$).

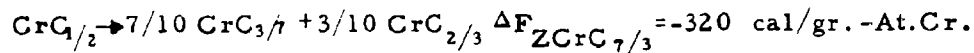


$$\Delta F_{\text{ZCrC}_{0.43}} (\text{Cr}_7\text{C}_3 \text{-type}) = + 370 \text{ cal/gr. -At. Cr.}$$

$$\Delta F_{\text{ZWC}_{0.43}} (\text{Cr}_7\text{C}_3 \text{-type}) = - 2620 \text{ cal/gr. -At. W.}$$

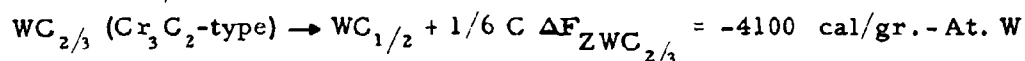
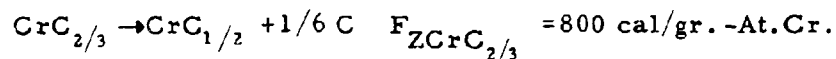
4. Three-Phase Equilibrium (Cr, W)₇C₃-(Cr, W)₂C-(Cr, W)₃C₂
(T = 1575°K)

$$(u = 3/7; v = 1/2, w = 2/3)$$

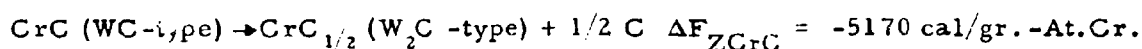
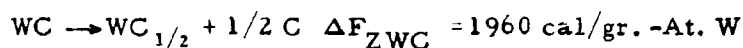


5. Three-Phase Equilibrium (Cr, W)₂C-(Cr, W)₃C₂-C
(T = 1863°K)

$$(u = 1/2, v = 2/3, w = \infty)$$



6. Three-Phase Equilibrium (W, Cr)C-(W, Cr)₂C-C (T = 1863°K)



In this system we have the interesting case that none of the lattice types observed in the one system, occur in the other. In order to enable a phase diagram calculation, the stability of all tungsten-phases with the structural characteristics of the chromium-carbon phases, and similarly, the structure of chromium-carbides with structures analogous to W₂C and WC have to be known. The calculation of each equilibrium in this system involves data for at least one hypothetical phase. Hence, based only on calorimetric data, not one equilibrium in the whole system could be predicted, or even estimated.

Except for the monocarbide, which is missing at the chosen equilibrium temperature, the phase relationships in the Mo-Cr-C system (Figure 34) are very similar to the system just treated with tungsten; the thermochemical evaluation is analogous and the data obtained ($\epsilon_{\text{MoC}_i} = 4000 \text{ cal/gr. -At. Metal}$) are summarized in Table 7. For comparison purposes, the data obtained from the W-Cr-C are included in the compilation. The various structure designations ($\alpha, \beta \dots \epsilon$) refer to the following types

<u>Designation</u>	<u>Lattice Type</u>
$\alpha \dots \dots \dots$	$\text{Mo}_2\text{C}, \text{W}_2\text{C}^*$
$\beta \dots \dots \dots$	WC
$\gamma \dots \dots \dots$	Cr_{23}C_6
$\delta \dots \dots \dots$	Cr_7C_3
$\epsilon \dots \dots \dots$	Cr_3C_2

A comparison of the data shows excellent agreement between the free energy changes obtained from the phase relationships in the two (independent) systems.

The free energies of formation of the stable chromium carbides are available from the literature, and representative values, taken from a recent compilation^(16,17), are given in Table (8).

* Mo_2C and W_2C differ at low temperatures in their sublattice order, however, since the exchange of chromium tends to outweigh the differences, a special distinction is immaterial for our present purposes.

Table 7: Summary of Thermochemical Results on Chromium-Carbides
 Derived from Phase Diagram Data in the W-Cr-C and Mo-Cr-C
 System. (Values in cal/gr. -At. Metal, T = 1575°K)

Reaction	Free Enthalpy of Reaction	
	From W-Cr-C	From Mo-Cr-C
$\text{CrC}_{6/23} (\gamma) \rightarrow 0.42 \text{Cr} + 0.58 \text{CrC}_{0.45} (\alpha)$	+ 970	+ 860
$\text{CrC}_{7/3} (\delta) \rightarrow 0.88 \text{CrC}_{0.45} (\alpha) + 0.12 \text{CrC}_{0.266} (\gamma)$	+ 370	+ 330
$\text{CrC}_{1/2} (\alpha) \rightarrow 0.7 \text{CrC}_{3/7} (\delta) + 0.3 \text{CrC}_{2/3} (\epsilon)$	- 320	- 220
$\text{CrC}_{2/3} (\epsilon) \rightarrow \text{CrC}_{1/2} (\alpha) + 1/6 \text{C}$	+ 800*	+ 945
$\text{CrC} (\beta) \rightarrow \text{CrC}_{1/2} (\alpha) + 1/2 \text{C}$	-5170	--

*T = 1873°K

Table 8: Free Enthalpies of Formation of Chromium
 Carbides (Compiled from the Literature)

$$\Delta F_f = A - B \cdot T \text{ (cal/gr. -At. Chromium)}$$

Carbide	A	B	Temperature Range, °K
Cr_{23}C_6	-4270±800	0.40±0.1	298° - 1673°
Cr_7C_3	-5710±800	0.81±0.1	298° - 1673°
Cr_3C_2	-6170±800	0.86±0.1	298 - 1673°

These data can now be used to assign free energy data to the hypothetical chromium carbides derived from the phase-diagram information (Table 9).

Table 9: Free Enthalpies of Formation of Unstable Chromium Carbide Lattice Types (Absolute Values are Based Upon the Data for the Stable Chromium Carbides)

$$\Delta F_f = A - B \cdot T \text{ (cal/gr. -At. Chromium)}$$

Carbide	A	B
Cr ₂ C (W ₂ C-type)	-5500	0.81 _{-1.5}
CrC (WC-type)	- 650	0.90 _{+0.5}
CrC _{2/3} (B1-type)*	-2100	1.86 _{+0.5}

*From Mo-Cr-C

For phase diagram calculations, however, it is usually preferable to use the differences directly as derived from the experimental sections, in order to avoid an unnecessary accumulation of errors. In either instance, however, it is advisable to countercheck the consistency of the values by back-calculating the phase relationships using the data derived from the experimental sections (Figures 35 and 36).

Compilations similar to those for the chromium carbides can now be made for the chromium carbide-type lattice structures in the molybdenum-carbon and tungsten-carbon system, providing us with base data for calculations in systems involving these lattice types. We shall not go into any further detail, since the relevant information has been collected elsewhere⁽¹⁶⁾; however, we will briefly discuss one aspect in the tungsten-chromium-carbon system, for certain discrepancies between observed and calculated thermodynamic values for the Me₂C phases initiated the search for, and finally resulted in the discovery of the sublattice transformations, which were observed to occur in nearly all subcarbide phases⁽⁹⁾ in the meantime.

In the evaluation of the three-phase equilibrium
 $(W,Cr)C-(W,Cr)_2C-C$ on one of the preceding pages, a value of $\Delta F_{ZWC} =$
 1960 cal/gr.-At. tungsten was obtained for the free enthalpy change of the
 reaction

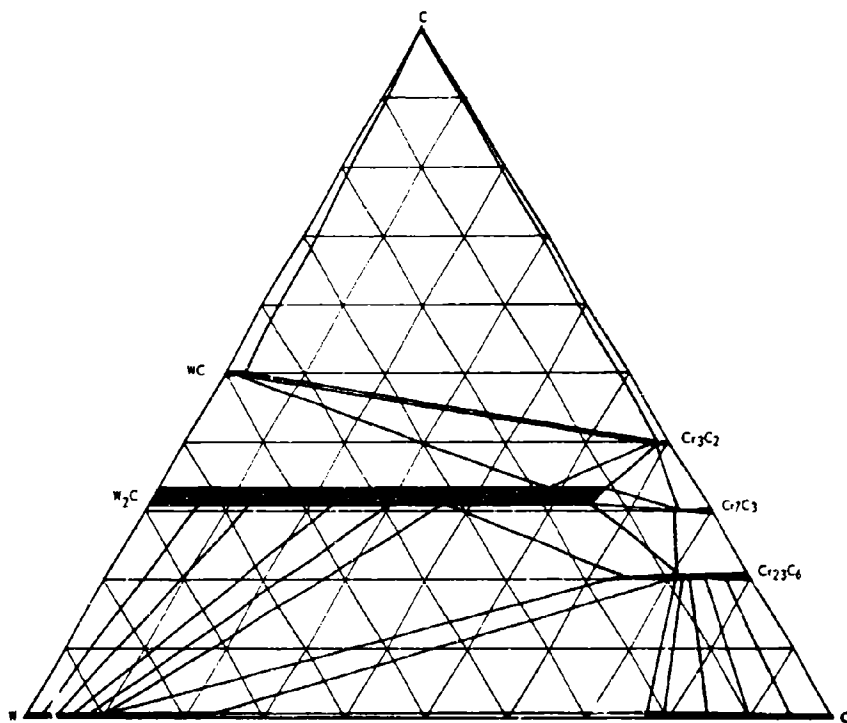
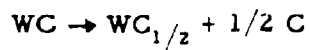


Figure 35. System Section W-Cr-C at 1600°K, Back-Calculated
 with the Thermodynamic Data derived from the
 Experimental Section in Figure 33.

In contrast to this, from the known, and apparently well established literature data for WC and W_2C (Table 1), the corresponding value should be 3700 cal/gr. - At. W. at a temperature of 1870°K. However, the calculated vertex of the three-phase equilibrium at the solid solution $(W,Cr)_2C$ would be $x_{WC_{1/2}} = 0.08$; this would extend the three-phase equilibrium far above the observed homogeneity range of the $(W,Cr)_2C$ solid solution, and therefore presents a discrepancy with the experimental findings.

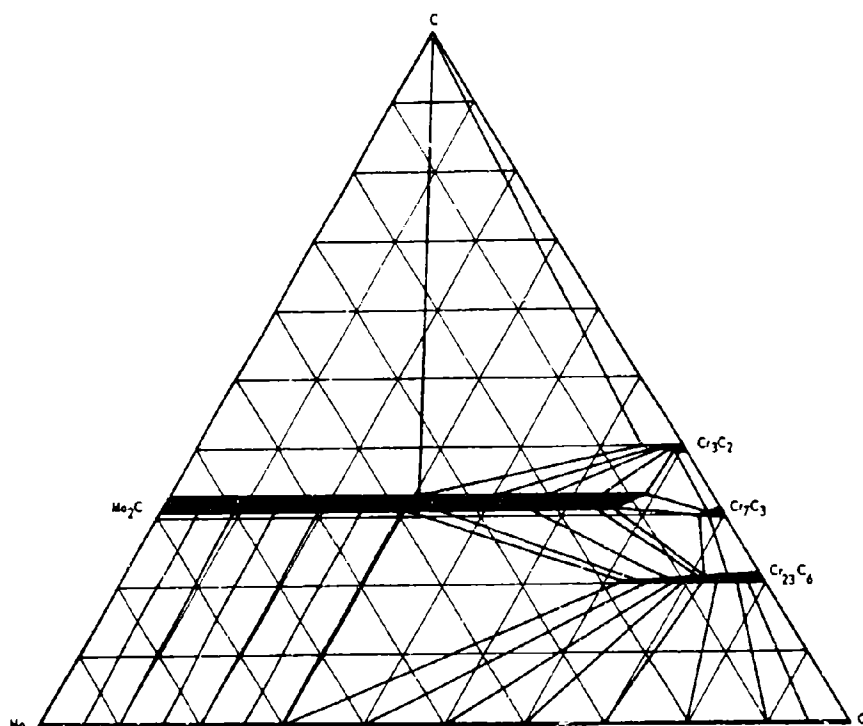


Figure 36. System Section Mo-Cr-C at 1500°K, Back-Calculated with the Thermodynamic Data Derived from the Experimental Section in Figure 34.

Since it was known from the literature⁽²⁰⁾ that the binary W_2C phase had an ordered distribution of carbon atoms, the only possibility in overcoming the observed discrepancy of approximately 1700 cal/gr. - At. tungsten, was to assume an essential disordered sublattice in the Me_2C phase at higher chromium exchanges. Thus, for the case of a narrow energy gap between ordered and disordered phase (low transformation temperature), the configurational entropy due to a statistical distribution of the N carbon atoms among the 2N lattice sites available in the hexagonal close-packed Me_2C structure (L'3-type) results in a free energy contribution of $1/2 RT \ln 2 = 1300$ cal per formula weight $MeC_{1/2}$, and thus eliminates the discrepancy. A subsequent intensive search to see, whether or not, the disordering extended to the binary phases, finally resulted in the establishment of order-disorder reactions for Nb_2C , Ta_2C , Mo_2C , and W_2C . (The question, whether V_2C undergoes a related transformation at low temperatures ($< 800^\circ C$), is not yet completely resolved).

C. DISCUSSION OF THE CARBON-RICH EQUILIBRIA IN URANIUM-TRANSITION METAL-CARBON SYSTEMS

An interesting problem was present in connection with the development of the fuel material for the European High Temperature Gas-Cooled Reactor (Dragon). It consisted of the question, whether it would be possible to stabilize the face-centered cubic monocarbide towards graphite by alloying it with other suitable refractory carbides. We recall that in the uranium-carbon system⁽²¹⁾, besides the monocarbide, two-carbon richer phases U_2C_3 and UC_2 exist, of which the latter undergoes a crystallographic transformation at approximately $1800^\circ C$. The resulting CaF_2 -type high temperature modification of UC_2 ultimately forms a complete solid solution with

the monocarbide. The problem was attacked in order to circumvent difficulties which might arise from the volume changes of the dicarbide phase in the transformation process, affecting the stability of the tight pyrolytic graphite shell into which the particles were embedded. Apart from these, as well as other factors, it was hoped that the increased melting temperatures of the alloyed material could improve the high temperature stability of the fuel materials. It was known from previous work, that uranium carbide forms complete solid solutions with a number of isostructural monocarbides^(22, 23, 24); the problem reduced to the question of, at what concentration of the alloying material would the three-phase equilibrium $(U, Me)C_2-(U, Me)C-C$ be replaced by a two-phase range monocarbide-graphite. The general phase-situation observed in these systems is shown in Figure 37.

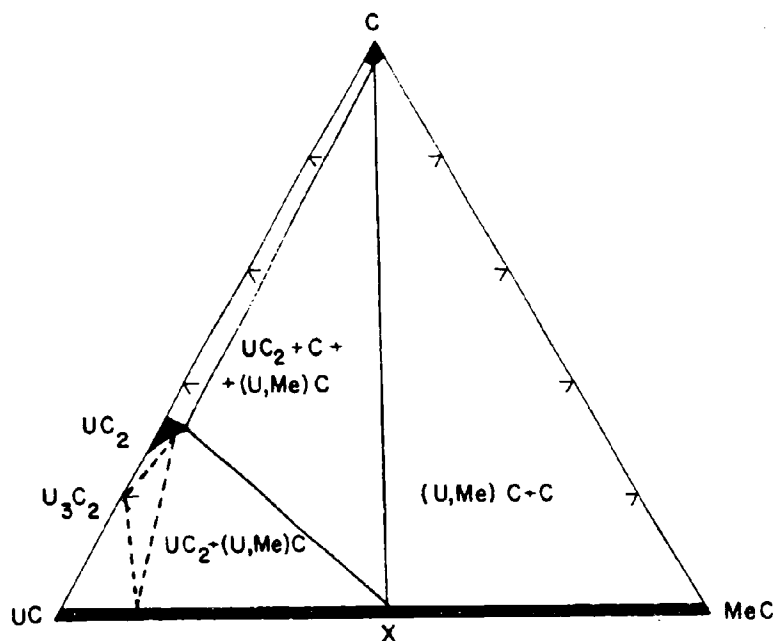


Figure 37. Basic Phase Distribution in the Carbon-Rich Portion of Uranium-Refractory Transition Metal-Carbon Systems.

Since the thermodynamic stability of a dicarbide in the refractory transition metal-carbon systems is considered low, the metal-exchange in UC_2 can, in a first approximation, be neglected. Thermodynamically, the point in Figure 37 is related to the thermodynamical properties of the phases by stability condition (8).

$$(v-w) \bar{F}_{A(u)} + (w-u) \bar{F}_{A(v)} + (u-v) \bar{F}_{A(w)} = 0$$

Applied to this case⁽²⁵⁾

$$\begin{aligned} u &= 1 && \text{solid solution (U, Me)C} \\ v &\approx 1.85 && UC_2 \\ w &\approx \infty && C \end{aligned}$$

we let w approach infinity, and the stability condition becomes

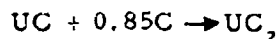
$$\bar{F}_{A(v)} - \bar{F}_{A(u)} = 0$$

i.e. the stoichiometry of the dicarbide does not enter into the result. Separating the partial terms in base and concentration-dependent functions, neglecting eventual metal exchanges in UC_2 , and replacing the free enthalpies by the respective free enthalpies of formation, we obtain

$$\Delta F_{fUC} + \bar{\Delta F}_{UC}^{mix} - \Delta F_{fUC_2} = 0$$

$$\bar{\Delta F}_{UC}^{mix} = \Delta F_{fUC_2} - \Delta F_{fUC} = \Delta F_R$$

The right hand side of the last equation represents the free enthalpy change of the reaction



The exact concentration-dependence of the partial molar free energy of UC in carbide solutions is unknown; however, the following interaction parameter in the vanLaar expression for the regular solution, which were derived from the tie line distributions within the miscibility gaps of pseudo-ternary systems U-Me-C⁽²⁶⁾ may serve as useful approximations to describe the average solution behavior:

$$\epsilon_{\text{UC-ZrC}} = 6,000, \epsilon_{\text{UC-HfC}} = 9,600, \epsilon_{\text{UC-NbC}} = 6,800 \text{ and } \epsilon_{\text{UC-TaC}} = 8,000 \text{ cal/mole.}$$

Approximating the solutions as being regular, we obtain

$$\epsilon_{\text{MeC-UC}} (1-x_{\text{U}})^2 + RT \ln x_{\text{U}} = \Delta F_{\text{R}}$$

x_{U}Uranium exchange in the monocarbide solutions
MeC-UC.

The equilibrium composition x , in effect therefore becomes a function of the free energy change ΔF_{R} . From the available thermodynamic data, ΔF_{R} should have been in the order of -20,000 cal per formula change, corresponding to $x_{\text{U}} < 2$ atomic percent. From these data, an effective stabilization should therefore, not have been expected. However, a closer examination of the values reveals that they are incompatible with the observed, low-temperature decomposition of UC₂, which rather indicated only a small value for ΔF_{R} . This was confirmed by experimental investigations of the phase-relationships in these systems⁽²⁶⁾, and showed the restraining three phase equilibria for the dicarbide to be located in the middle portions of the systems. The vertices of the three-phase equilibrium (U, Me)C-(U, Me)₂C-C at the monocarbide solid solution for the various carbide solutions and a number of different temperatures are presented in Figure 38.

Back calculation of ΔF_R from these phase data, and taking into account the transformation of UC_2 at 1820°, yields after linearization,

$$\Delta F_R = -10,350 - 5.57 T \text{ cal/formula change, } (T = 2100-2300^\circ K)$$

and

$$\Delta F_R' = -7710 - 4.31 T \text{ cal/formula change } (T = 1900-2100^\circ K)$$

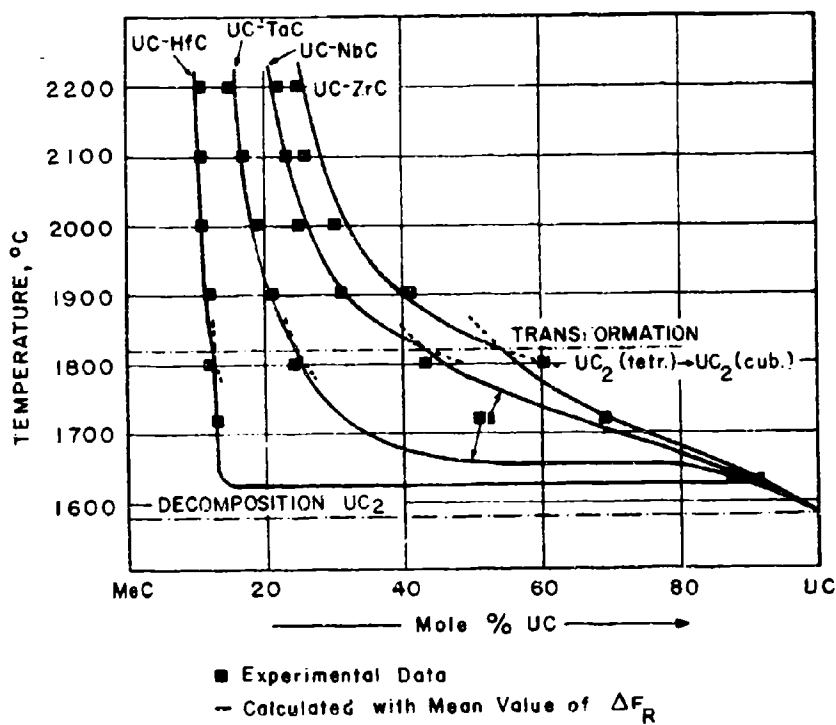
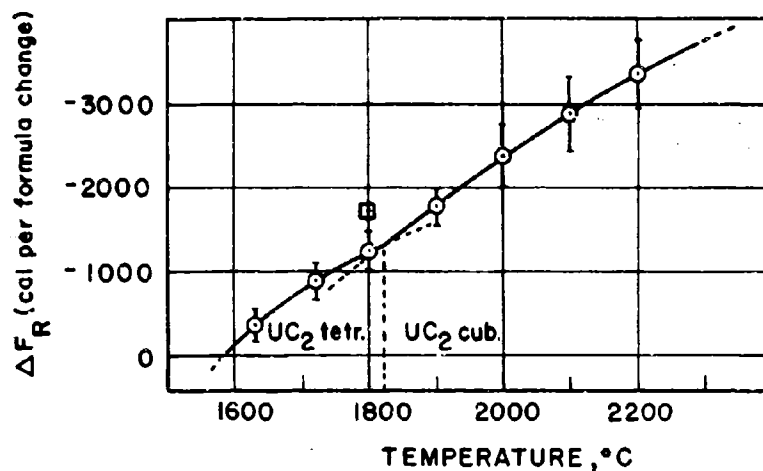


Figure 38. Temperature Dependence of the Graphite-Stable Ranges in Uranium-Containing Monocarbide Solutions.

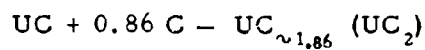
The calculated data for ΔF_R are illustrated in

Figure 39.



- Mean Values
- I Mean Error
- Calculated from the System U-N-C

Figure 39. Free Enthalpy Changes for the Reaction



(Data Calculated from Phase Diagrams U-Me-C)

The free enthalpy of transformation of the tetragonal into the cubic modification of UC_2 is given by the difference of $\Delta F_R'$ and ΔF_R ; we obtain, as a first approximation, from the data given above:

$$\Delta F_{\text{tr}} = 2640 - 1.26 T \text{ cal/mole UC}_2$$

The phase diagram data, calculated with the mean values of ΔF_R and ΔF_R^1 are in excellent agreement with the experiment (Figure 38). The binary temperature stability limit T_c for the tetragonal UC_2 -phase is given by

$$\Delta F_R^1 = 0$$

$$T_c = 1550^\circ\text{C}$$

and agree well with the experiment⁽²⁵⁾. Also, more recent thermochemical values for the free enthalpies of formation of the uranium carbides^(27,28) closely confirm the data derived from the phase diagrams.

V. GENERAL DISCUSSION OF THE PHASE RELATIONSHIPS IN
TERNARY SYSTEMS OF REFRACTORY TRANSITION METALS
WITH B-ELEMENTS

A. METAL-CARBON SYSTEMS

During the past few years, temperature sections for a large number of ternary transition metal-carbon alloys have been investigated or calculated. Their detailed evaluation, however, would exceed the framework of the present discussion, and, therefore, reference is made to the literature compilation at the end of the text⁽³⁹⁾. In general, the previous investigations cover only one temperature section of the system, and the investigation of complete systems has been initiated only recently under the sponsorship of the Wright-Patterson Air Force Materials Laboratory.

As a rule, no ternary phases are formed in the ternary carbide systems, i.e. the ternary phase relationships are governed by the binary

compounds. Where the radius-ratio rule is fulfilled, the isostructural monocarbides of the group IV and group V transition metals form complete series of solid solutions. In the systems involving the group VI metals, the cubic (B1) phases are stable at high temperatures only, and, therefore, the homogeneity ranges of the cubic solution are temperature-dependent; above the eutectoid temperatures, however, which are 1960°C for α -MoC_{1-x} (B1), 2530°C for α -WC_{1-x} (B1), solid solution formation with the other cubic monocarbides is complete.

As for the subcarbides, complete solid solutions at higher temperatures are formed between the Me₂C-phases of the group V metals as well as between V₂C and Mo₂C, and V₂C and W₂C, respectively. In the carbon systems of niobium and tantalum with the heavier group VI metals, the subcarbide solid solutions are unstable in respect to mechanical mixtures of monocarbide and metal solution, but Me₂C single phase fields tend to increase with temperature, or even show a continuous transition, as found for the Ta-W-C system⁽¹²⁾. In the group IV metal-carbon systems, the Me₂C-phases are unstable in respect to mixtures of metal + monocarbide; the ternary homogeneity ranges of the Me₂C phases in systems Me₁ (V, VI)-Me₂(IV)-C are therefore restricted.

In the ternary systems Me₁(group V or VI)-Me₂C(group IV)-C, due to the instability of the Me₂C-phase in the binary carbon systems of Ti, Zr, and Hf, the ternary homogeneity ranges of the Me₂C-phases are very restricted.

In their basic layout, the ternary systems involving chromium are similar to the molybdenum-containing systems, although the phase

distribution near the Cr-C edge systems are somewhat modified as a result of the different structural characteristics of the chromium carbides.

The high temperature phase relationships in all ternary metal-carbon systems are complicated by the fact that in many of them even the solid-state equilibria change rapidly with temperature, and the order-disorder-transformations in the Me_2C -phases proceed as concentration-temperature dependent reactions in the ternary phase fields. A few phase diagrams, together with their reaction diagrams and liquidus projections, which were taken from the work referenced in (10), may serve to illustrate the general appearance of the complete constitution diagrams (Figures 40 through 48).

In neither of the previously indicated systems⁽³⁰⁾ do melting point maxima of the monocarbide solid solutions occur, and earlier findings are related to the fact that maximum melting of the interstitial monocarbides does not occur at stoichiometry, i. e., melting of the ternary alloys is a function of the metal as well as the carbon concentration (Figure 49).

B. METAL-BORON SYSTEM

Many of the structural characteristics of the intermediate phases, are repeated throughout the systems of the group IV to the group VI metals; hence, where these conditions prevail, and the radius ratios are within the tolerable limits, complete solid solutions usually are formed. The stability of the borides decreases with increasing group number; consequently, the selectivity of the metal-exchange increases upon combining group IV with group V or group VI metal borides.

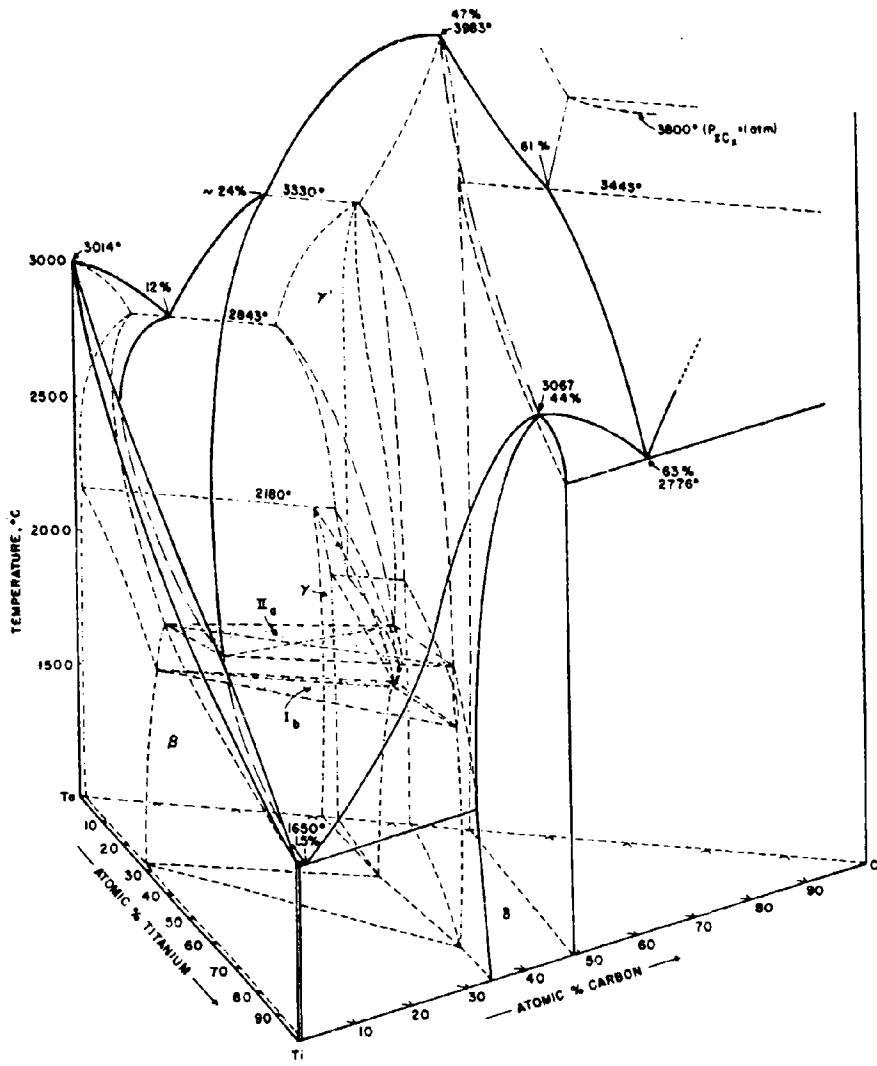


Figure 40. Constitution Diagram Titanium-Tantalum-Carbon.
 (C.E. Bruki and D. P. Harmon, 1965)⁽¹⁰⁾

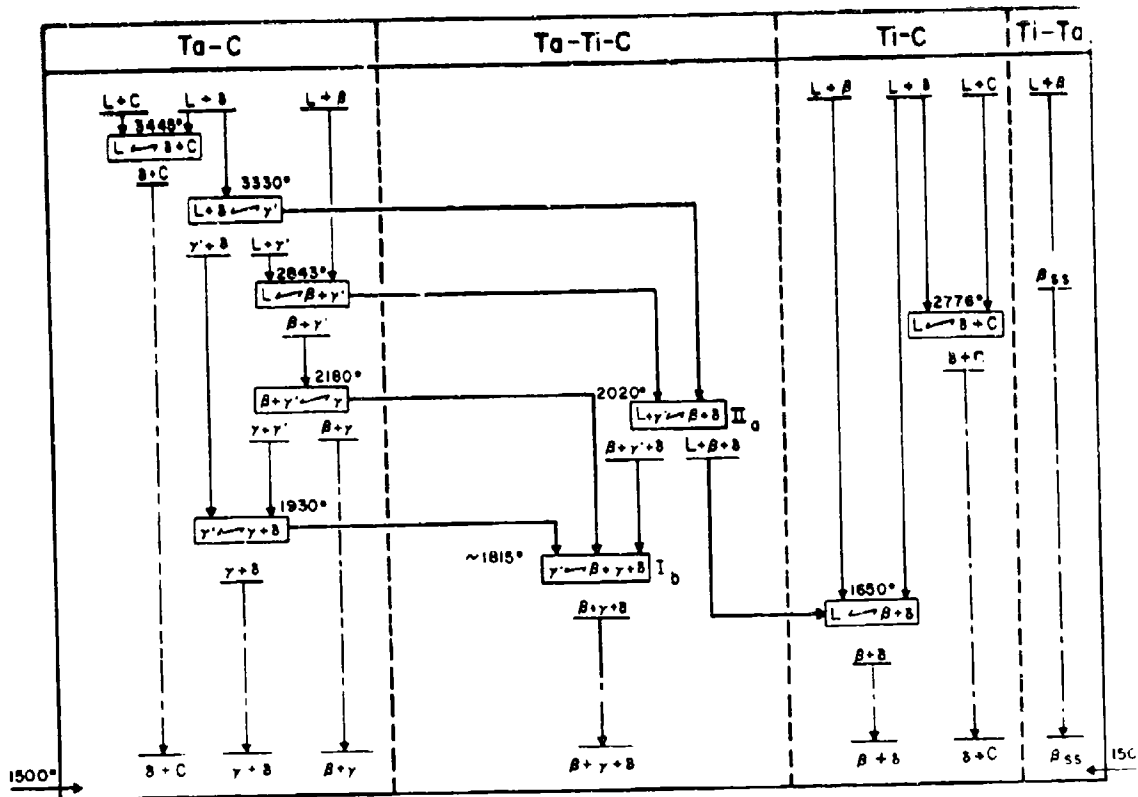


Figure 41. Scheil-Schultz Reaction Diagram for the Ti-Ta-C System

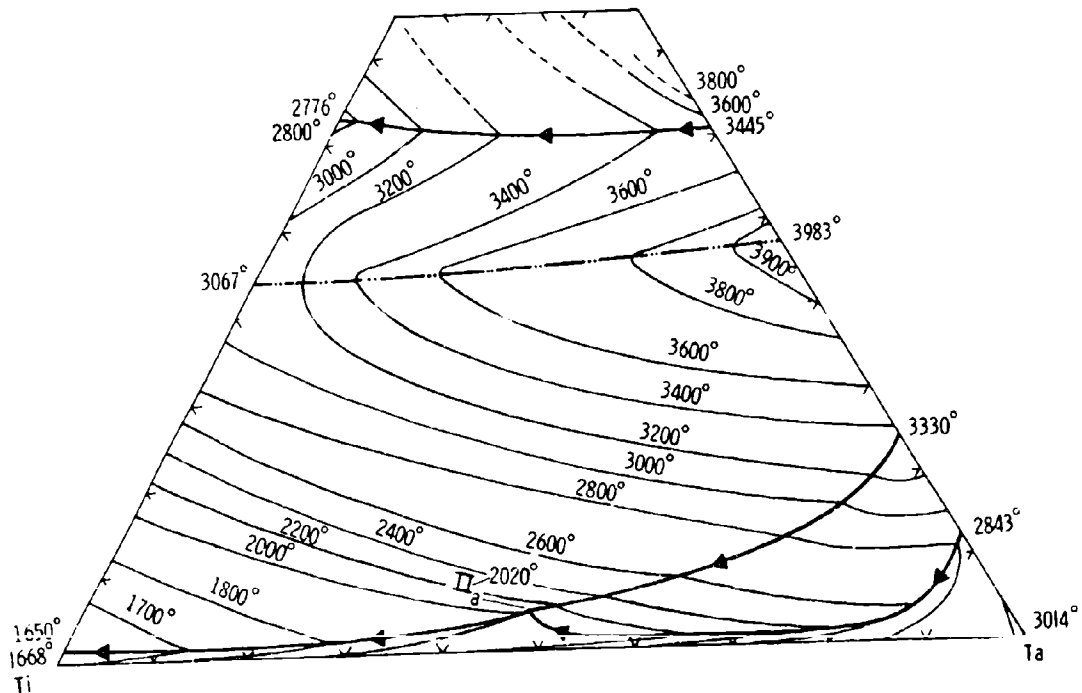


Figure 42. Liquidus Projections in the Ti-Ta-C System.

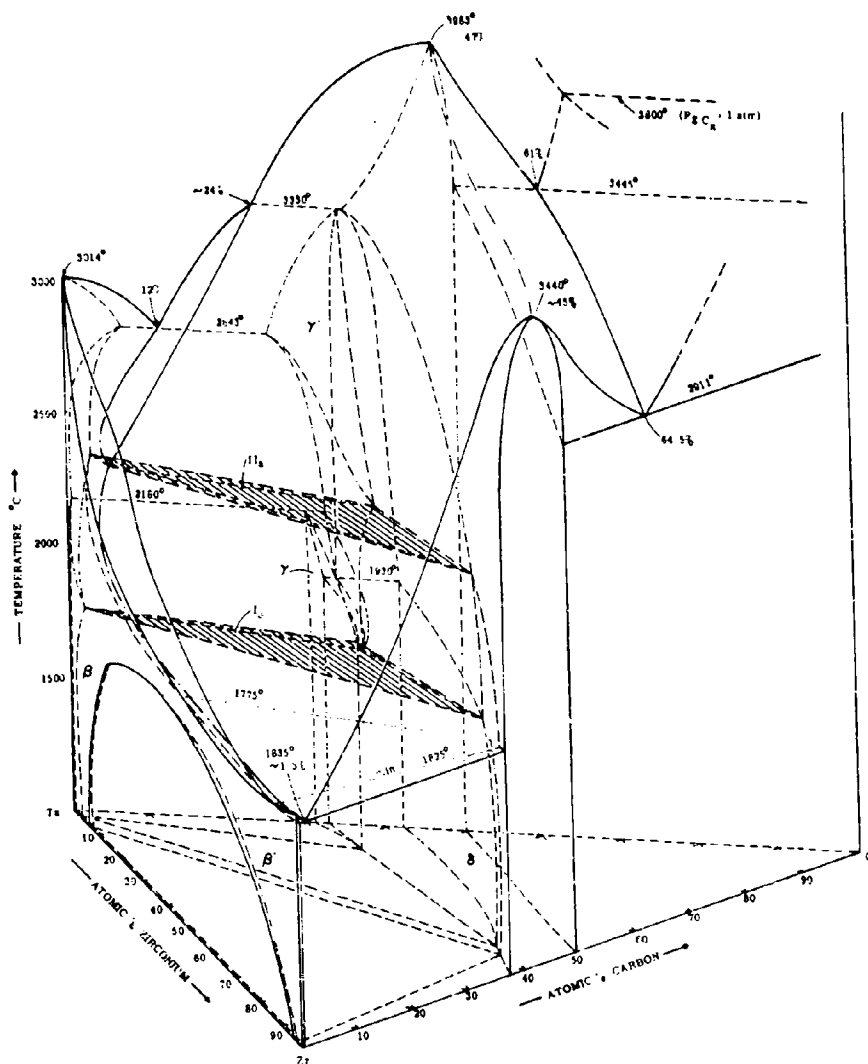


Figure 43. Constitution Diagram Zirconium-Tantalum-Carbon.
 (D. P. Harmon and C. E. Bruhl, 1965)⁽¹⁰⁾

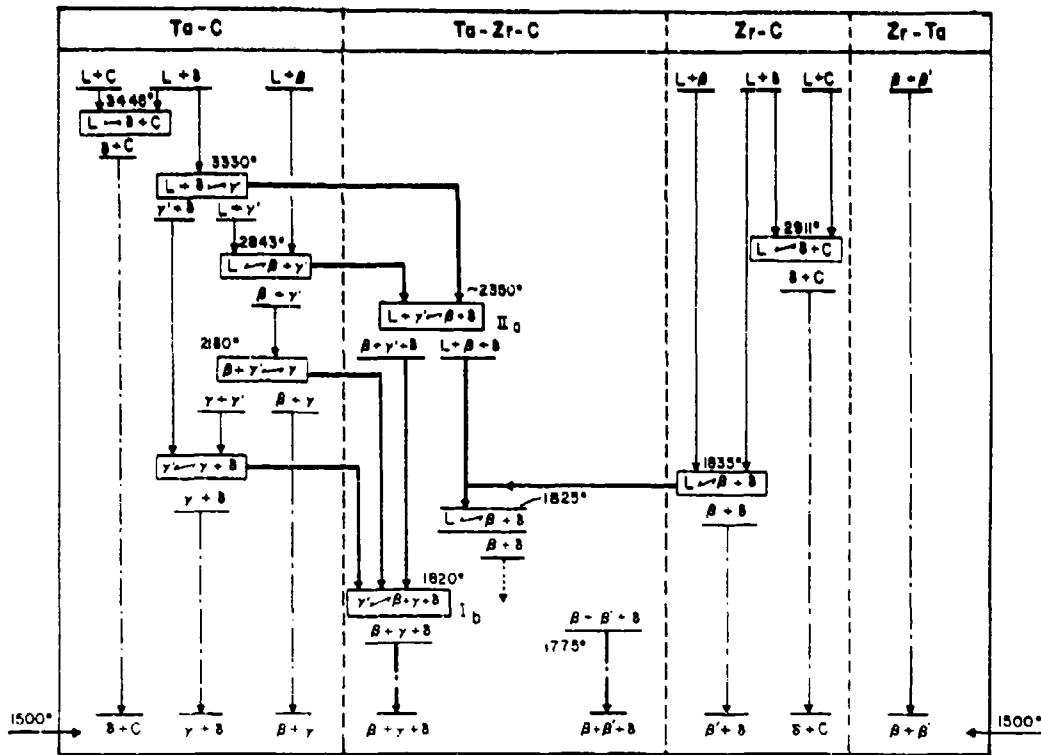


Figure 44. Scheil-Schultz Reaction Diagram for the Zr-Ta-C System.

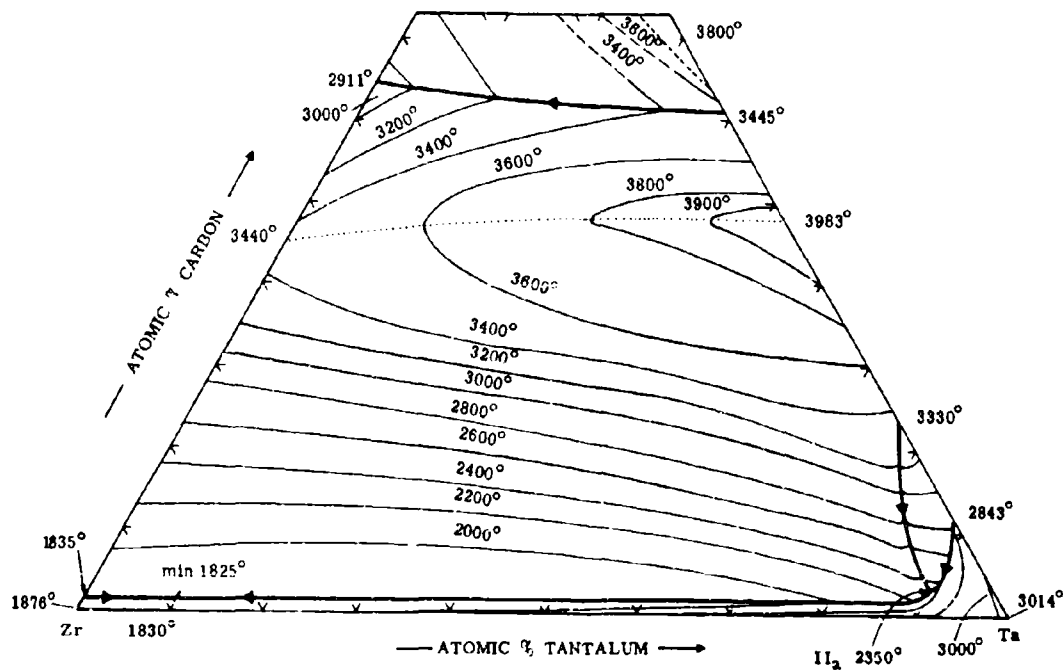


Figure 45. Liquidus Projections in the Zr-Ta-C System.

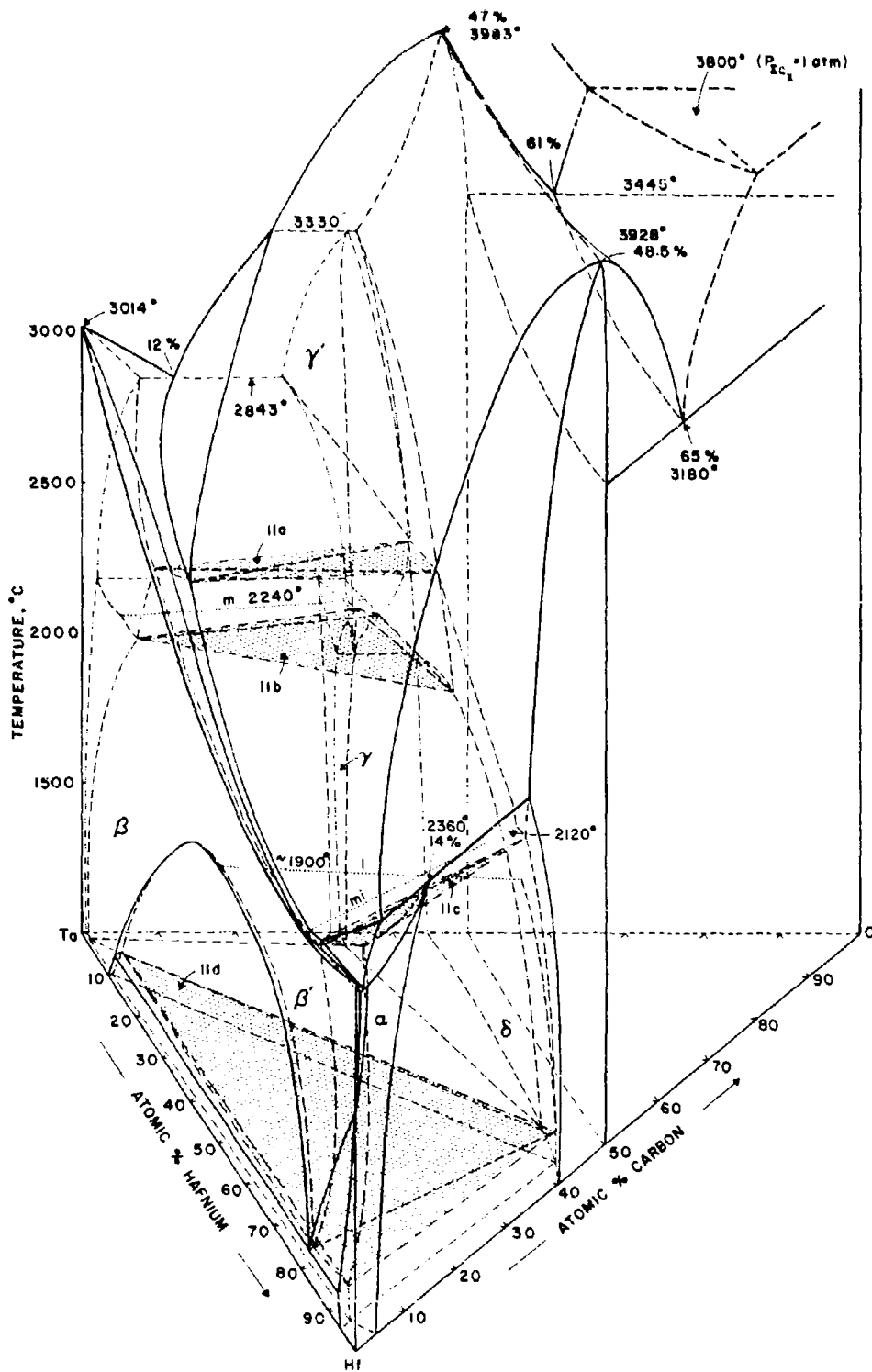


Figure 46. Constitution Diagram Hafnium-Tantalum-Carbon
(E. Rudy, 1965) (10)

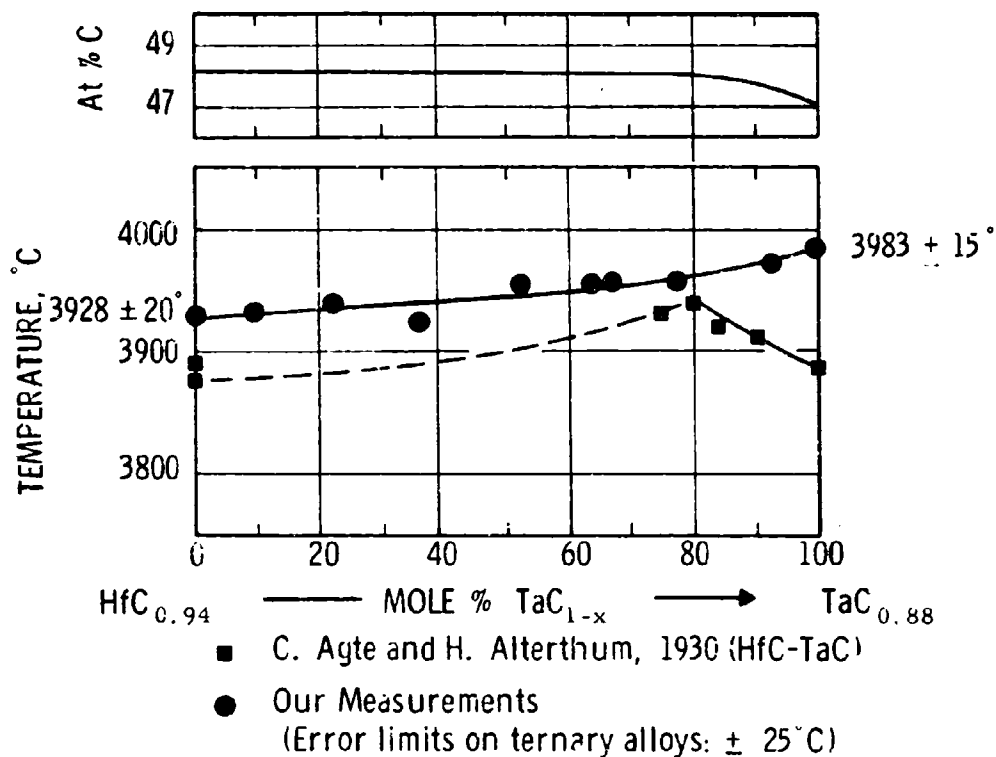


Figure 49. Maximum Solidus Temperatures for the $(Ta,Hf)C_{1-x}$ Monocarbide Solution.

Top: Concentration line of maximum melting.

Apart from the technically most interesting group IV metal-boron systems which presently are being investigated under Air Force sponsorship⁽¹⁰⁾, very little experimental work has been performed in this system class. The phase relationships in the Zr-Hf-B system, which are representative of the phase behavior of all ternary group IV metal borides, are shown in Figures 50, 51, and 52.

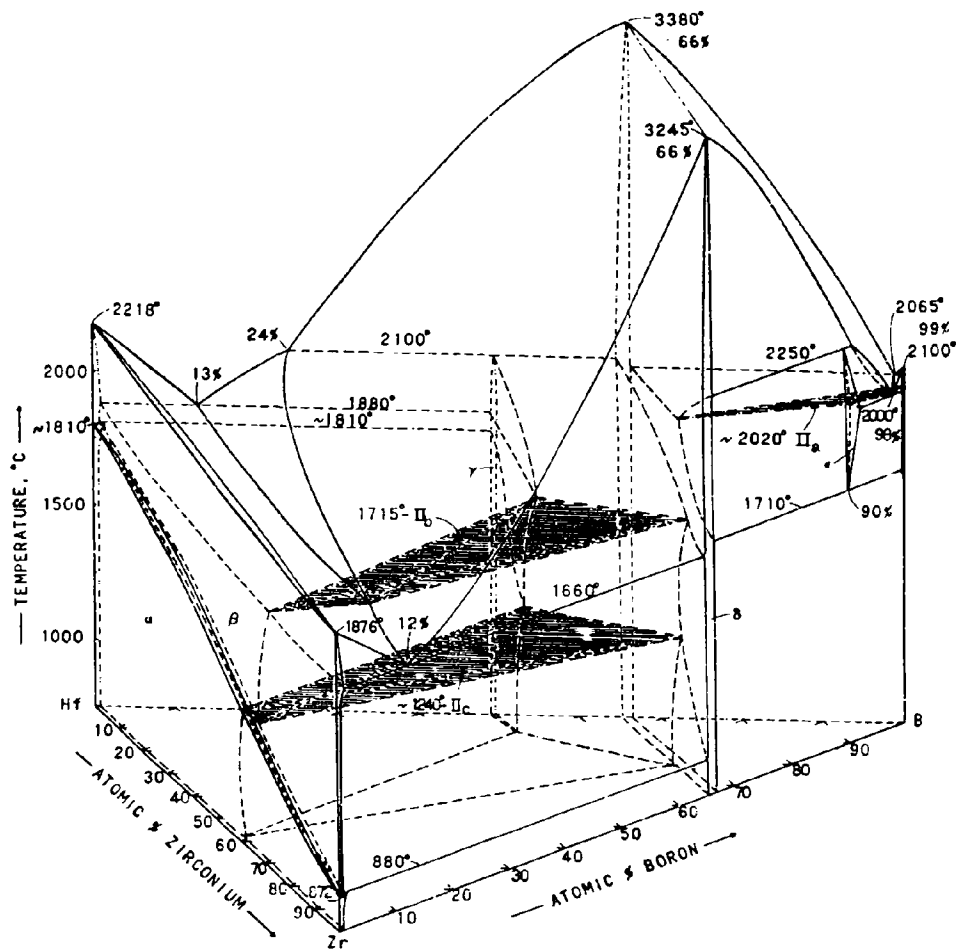


Figure 50. Constitution Diagram Zirconium-Hafnium-Boron
(D.P. Harmon, 1965)⁽¹⁰⁾

C. REFRACTORY TERNARY SYSTEMS INVOLVING A TRANSITION METAL AND TWO B-ELEMENTS.

The group of systems considered are Me-X₁-X₂, where Me stands for a refractory transition metal, and X₁ and X₂ are either N, C, Si, or B.

Interstitials, such as oxygen and hydrogen, as well as other elements, which to a certain degree might be equivalent to one of the elements listed above and hence would fall into the same category, have been omitted since they form either comparatively low-melting phases, or gaseous reaction products with the other B-elements at high temperatures (O-Si, N, C).

Nitrogen in the refractory transition metals behaves similarly to carbon, and a large number of interstitial compounds formed by this element are isostructural with the carbides. Hence, extended or complete intersolubility between nitrides and carbide phases is observed⁽¹⁹⁾.

Nitrides and carbides on the one hand, and borides as well as silicides on the other, are quite different in their structural characteristics. Solid solution formation between these compounds usually is very restricted, indicating high mutual transformation or disproportionation energies of the lattice structures. The silicon-containing systems are further characterized by the appearance of carbon (nitrogen, oxygen, boron)-stabilized ternary phases⁽¹⁹⁾.

Although for the majority of the systems isothermal sections are available from previous work⁽¹⁹⁾, the high temperature portions of the majority of the ternary alloy systems are still unknown, and even a number of binary systems would require extensive revision. High temperature portions

of selected ternaries of these system classes are presently being investigated under current Air Force programs⁽³²⁾. From these systems, in particular the borocarbides of the group IV metals have recently become of interest in the development of oxidation-resistant graphites. Important equilibrium characteristics of these systems are the formation of pseudo-binary systems of the diborides with graphite and B_4C . Examples of the latter system group are given in Figures 53 through 61.

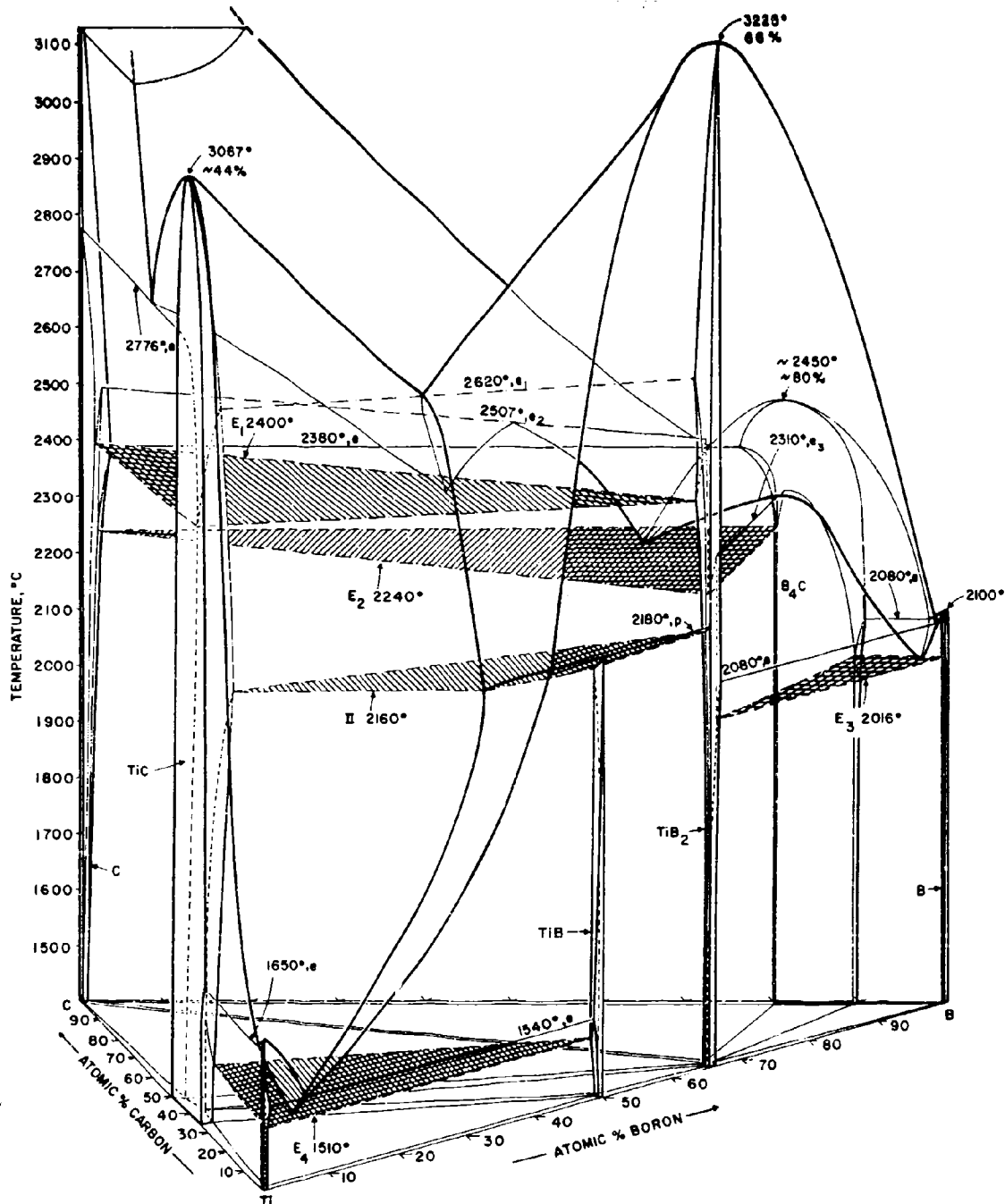


Figure 53. Constitution Diagram Titanium-Boron-Carbon.
(E. Rudy and St. Windisch, 1965) (10).

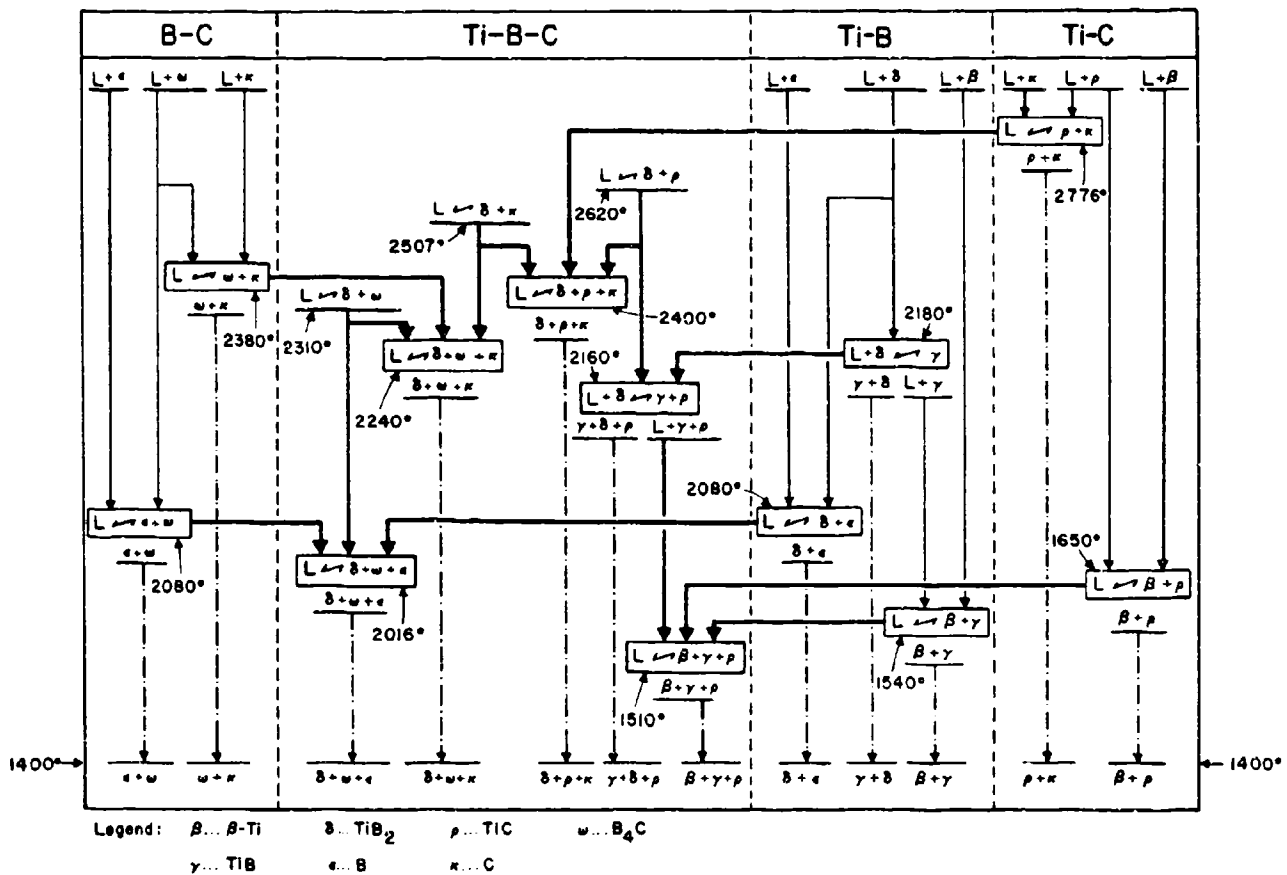


Figure 54. Schell-Schultz Reaction Diagram for the Titanium-Boron-Carbon System.

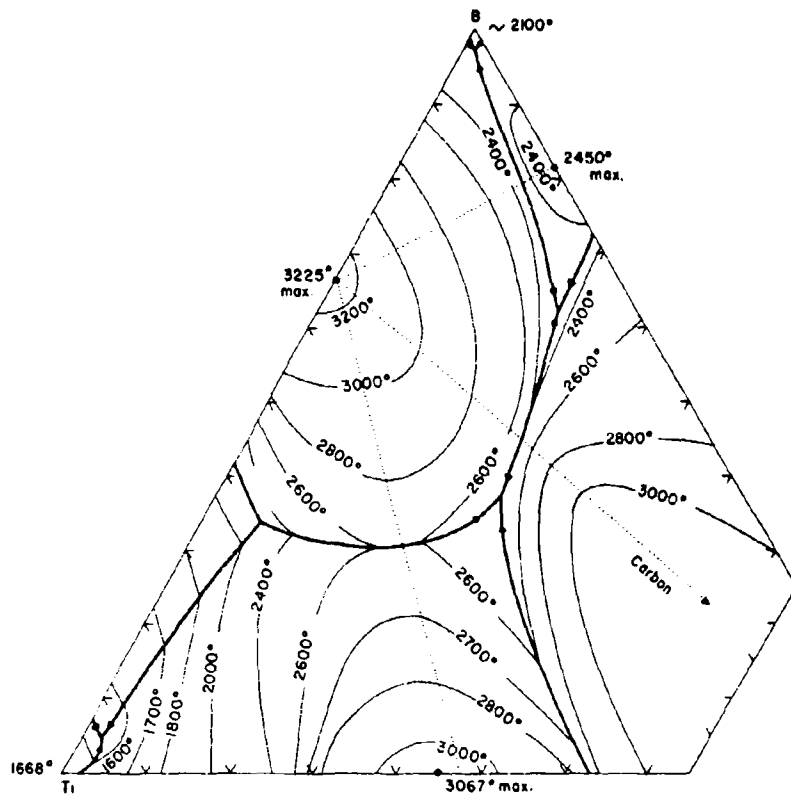


Figure 55. Liquidus Projection in the Ti-B-C System.

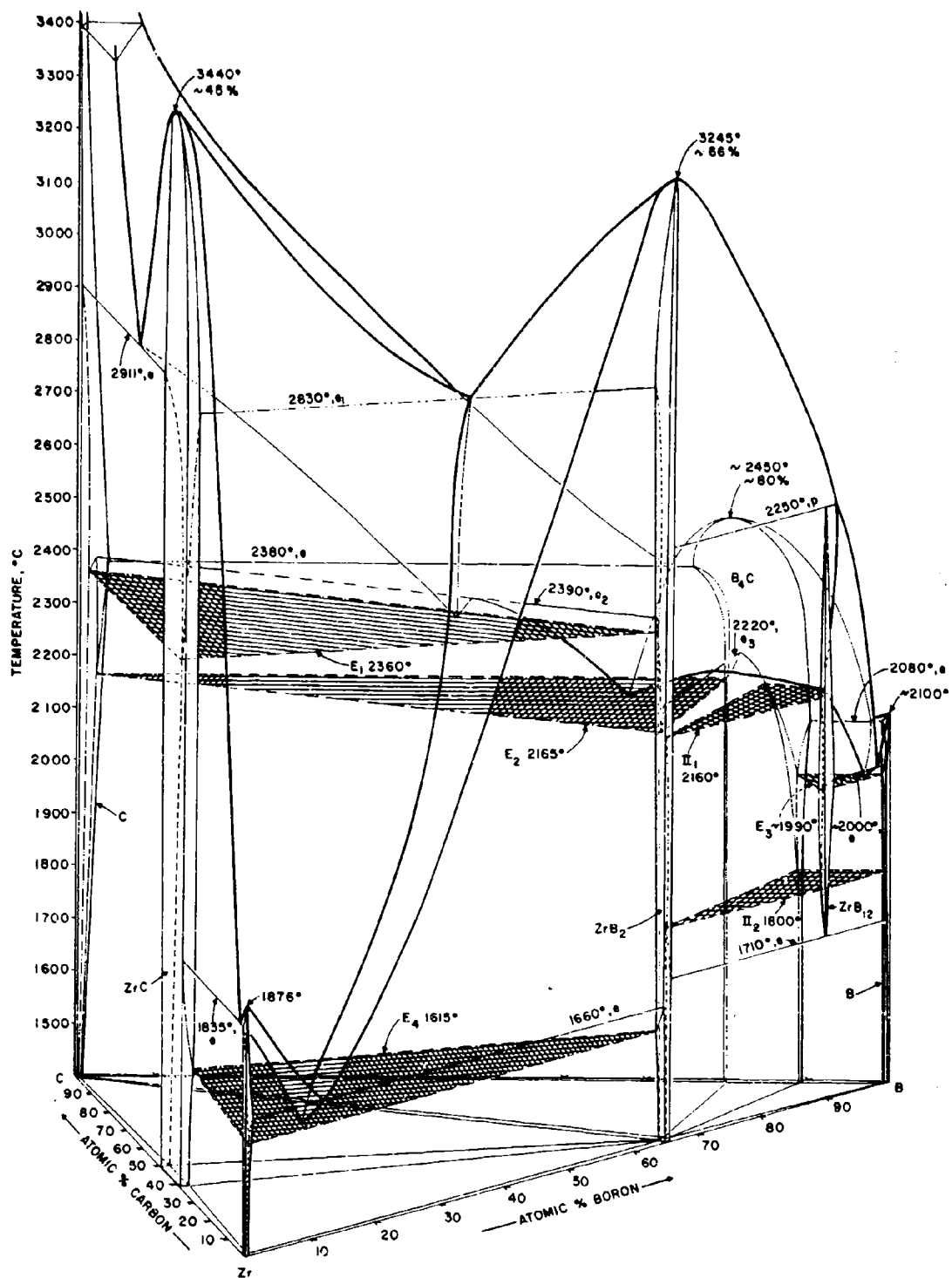


Figure 56. Constitution Diagram Zirconium-Boron-Carbon
(E. Rudy and St. Windisch)⁽¹⁰⁾

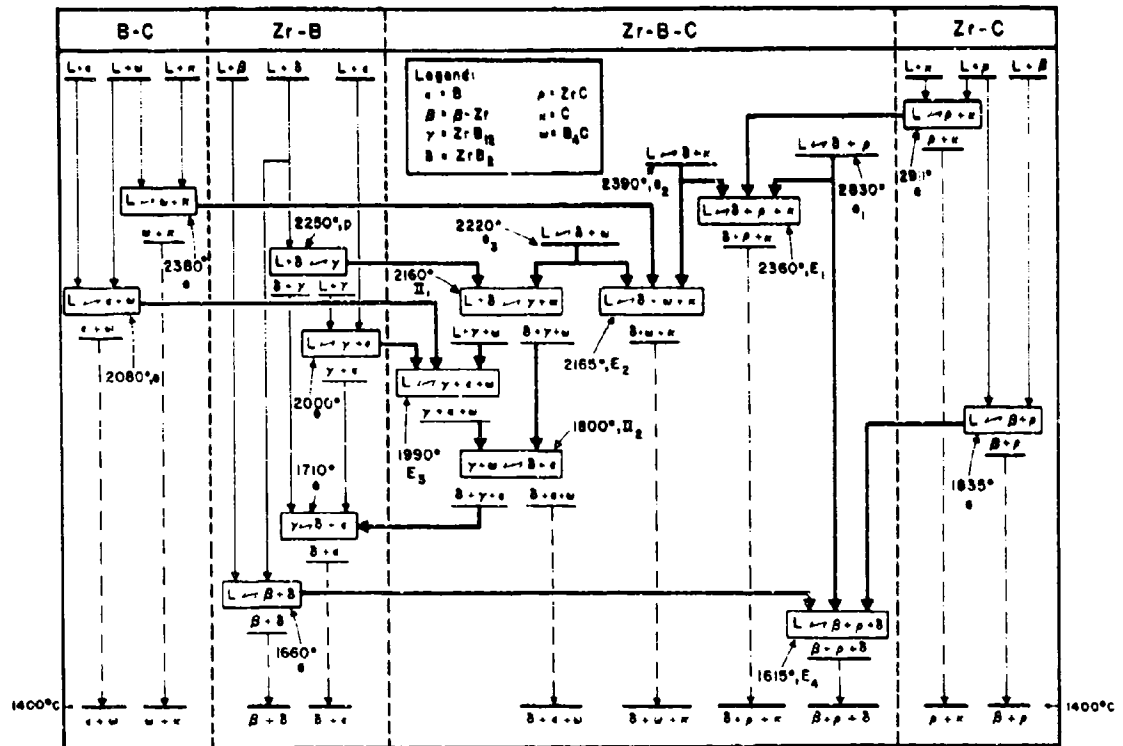


Figure 57. Scheil-Schulz Reaction Diagram for the Zirconium-Boron-Carbon System.

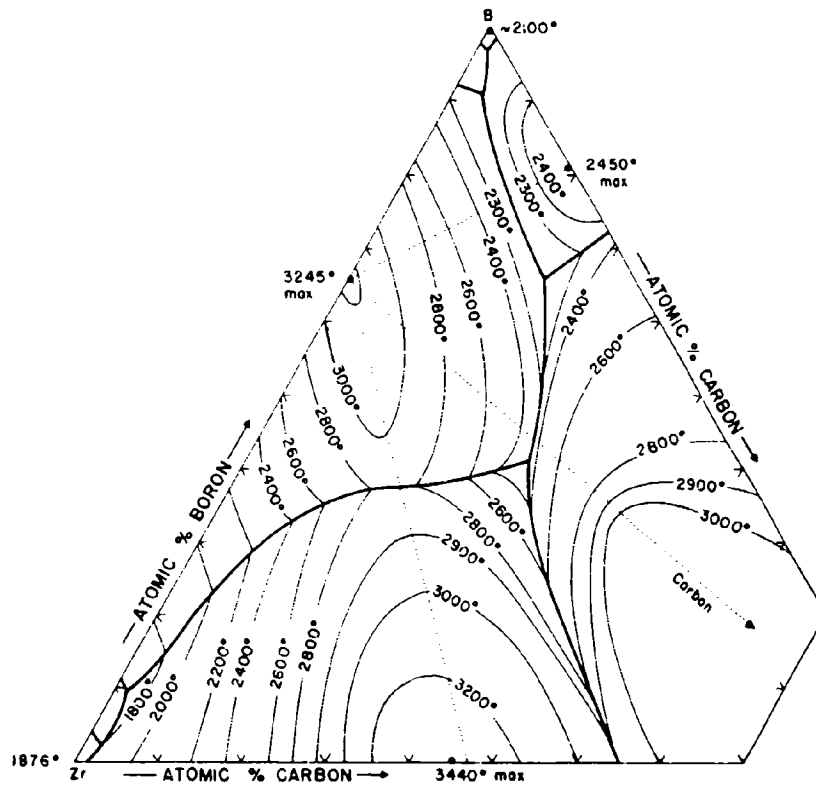


Figure 58. Liquidus Projection in the Zr-B-C System.

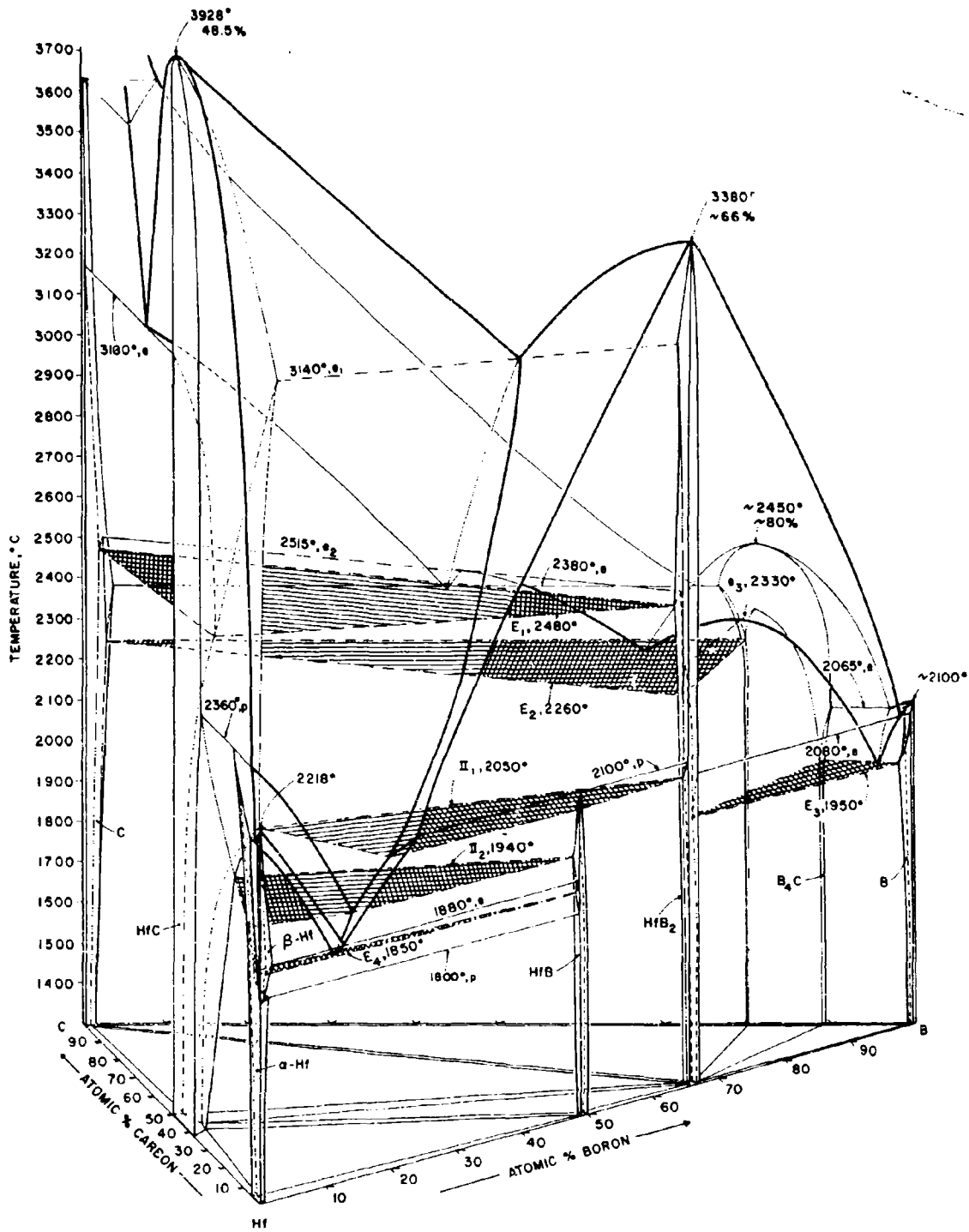


Figure 59. Constitution Diagram Hafnium-Boron-Carbon.
 (E. Rudy and St. Windisch, 1965)⁽¹⁰⁾

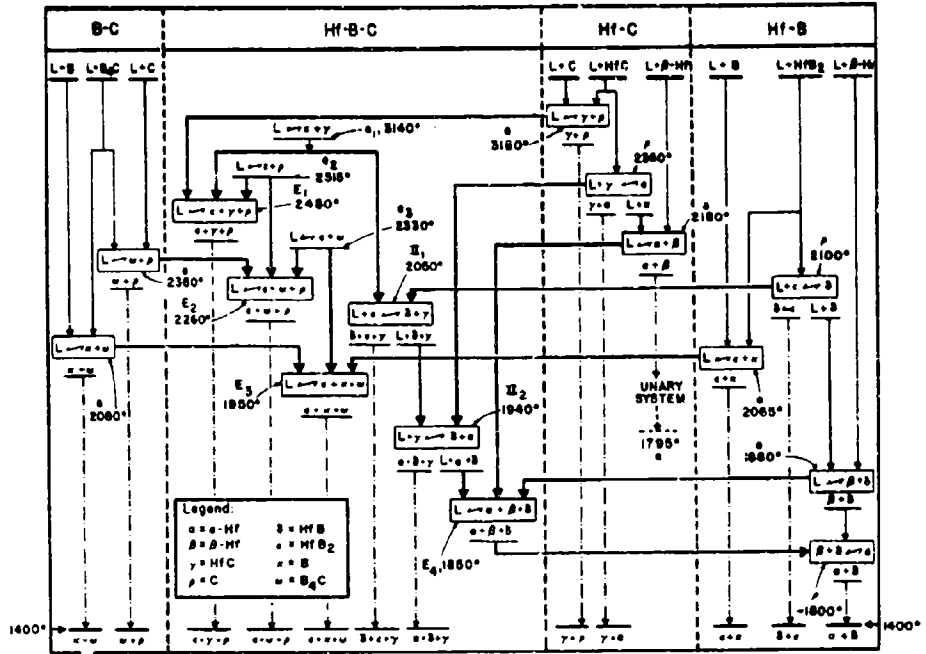


Figure 60. Scheil-Schulz Reaction Diagram for the Hf-B-C System.

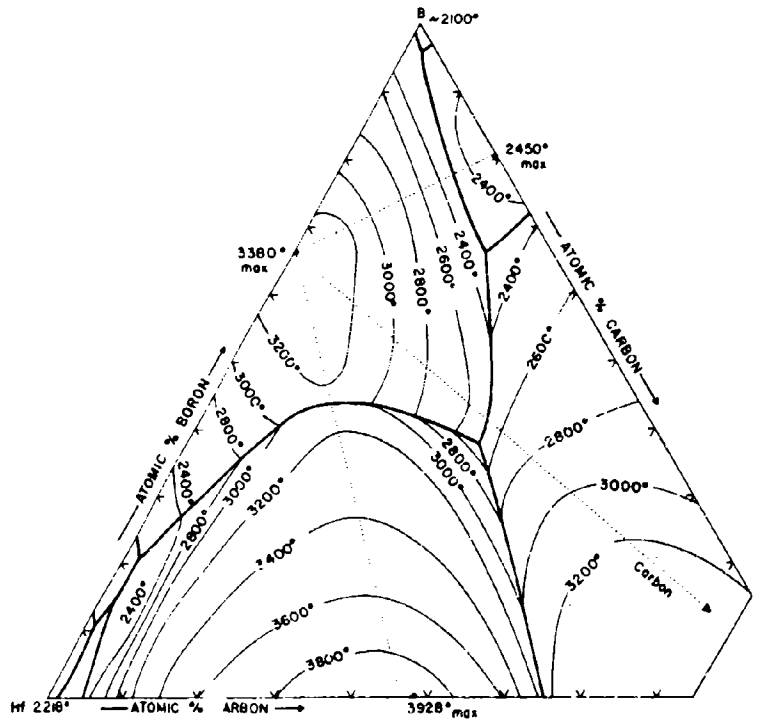


Figure 61. Liquidus Projections in the Hf-B-C System.

VI. NOTES ON THE RELATION OF PHASE DIAGRAM DATA TO APPLICATION PROBLEMS

The purpose of a constitution or phase diagram of a system is to depict in condensed form the equilibria existing between the phases in the given alloy system. Consultation of the phase diagram will tell us, whether or not, or to what extent, given alloy mixtures will undergo reaction when heated to temperatures and for times which are sufficient to allow equilibration to take place. The information is quantitative with respect to the nature and composition of the phases. A phase diagram, combined with kinetic data, provides us with a whole spectrum of means to modify the properties of alloys, of which extensive use has been made in the past. However, the increasing demand for materials capable of operating for prolonged lengths of time at extremely high temperatures has introduced additional variables which have to be taken into consideration. In reviewing problem areas in the field of high-temperature materials, oxidation-resistant coatings, etc., it is seen that the main problem is not so much found in not having materials with any of the desired properties, but rather in the lack of a single-phased material, which combines all of the necessary properties. The conception of a composite, or heterogeneous system, therefore, involves the task of combining, the beneficial properties of a number of constituents within a quasi-homogeneous structure without degradation.

Consideration of a composite system always implies a certain degree of pre-fixation, since we normally have a certain base material already in mind. The main problem to be solved concerns the modification of certain undesirable properties, so that the system will be capable of performing under the prescribed

condition. Typical cases may involve the protection of exposed surfaces from corrosive gas attack, reinforcement of ceramic or plastic structures, and transpiration systems, etc. Each case may have its specific extra requirements, thus placing further restraints upon the usability of particular material systems; however, chemical compatibility between the alloy phases will be an eliminative prerequisite if the conditions are such, that non-equilibrium states cannot be maintained over significant lengths of time. The recognition of such prerequisites, their experimental and/or theoretical rationalization, and, as a result, the establishment of an effective elimination and selection system, constitutes an important first step in an intelligently conducted attack on the problem. The largest part of the information required for the initial screening can be obtained from phase diagrams, and the only possible, or the optimum, compositions determined from the existing phase relationships. Detailed phase diagram information is also necessary in order to predict the reaction paths in a system of reacting species. While phase compatibility can prevail between only two phases in binary systems, the additional degree of freedom in ternary alloys allows much wider variations in the equilibria formed. Obviously, the multiplicity of combinations becomes still greater in higher order alloys. Without going into too great detail, we shall try qualitatively to demonstrate on a simple example the variety of reactions, which may occur in two-phased ternary alloys having the same overall composition.

For this purpose, let us arbitrarily assume a diffusion couple made up of interstitial phase solutions $(A,B)C_u$ and $(A,B)C_v$. We shall choose the starting compositions (dashed line in Figure 61) so that a conjugate system is formed with respect to the equilibrium compositions X_{e_I} and $x_{e_{II}}$.

To make the example more concrete and easier to follow, we may, for example, think, that $u = 0$ (metal solution), and $v = \frac{1}{2}$ (thus making it, if C stands for carbon, a Me_2C solid solution). Equilibrium in the couple

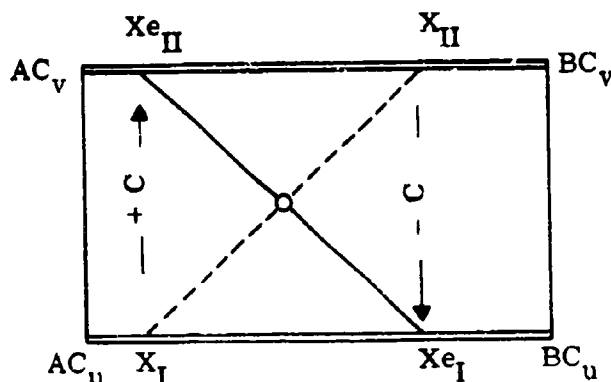


Figure 62. Conjugate Diffusion Couple, Consisting of Two Ternary Solutions $(A, B)C_u$ and $(A, B)C_v$.

(Equilibrium by Interstitial Atom Diffusion)

will be attained, if the composition of the solution $(A, B)C_v$ reaches $X_{e_{II}}$, and that of $(A, B)C_u$ assumes the equilibrium composition, denoted by X_{e_I} .

We first consider the following extreme cases:

- a. The interstitial atom C is the only diffusing species in the system.
- b. The diffusion current is carried only by metal atoms (A, B)

In process (a), equilibration can only be achieved by migration of carbon atoms across the metal-carbide interface (Figure 62); thus, the subcarbide solution, having the non-equilibrium starting composition X_{II} , gradually gets converted

into a metal solution with the equilibrium concentration X_{e_I} . Simultaneously, the transfer of carbon atoms results in a carburization of the metal solution (starting composition X_I) into a subcarbide solution of the equilibrium composition $X_{e_{II}}$. The ultimate result is a complete phase interchange (Figure 63).

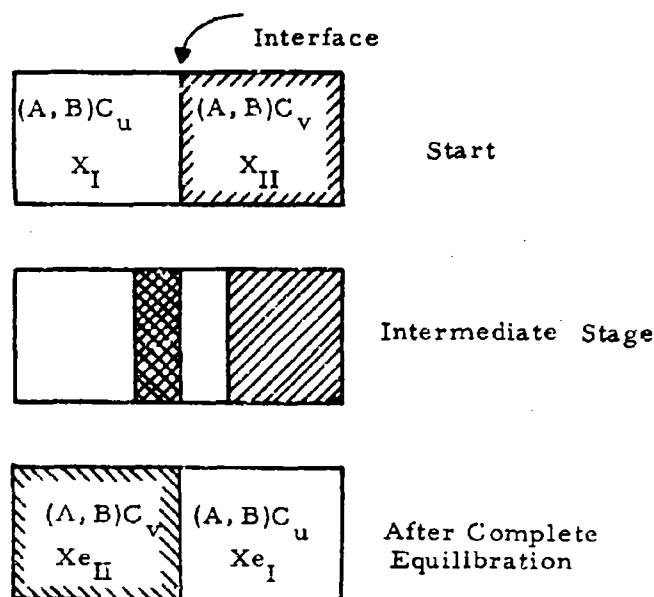


Figure 63. Phase Interchange in a Conjugate Ternary Diffusion Couple, for the Case that the Interstitial Atom C is the Only Diffusing Species.

Considering the second case, we see that the compositions of the individual phases gradually change along the lines indicated by the arrows in Figure 64, until the equilibrium concentrations X_{e_I} and $X_{e_{II}}$ are finally reached. We note, that for host atom diffusion both phases do not physically interchange.

In practice, we never will have to deal with either extreme, but generally will be confronted with a superposition of both types. However,

assume now, that, without changing the overall composition of the couple as well as the position of the equilibrium tie line, we had chosen the initial compositions of the couple such that $X_I = X_{II}$, i.e., equal exchanges of A and B in both solutions. Exchange of the interstitial atom would not produce any decrease in the total free energy of the diffusion system; hence, no net transfer of interstitial atoms would occur, and equilibration would take place via diffusion of atoms A and B only.

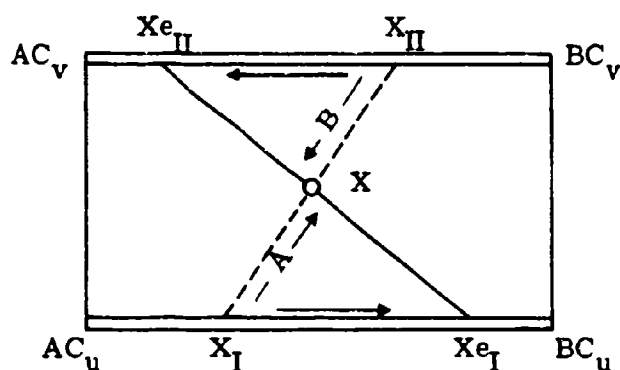


Figure 64. Equilibration by Host (A,B) Atom Diffusion in a Ternary Diffusion Couple $(A,B)C_u + (A,B)C_v$.

A closer analysis of the assumed example will reveal, that for all compositions lying between the line $X_I = X_{II}$ and the equilibrium compositions X_{e_I} and $X_{e_{II}}$, and regardless of the magnitude of the diffusion coefficient for the interstitial phase, the diffusion current would be carried only by the host atoms (Figure 65). For concentrations on the opposite side of the dividing line $X_I = X_{II}$, equilibration will take place by a combination of host and interstitial atom diffusion resulting in at least a partial phase interchange. Thus, in spite of the fact, that no structural changes, or additional phases are

involved, the physical appearance and phase distribution of the ultimately equilibrated alloy will vary significantly with the initially chosen starting compositions.

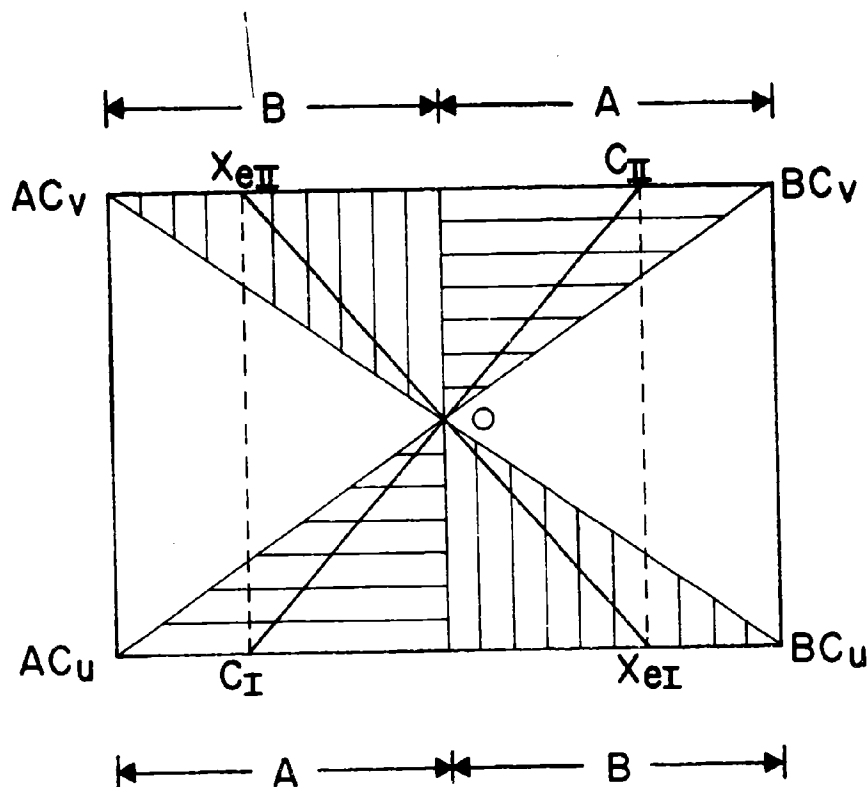


Figure 65. Effect of Composition Upon the Equilibration Reactions in a Ternary Diffusion Couple $(A,B)C_u + (A,B)C_v$ ($c =$ Interstitial Element)

O ... Overall Composition of the Couple

$X_{eI} X_{eII}$... Equilibrium Tie Line

$\overline{C_I C_{II}}$... Conjugate Compositions

Vertical Shading ... Host Atom Diffusion Only

Horizontal Shading... Host + Interstitial Atom Diffusion (Partial Phase Interchange)

Since the type of diffusion proceeding at the couple interface is — apart from the variation of the composition — dependent on the course of the tie lines, the diffusion process is closely linked to the equilibrium conditions prevailing in the system. We will, however, not pursue these questions any further at this time, but emphasize the principal recognition of these factors for the solution of practical diffusion problems. The possibility, to derive free energy gradients for the interpretation and quantitative evaluation of diffusion data, by combining the thermodynamic approaches described in the previous chapters with pertinent phase information, shall only be mentioned

VII. CONCLUDING REMARKS

Although the presently available experimental and theoretical material is still insufficient to allow a fairly complete correlation of phase diagram with thermodynamic data, it has been shown that with relatively simple thermodynamic approaches, useful information regarding phase stability can be derived, and in turn applied to evaluate the phase relationships in still unknown systems. The examples given also show some of the difficulties encountered in applying mathematical models to actual systems; they reveal the need for more complete and accurate data to enable more refined calculations. In many instances this will require an extension of the measuring techniques to higher temperatures in order to account for thermal effects due to excitation of other internal degrees of freedom.

REFERENCES

- 1 E. Rudy: Z. Metallkde 54 (1963), 112.
- 2 Compare the Treatment of Corresponding Cases by
J.L. Meijering: Acta Met. 4 (1956), 249
J.L. Meijering and H.K. Hardy: ibid. 5 (1957), 257
J.L. Meijering: Philips Res. Rept. 5 (1950), 333
J.L. Meijering in: "The Physical Chemistry of Metallic
Solutions and Intermetallic Compounds, Vol. II. (Her
Majesty's Stationery Office, London, 1959)
E. Rudy, H. Nowotny, R. Kieffer, F. Benesovsky, and
A. Neckel: Mh. Chem. 91 (1960), 176
- 3 L.S. Darken and R.W. Gurry: Physical Chemistry of Metals
(McGraw-Hill, New York, 1953).
- 4 W. Schottky and C. Wagner: Z. Phys. Chem. B11 (1930), 163.
- 5 L. Kaufmann, H. Bernstein, and A. Sarney: ASD-TR-6-445, Part IV
(1963).
- 6 C. Wagner: Thermodynamics of Alloys (Addison-Wesley, Reading,
Mass, 1952).
- 7 J.S. Anderson: Proc. Roy. Soc. A 185 (1946) 69.
- 8 A.L.G. Rees: Chemistry of the Defect Solid State (Methuen, London, 1955).
- 9 E. Rudy, St. Windisch, and Y.A. Chang: AFML-TR-65-2, Part I, Vol. I,
(Dec, 1964).
- 10 Ternary Phase Equilibria in Transition Metal-Boron-Carbon-Silicon
Systems. Contract AF 33(615)-1249, Air Force Materials Laboratory,
Wright-Patterson Air Force Base. Report Series AFML-TR-65-2,
Parts I, II, and IV. (1964 to 1966).
- 11 E. Rudy, El. Rudy, and F. Benesovsky: Mh. Chem. 93 (1962), 1776.
- 12 E. Rudy: AFML-TR-65-2, Part II (Jan 1966).
- 13 H. Buckle: Z. Metallkde 37 (1946), 53
- 14 C.H. Schramm, P. Gordon, and A.R. Kaufmann: Trans. Amer. Inst.
Min. Met. Eng. 188 (1950), 195.
- 15 R. Kieffer, K. Sedlatschek, and H. Braun: Z. Metallkde, 50 (1959), 18.
- 16 E. Rudy and Y.A. Chang: Plansee Proc., 1964, p. 786.

REFERENCES (Cont'd)

- 17 Y.A. Chang: AFML-TR-65-2, Part IV, Vol. I (Sept. 1965).
- 18 E. Rudy and H. Nowotny: Mh. Chem. 94 (1963), 508.
- 19 Compare the compilation of related data in R. Kieffer and F. Benesovsky, Hartstoffe (Springer, Wien, 1963).
- 20 L.N. Butorina, and Z.G. Pinsker: Soviet Physics, Crystallography, 5 (1960), 560.
- 21 M.G. Bowman: Plansee Proc. 1964, 701.
- 22 R. Kieffer, F. Benesovsky, and H. Nowotny: Planseeber f. Pulvermetallurgie, 5 (1957), 33.
- 23 H. Nowotny, R. Kieffer, and F. Benesovsky, and E. Laube: Mh. Chem. 88 (1957), 336; Rev. Met. 55 (1958), 454.
- 24 L.D. Brownly: J. Inst. Met. 87 (1958), 58.
- 25 E. Rudy and F. Benesovsky: Mh. Chem. 94 (1963), 204.
- 26 E. Rudy, H. Nowotny, F. Benesovsky, R. Kieffer, and A. Neckel: Mh. Chem. 91 (1960), 176.
- 27 C. B. Alcock and P. Grieveson: I.A.E.A. Symposium on the Thermodynamics of Nuclear Material, Vienna (May, 1962).
- 28 M.H. Rand and O. Kubaschewski: AERE: Report 3487 (1960).
- 29 Compilation of References on Ternary Transition Metal-Carbon Systems
- Ti-Zr-C: C.E. Brukl, and D.P. Harmon (AFML-TR-65-2, Part II, Vol. IV., Sept, 1965).
- Ti-Hf-C: C.E. Brukl and D.P. Harmon: AFML-TR-65-2, Part II, Vol. II (Jul 1965).
- Zr-Hf-C:
- Ti-V-C: W.N. Eremenko and L.A. Tretjatsenko: Poroshkaia Metallurgia 6 (1964), 27.
- Ti-Ta-C: J.G. McMullin and J.T. Norton: J. Met. 5 (1953), 1205.
- C.E. Brukl and D.P. Harmon: AFML-TR-65-2, Part II, Vol. II (Jul 1965).
- Ti-Nb-C: P. Stecher, F. Benesovsky, A. Neckel, and H. Nowotny: Mh. Chem. 95 (1964), 1630.
- Ti-Cr-C: W.N. Eremenko, S.I. Tolmatseva, T.J. Velikanova: Report on Temperature-Resistant Alloys, AN SSSR, M., (1963)-95.

REFERENCES (Cont'd)

- Ti-Mo-C: H.J. Albert and J. T. Norton: Planseeber f. Pulvermet. 4 (1956), 2-6.
- Ti-W-C: H. Nowotny, E. Parthé, R. Kieffer, and F. Benesovsky: Z. Metallkunde 45 (1954), 97.
- Zr-Nb-C: P. Stecher, F. Benesovsky, A. Neckel, and H. Nowotny: Mh. Chem. 95 (1964), 1630.
- Zr-Ta-C: D.P. Harmon and C.E. Brukl: AFML-TR-65-2, Part II, Vol. III (August 1965).
- Zr-Cr-C: T.F. Fedorov and Yu.B. Kuzma: Poroshkova Metall. 3 (1965), 76.
- Zr-Mo-C: (a) T.C. Wallace, C.P. Guitierrez, and P.L. Stone: J. Phys. Chem. 67 (1963), 796.
(b) T.F. Fedorov, Yu.B. Kuzma, and L.W. Gorshkova: Poroshkovaia Metall. 3 (1965), 69.
- Zr-W-C: E. Rudy: 2nd Progress Report, AF 33(615)-1249 (October 1964).
- Hf-Nb-C: (a) E. Rudy: Z. Metallkunde 54 (1963), 213 (calculated).
(b) P. Stecher, F. Benesovsky, A. Neckel, and H. Nowotny: Mh. Chem. 95 (1964), 1630.
- Hf-Ta-C: E. Rudy and H. Nowotny: Mh. Chem. 94 (1963), 507.
E. Rudy: AFML-TR-65-2, Part II, Vol. I (June 1965).
- Hf-Mo-C: E. Rudy: 2nd Progress Report, AF 33(615)-1249
Hf-W-C: (October 1964).
- V-Nb-C: E. Rudy: Z. Metallkunde, 54 (1963), 213 (calculated).
V-Ta-C:
Nb-Ta-C:
- V-Cr-C: H. Rassaerts, R. Kieffer, and H. Nowotny: Mh. Chem. 96 (1965), 1536.
- V-Mo-C: E. Rudy, El. Rudy, and F. Benesovsky: Planseeber Pulvermet. 10 (1962), 42.
- V-W-C: E. Rudy, F. Benesovsky, and El. Rudy: Mh. Chem. 93 (1962), 693.

REFERENCES (Cont'd)

- Nb-Mo-C: E. Rudy, F. Benesovsky, and K. Sedlatschek: *Mh. Chem.* 92 (1961), 841.
- Nb-W-C: E. Rudy and Y.A. Chang: *Plansee Proc.* 1964, pp 786.
- Ta-Mo-C: E. Rudy and Y.A. Chang: *Plansee Proc.*, 1964, pp 786.
- Ta-W-C: E. Rudy, El. Rudy, and F. Benesovsky: *Mh. Chem.* 93 (1962), 1176.
- Cr-Mo-C: E. Rudy and Y.A. Chang: *Plansee Proc.* 1964, 786.
- Cr-W-C: (a) E. Rudy and Y.A. Chang: *Plansee Proc.* 1964.
 (b) P. Stecher, F. Benesovsky, and H. Nowotny: *Planseeber Pulvermet.* 12 (1964).
- Mo-W-C: H.J. Albert and J. T. Norton: *Planseeber Pulvermet.* 4 (1956), 2.
- 30 C. Agte and H. Alterthum: *Z. Techn. Phys.* 11 (1930), 182.
- 31 E. Rudy, D.P. Harmon, and C.E. Brukl: AFML-TR-65-2, Part I, Vol. II (May 1965).
- 32 R.V. Sara, C.E. Lowell, and R. T. Doloff: WADD-TR-60-143, Part IV. (1963).
- 33 R.V. Sara: *J. Amer. Ceram. Soc.* 48 (1965), 243.
- 34 E. Rudy: AFML-TR-65-2, Part I, Vol. IV (Sept. 1965).
- 35 E.K. Storms and R.J. McNeal: *J. Phys. Chem.* 66 (1962), 1401.
- 36 H. Kimura and Y. Sasaki: *Trans. Jap. Inst. Met.* 2 (1961), 98.
- 37 E. Rudy and D.P. Harmon: AFML-TR-65-2, Part I, Vol. V, (December 1963)
- 38 D.S. Bloom and N.S. Grant: *Trans. Am. Inst. Met. Eng.* 188 (1950), 41.
- 39 E. Rudy, St. Windisch, and J.R. Hoffman: AFML-TR-65-2, Part I, Vol. VI (December 1965).
- 40 E. Rudy and St. Windisch: AFML-TR-65-2, Part I, Vol. VII (Dec. 1965).
- 41 E. Rudy and St. Windisch: AFML-TR-65-2, Part I, Vol VIII (Jan 1966).

REFERENCES (Cont'd)

- 42 E. Rudy and St. Windisch: AFML-TR-65-2, Part I, Vol. IX. (Jan 1966).
- 43 E. Rudy and St. Windisch: AFML-TR-65-2, Part I, Vol. X (Feb 1966).
- 44 H. Nowotny, E. Piegger, R. Kieffer, and F. Benesovsky: Mh.Chem.
89 (1958), 611.
45. E. Rudy and St. Windisch: AFML-TR-65-2, Part I, Vol. III (July 1965).

APPENDIX I

Proof of the Identity of the Functions $\phi_A(x_{iA})$ and $\phi_B(x_{iB})$

$$\Delta F_{ZAC_v} + \overline{\Delta F}_{ZAC_v}^{\text{mix}} = \phi_A(x_{iA}) \quad (1)$$

$$\Delta F_{ZBC_v} + \overline{\Delta F}_{ZBC_v}^{\text{mix}} = \phi_B(x_{iB}) \quad (2)$$

with

$$\Delta F_{ZAC_v} = (w-v) \Delta F_{fAC_u} + (v-u) \Delta F_{fAC_w} - (w-u) \Delta F_{fAC_v} \quad (3)$$

$$\Delta F_{ZBC_v} = (w-v) \Delta F_{fBC_u} + (v-u) \Delta F_{fBC_w} - (w-u) \Delta F_{fBC_v} \quad (4)$$

Mixing Terms:

$$\Delta F_{(A,B)C_u}^{\text{mix}} = \phi_{1m}(x_A) \quad x_A + x_B = 1$$

$$\Delta F_{(A,B)C_v}^{\text{mix}} = \phi_{2m}(x'_A) \quad x'_A + x'_B = 1$$

$$\Delta F_{(A,B)C_w}^{\text{mix}} = \phi_{3m}(x''_A) \quad x''_A + x''_B = 1$$

The partial quantities $\overline{\Delta F}^{\text{mix}}$ are related to the integral terms by:

$$\overline{\Delta F}_{AC_v}^{\text{mix}} = \phi_{1m} + x_B \frac{\partial \phi_{1m}}{\partial x_A},$$

$$\overline{\Delta F}_{AC_v}^{\text{mix}} = \phi_{2m} + x'_B \frac{\partial \phi_{2m}}{\partial x'_A},$$

$$\overline{\Delta F}_{AC_w}^{\text{mix}} = \phi_{3m} + x''_B \frac{\partial \phi_{3m}}{\partial x''_A},$$

$$\begin{aligned}
\overline{\Delta F}_{ZAC_v}^{mix} &= (v-u) \overline{\Delta F}_{AC_w}^{mix} + (w-v) \overline{\Delta F}_{AC_u}^{mix} - (w-u) \overline{\Delta F}_{AC_v}^{mix} \\
&= (w-u) \phi_{3m} + (w-v) \phi_{1m} - (w-u) \phi_{2m} + (w-u) x''_B \frac{\partial \phi_{3m}}{\partial x''_A} + \\
&\quad + (w-v) x_B \frac{\partial \phi_{1m}}{\partial x_A} - (w-u) x'_B \frac{\partial \phi_{2m}}{\partial x'_A}
\end{aligned} \tag{5}$$

The analogous calculation performed for the component B yields:

$$\begin{aligned}
\overline{\Delta F}_{ZAC_v}^{mix} &= (w-u) \phi_{3m} + (w-v) \phi_{1m} - (w-u) \phi_{2m} + (w-u) x''_A \frac{\partial \phi_{3m}}{\partial x''_B} + \\
&\quad + (w-v) x_A \frac{\partial \phi_{1m}}{\partial x_B} - (w-u) x'_A \frac{\partial \phi_{2m}}{\partial x'_B}
\end{aligned} \tag{6}$$

From the gradient condition we derive:

$$\left[\frac{\partial \Delta F_{f(A,B)C_u}}{\partial x} \right]_{T,P} = \left[\frac{\partial \Delta F_{f(A,B)C_v}}{\partial x'} \right]_{T,P} = \left[\frac{\partial \Delta F_{f(A,B)C_w}}{\partial x''} \right]_{T,P}$$

$$\Delta F_{f(A,B)C_u} = x_A \Delta F_{fAC_u} + x_B \Delta F_{fBC_u} + \phi_{1m}$$

$$\Delta F_{f(A,B)C_v} = x'_A \Delta F_{fAC_v} + x'_B \Delta F_{fBC_v} + \phi_{2m}$$

$$\Delta F_{f(A,B)C_w} = x''_A \Delta F_{fAC_w} + x''_B \Delta F_{fBC_w} + \phi_{3m}$$

Differentiation and rearrangement of the terms yields:

$$\Delta F_{fAC_u} - \Delta F_{fBC_u} + \frac{\partial \phi_{1m}}{\partial x_A} = \Delta F_{fAC_v} - \Delta F_{fBC_v} + \frac{\partial \phi_{2m}}{\partial x'_A} \tag{7}$$

$$\Delta F_{fAC_v} - \Delta F_{fBC_v} + \frac{\partial \phi_{zm}}{\partial x_A} = \Delta F_{fAC_w} - \Delta F_{fBC_w} + \frac{\partial \phi_{zm}}{\partial x_A} \quad (8)$$

Combining equations (1) and (2), with (5) and (6), and rearranging the terms, we obtain

$$\phi_A(x_{iA}) - \phi_B(x_{iB}) = \Delta F_{ZAC_v} - \Delta F_{ZBC_v} + (v-u) \frac{\partial \phi_{zm}}{\partial x_A} + (w-v) \frac{\partial \phi_{im}}{\partial x_A} - (w-u) \frac{\partial \phi_{zm}}{\partial x_A}$$

Substituting for $\frac{\partial \phi_{zm}}{\partial x_A}$ and $\frac{\partial \phi_{im}}{\partial x_A}$ from equations (7) and (8) yields:

$$\begin{aligned} \phi_A(x_{iA}) - \phi_B(x_{iB}) &= \Delta F_{ZAC_v} - \Delta F_{ZBC_v} + (v-u) (\Delta F_{fAC_u} - \Delta F_{fBC_u} - \Delta F_{fAC_w} + \Delta F_{fBC_w}) - \\ &\quad - (w-u) (\Delta F_{fAC_u} - \Delta F_{fBC_u} - \Delta F_{fAC_v} + \Delta F_{fBC_v}) \end{aligned}$$

From relations (3) and (4) follows immediately, that the last two terms in the equation above are equivalent to $\Delta F_{ZBC_v} - \Delta F_{ZAC_v}$; hence,

$$\phi_A(x_{iA}) - \phi_B(x_{iB}) = 0$$

or

$$\underline{\underline{\phi_A(x_{iA}) = \phi_B(x_{iB})}}$$

APPENDIX II

Collection of the Most Recent Phase Diagrams for Binary Transition Metal-Carbon, and Transition Metal-Boron Systems.

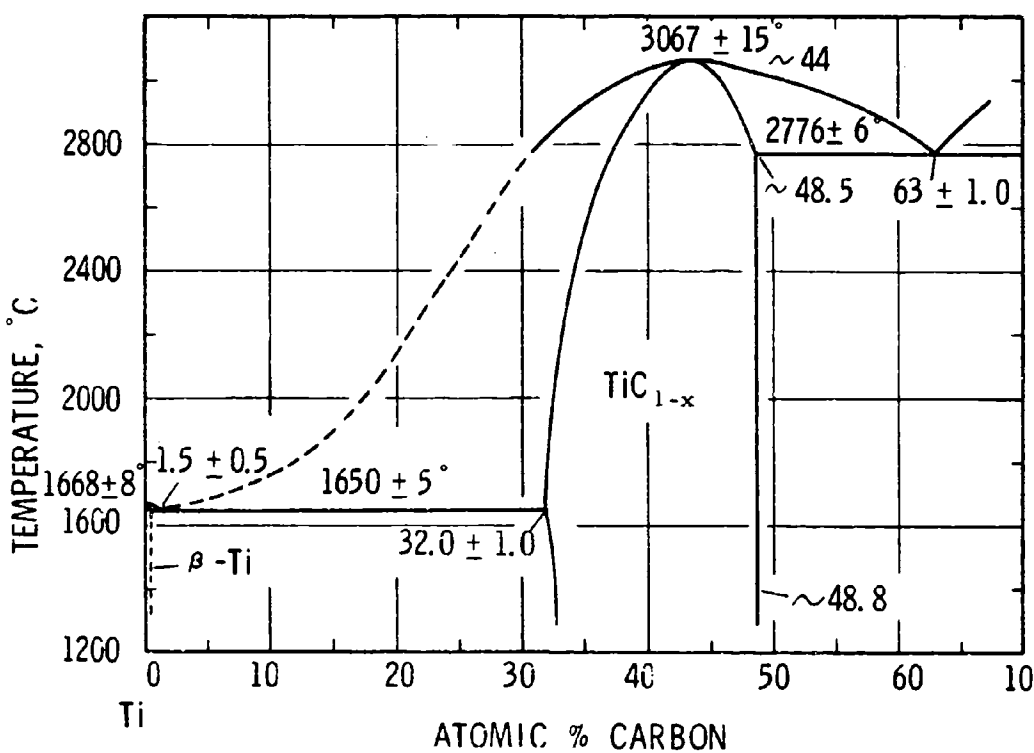


Figure 66. Constitution Diagram Titanium-Carbon.

(E. Rudy, D. P. Harmon, and C. E. Brukl, 1965)⁽³¹⁾

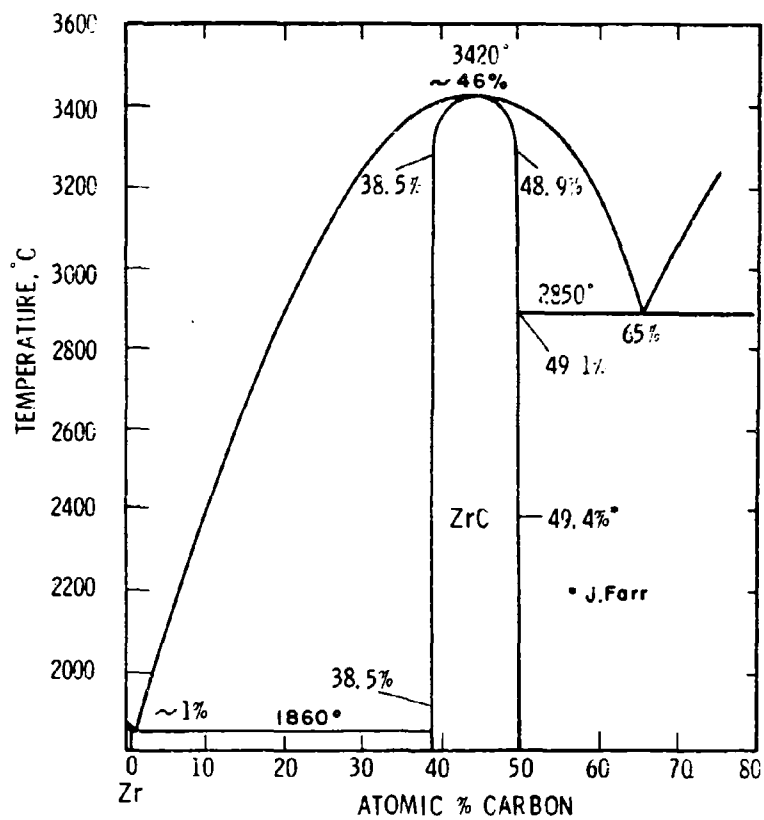


Figure 67. Constitution Diagram Zirconium-Carbon.

(R.V. Sara, C.E. Lowell, and R. T. Doloff, 1963 and 1965)^(32, 33)

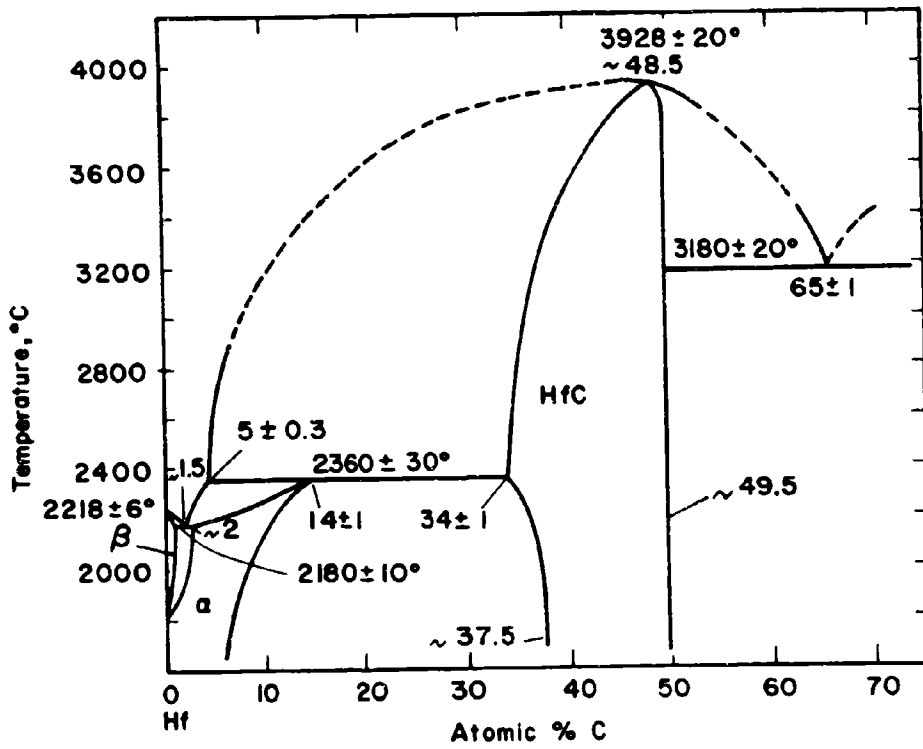


Figure 68. Constitution Diagram Hafnium-Carbon.

(E. Rudy, 1965)⁽³⁴⁾

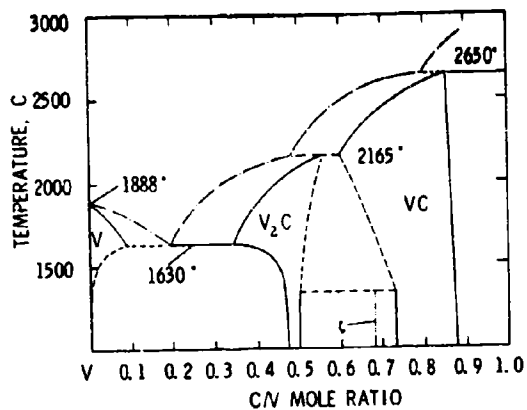


Figure 69. Constitution Diagram Vanadium-Carbon).
 (E.K. Storms and R.J. McNeal, 1962)⁽³⁵⁾

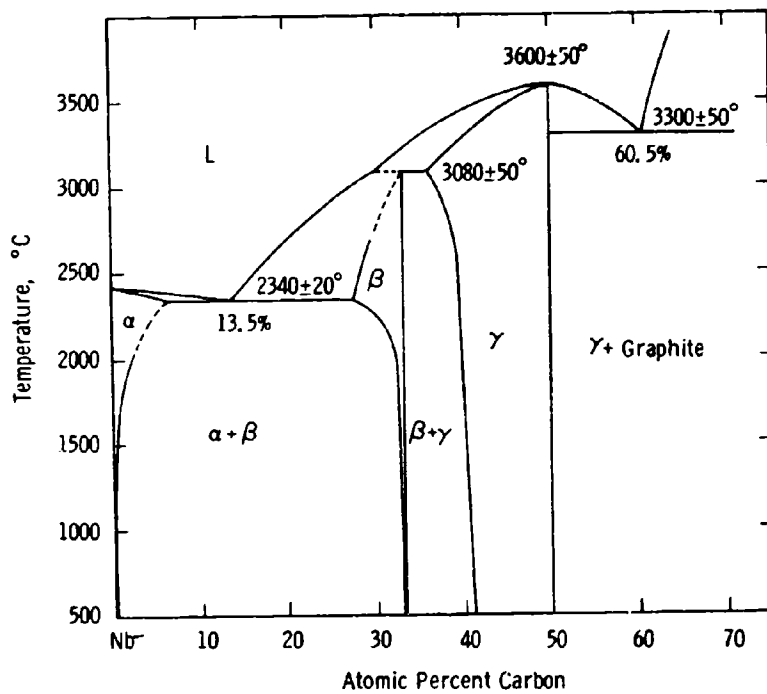


Figure 70. Constitution Diagram Niobium-Carbon
 (H. Kimura and Y. Sasaki, 1961)⁽³⁶⁾

Note: The order-disorder reaction of the Nb_2C -phase at $\sim 2450^\circ C$ ⁽³⁶⁾ is not recorded in the diagram.

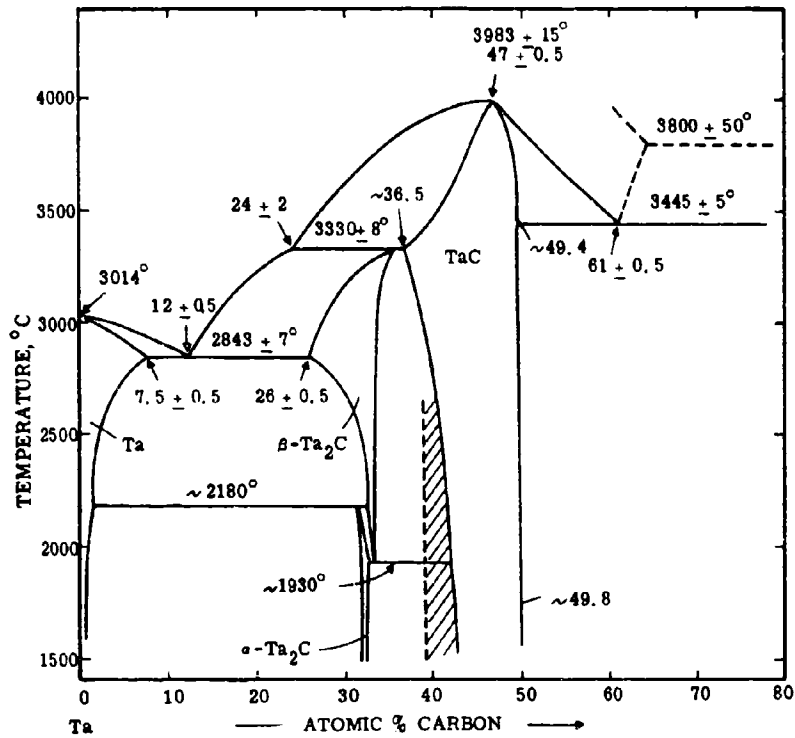


Figure 71. Constitution Diagram Tantalum-Carbon.
 (E. Rudy and D. P. Harmon, 1965)⁽³⁷⁾

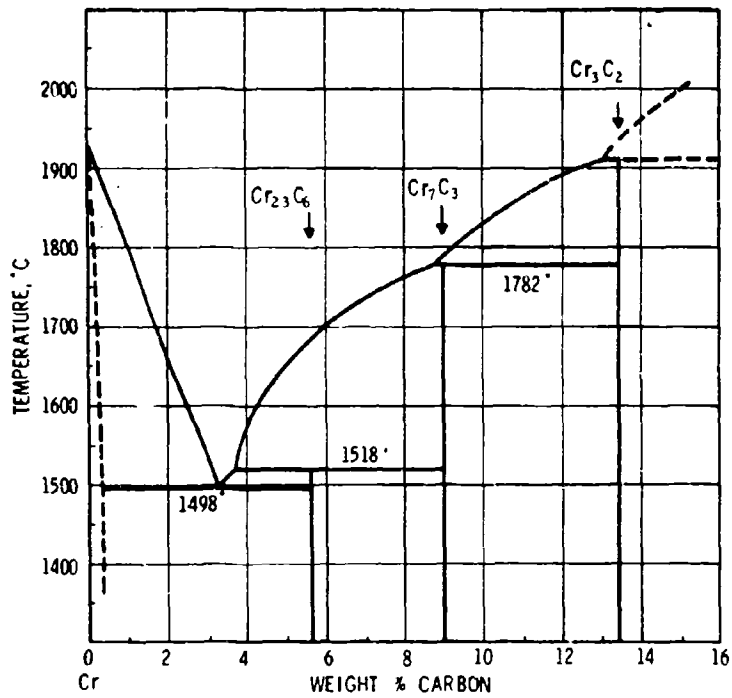


Figure 72. Constitution Diagram Chromium-Carbon.
 (D.S. Bloom and N.J. Grant, 1950)⁽³⁸⁾

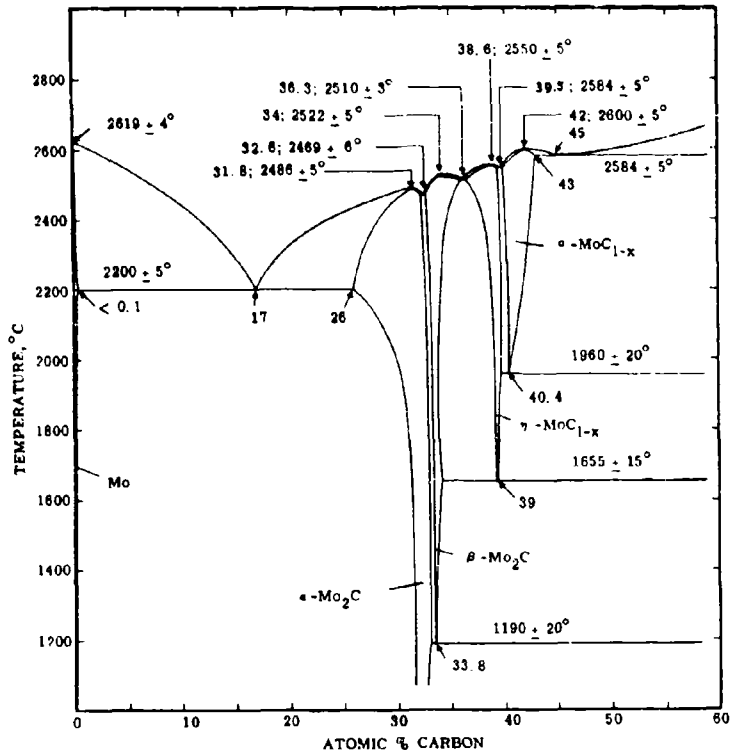


Figure 73. Constitution Diagram Molybdenum-Carbon.
 (E. Rudy, St. Windisch, and Y. A. Chang, 1965)⁽⁹⁾

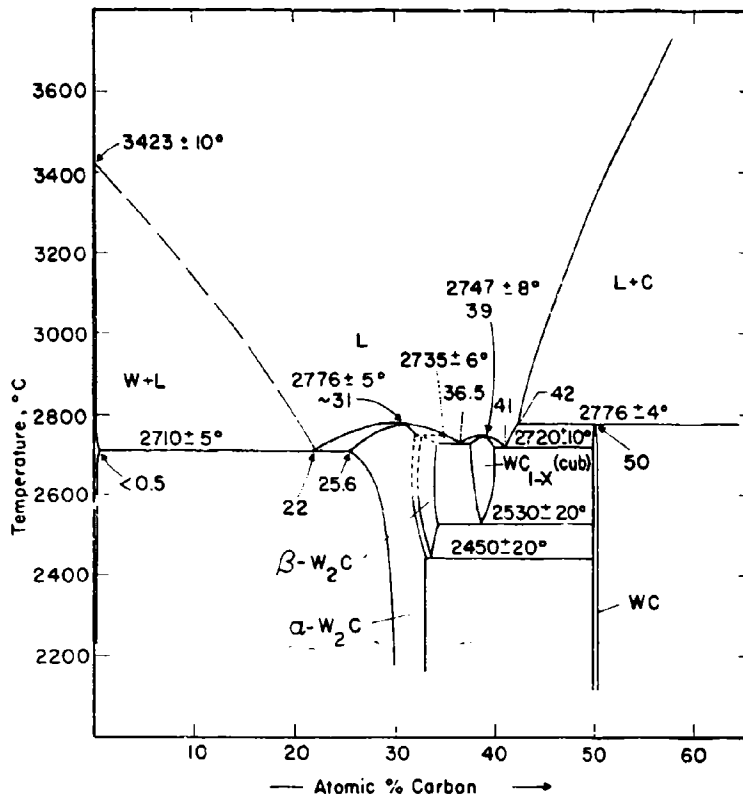


Figure 74. Constitution Diagram Tungsten-Carbon.

(E. Rudy, St. Windisch, and J. R. Hoffman, 1965)⁽³⁹⁾

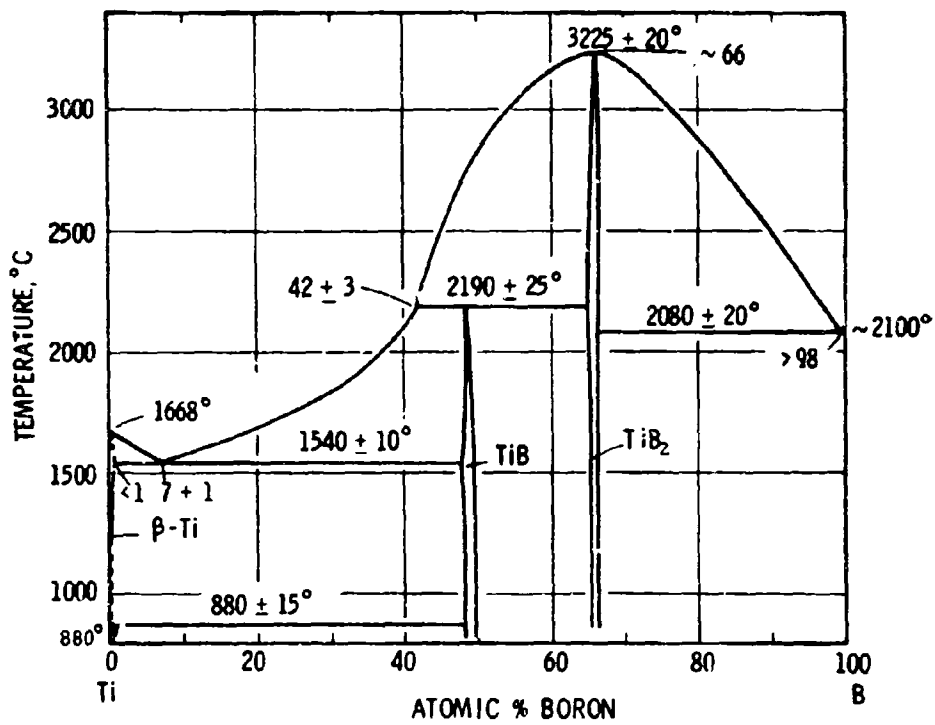


Figure 75. Constitution Diagram Titanium - Boron.

(E. Rudy and St. Windisch, 1965)⁽⁴⁰⁾

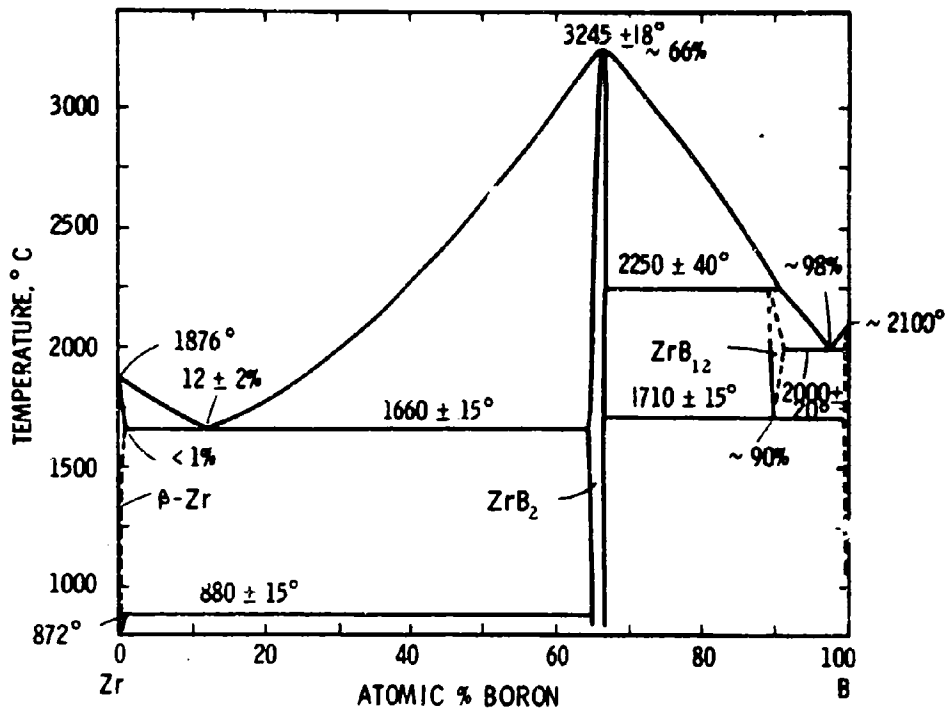


Figure 76. Constitution Diagram Zirconium-Boron.
 (E. Rudy and St. Windisch, 1965)⁽⁴¹⁾

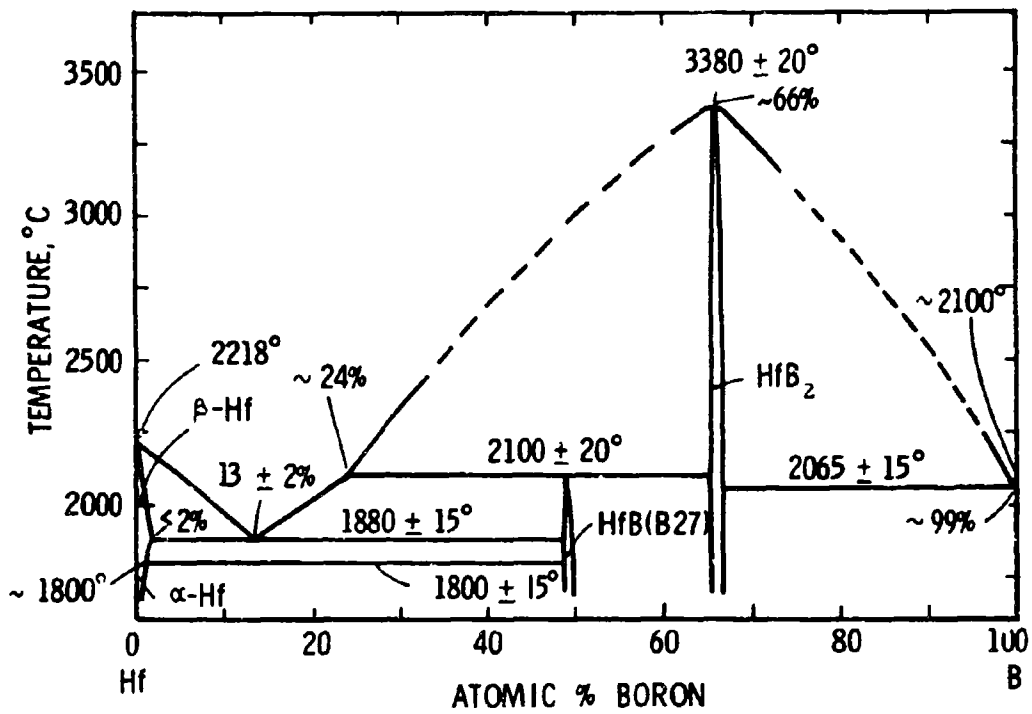


Figure 77. Constitution Diagram Hafnium-Boron.
 (E. Rudy and St. Windisch, 1965)⁽⁴²⁾

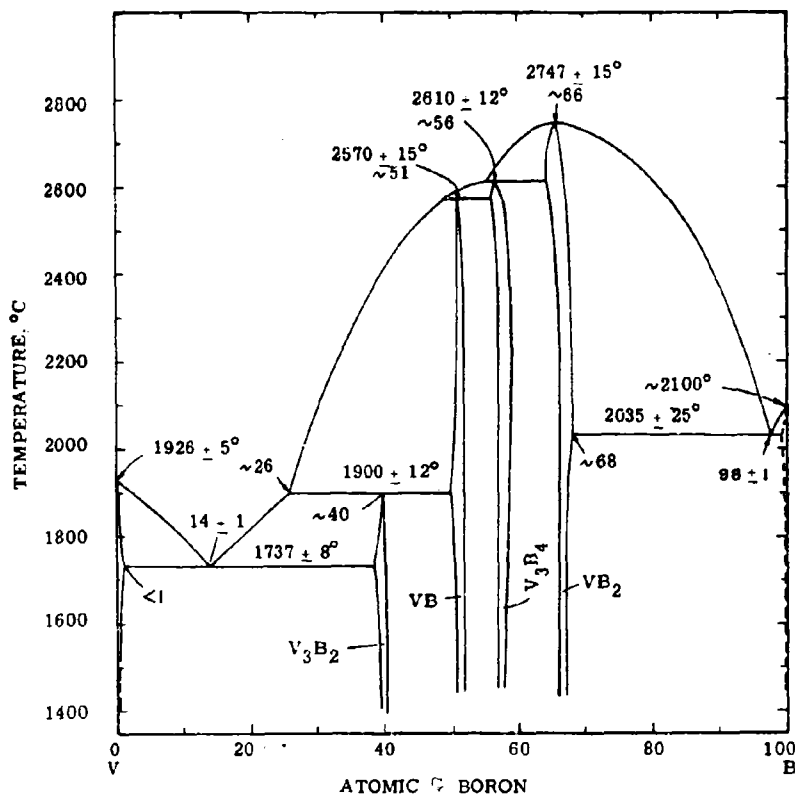


Figure 78. Constitution Diagram Vanadium - Boron
(E. Rudy and St. Windisch, 1965)⁽⁴³⁾

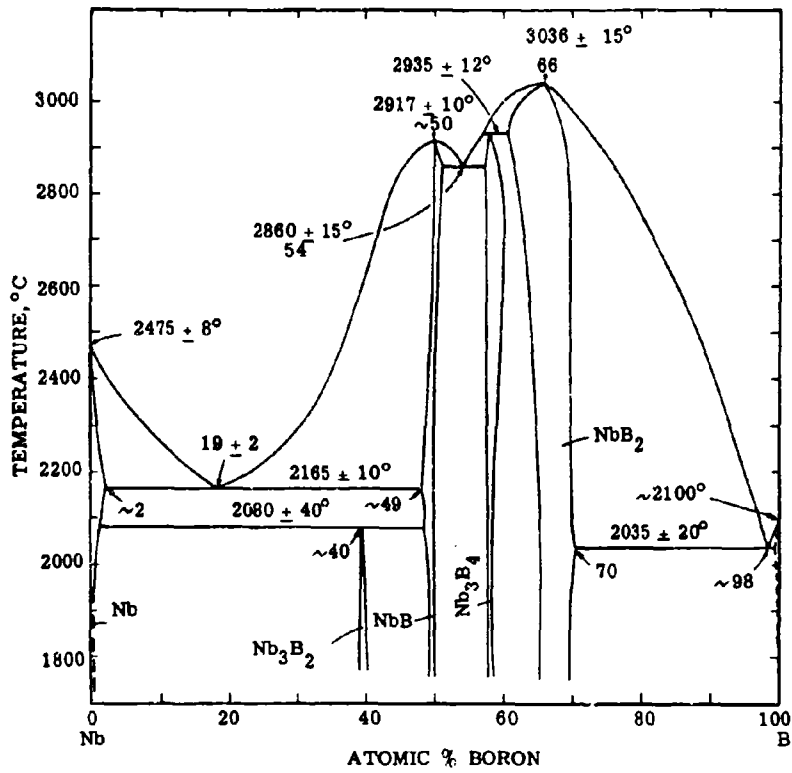


Figure 79. Constitution Diagram Niobium-Boron.
 (E. Rudy and St. Windisch, 1965)⁽⁴³⁾

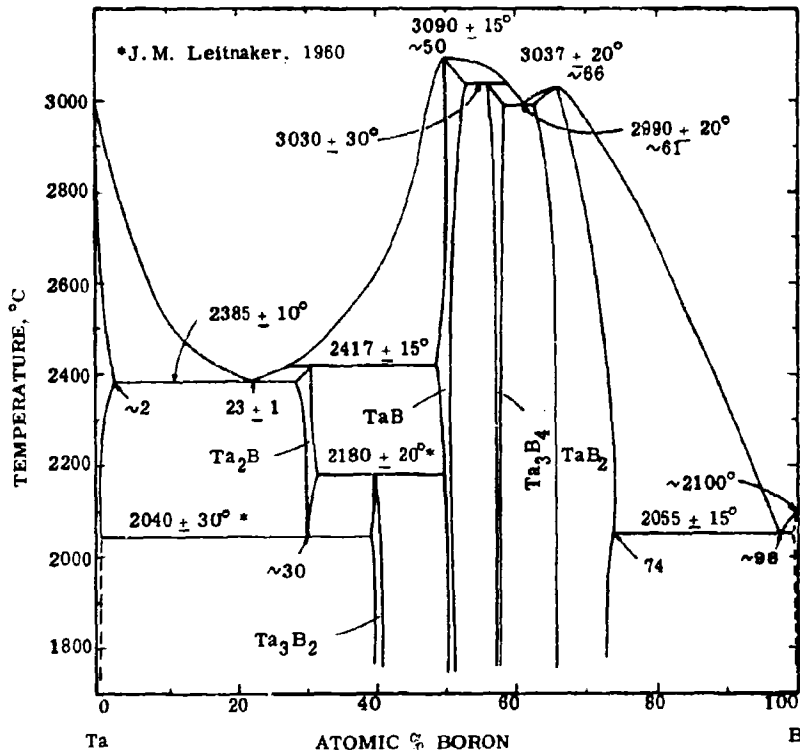


Figure 80. Constitution Diagram Tantalum-Boron
(E. Rudy and St. Windisch, 1965)⁽⁴³⁾

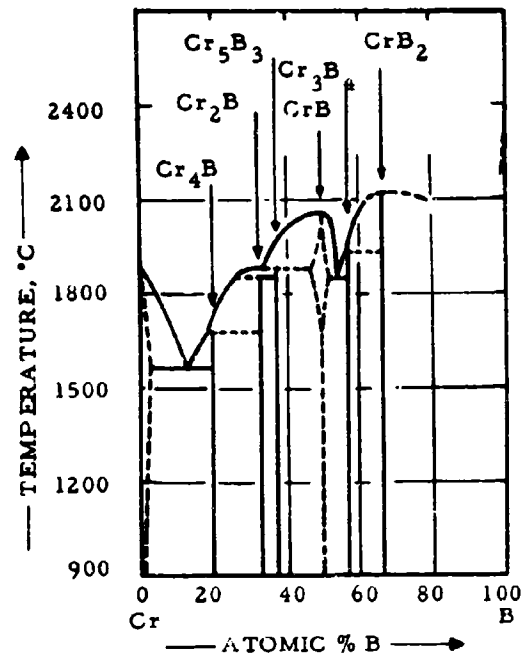


Figure 81. Constitution Diagram Chromium-Boron

(H. Nowotny, E. Piegger, R. Kieffer, and F. Benesovsky, 1958)(44)

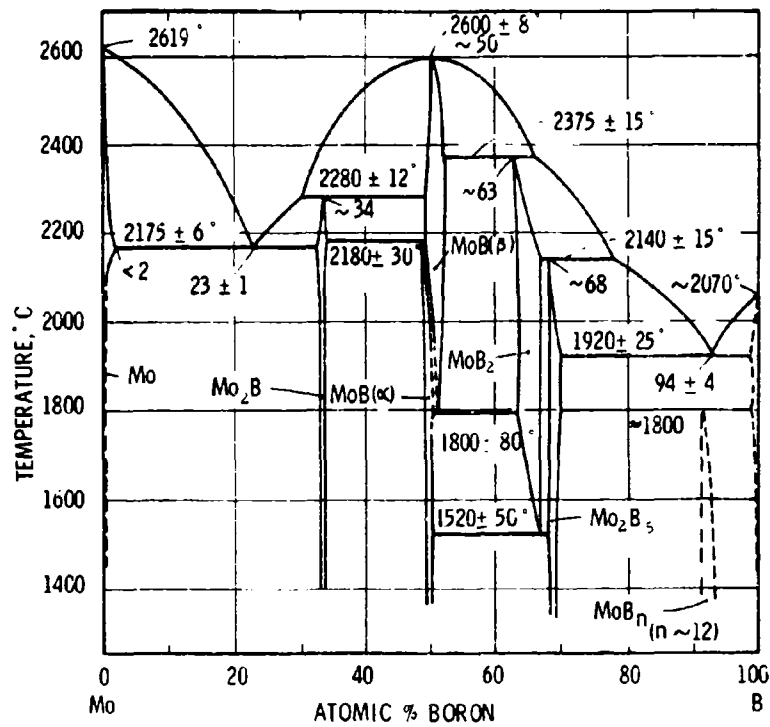


Figure 82. Constitution Diagram Molybdenum-Boron.

(E. Rudy and St. Windisch, 1965)⁽⁴⁵⁾

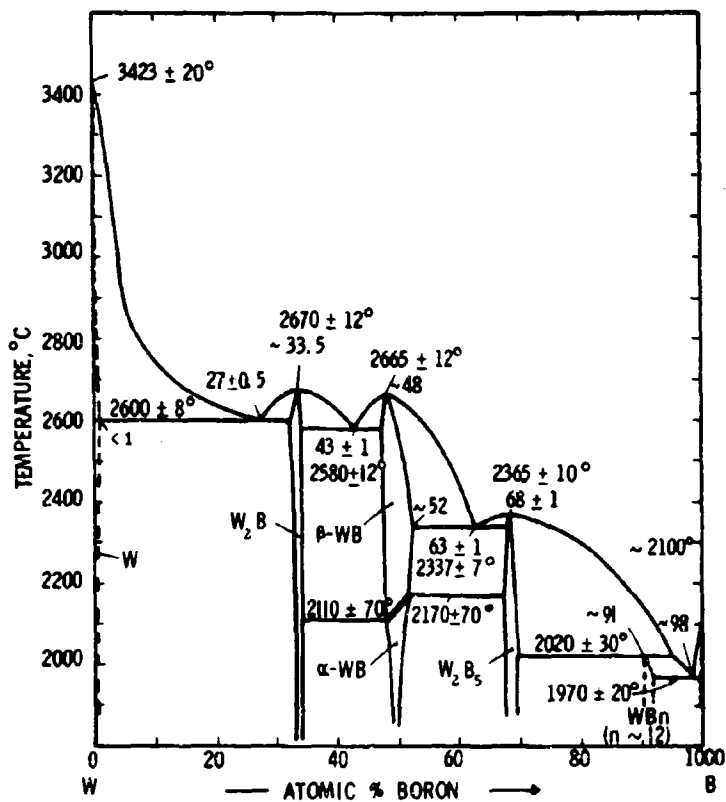


Figure 83. Constitution Diagram Tungsten-Boron.
 (E. Rudy and St. Windisch, 1965)⁽⁴⁵⁾

DOCUMENT CONTROL DATA - R&D

(Security classification of title, body of abstract and indexing annotation must be entered when the overall report is classified)

1. ORIGINATING ACTIVITY (Corporate author) Materials Research Laboratory Aerojet-General Corporation Sacramento, California		2a. REPORT SECURITY CLASSIFICATION <p align="center">Unclassified</p>	
		2b. GROUP <p align="center">N.A.</p>	
3. REPORT TITLE Ternary Phase Equilibria in Transition Metal-Boron-Carbon-Silicon Systems Part IV. Thermochemical Calculations: Vol. II. Thermodynamic Interpretation of Ternary Phase Diagrams.			
4. DESCRIPTIVE NOTES (Type of report and inclusive dates) <p align="center">Documentary Report.</p>			
5. AUTHOR(S) (Last name, first name, initial) <p align="center">Rudy, Erwin</p>			
6. REPORT DATE <p align="center">January 1966</p>		7a. TOTAL NO. OF PAGES <p align="center">147</p>	7b. NO. OF REFS <p align="center">45</p>
8a. CONTRACT OR GRANT NO. <p align="center">AF 33(615)-1249</p>		9a. ORIGINATOR'S REPORT NUMBER(S) <p align="center">AFML-TR-65-2 Part IV, Volume II.</p>	
b. PROJECT NO. 7350 		9b. OTHER REPORT NO(S) (Any other numbers that may be assigned this report) <p align="center">N.A.</p>	
c. Task No. 735001 			
d.			
10. AVAILABILITY/LIMITATION NOTICES This document is subject to special export controls, and each transmittal to foreign governments or foreign nationals may be made only with prior approval of Metals & Ceramics Div., AF Materials Laboratory, Wright-Patterson AFB, Ohio.			
11. SUPPLEMENTARY NOTES		12. SPONSORING MILITARY ACTIVITY <p align="center">AFML (MAMC) Wright-Patterson AFB, Ohio 45433</p>	
13. ABSTRACT <p>The equilibrium conditions for two-phase and three-phase equilibria in ternary systems are derived from the minimum condition for the free energy, and special solutions are discussed on model examples. The predictive capabilities of the thermodynamic approach are demonstrated on a number of refractory carbide systems, and methods for the determination of phase stabilities from experimental phase equilibrium data are outlined. The thermodynamic discussions are supplemented by a general review of recent phase diagram work on refractory transition metal-B element systems.</p>			

14 KEY WORDS	LINK A		LINK B		LINK C	
	ROLE	WT	ROLE	WT	ROLE	WT
Phase Equilibria Thermodynamics Refractory Alloys						

INSTRUCTIONS

1. **ORIGINATING ACTIVITY:** Enter the name and address of the contractor, subcontractor, grantee, Department of Defense activity or other organization (*corporate author*) issuing the report.

2a. **REPORT SECURITY CLASSIFICATION:** Enter the overall security classification of the report. Indicate whether "Restricted Data" is included. Marking is to be in accordance with appropriate security regulations.

2b. **GROUP:** Automatic downgrading is specified in DoD Directive 5290.10 and Armed Forces Industrial Manual. Enter the group number. Also, when applicable, show that optional markings have been used for Group 3 and Group 4 as authorized.

3. **REPORT TITLE:** Enter the complete report title in all capital letters. Titles in all cases should be unclassified. If a meaningful title cannot be selected without classification, show title classification in all capitals in parentheses immediately following the title.

4. **DESCRIPTIVE NOTES:** If appropriate, enter the type of report, e.g., interim, progress, summary, annual, or final. Give the inclusive dates when a specific reporting period is covered.

5. **AUTHOR(S):** Enter the name(s) of author(s) as shown on or in the report. Enter last name, first name, middle initial. If military, show rank and branch of service. The name of the principal author is an absolute minimum requirement.

6. **REPORT DATE:** Enter the date of the report as day, month, year, or month, year. If more than one date appears on the report, use date of publication.

7a. **TOTAL NUMBER OF PAGES:** The total page count should follow normal pagination procedures, i.e., enter the number of pages containing information.

7b. **NUMBER OF REFERENCES:** Enter the total number of references cited in the report.

8a. **CONTRACT OR GRANT NUMBER:** If appropriate, enter the applicable number of the contract or grant under which the report was written.

8b, 8c, & 8d. **PROJECT NUMBER:** Enter the appropriate military department identification, such as project number, subproject number, system numbers, task number, etc.

9a. **ORIGINATOR'S REPORT NUMBER(S):** Enter the official report number by which the document will be identified and controlled by the originating activity. This number must be unique to this report.

9b. **OTHER REPORT NUMBER(S):** If the report has been assigned any other report numbers (*either by the originator or by the sponsor*), also enter this number(s).

10. **AVAILABILITY/LIMITATION NOTICES:** Enter any limitations on further dissemination of the report, other than those

imposed by security classification, using standard statements such as:

- (1) "Qualified requesters may obtain copies of this report from DDC."
- (2) "Foreign announcement and dissemination of this report by DDC is not authorized."
- (3) "U. S. Government agencies may obtain copies of this report directly from DDC. Other qualified DDC users shall request through _____."
- (4) "U. S. military agencies may obtain copies of this report directly from DDC. Other qualified users shall request through _____."
- (5) "All distribution of this report is controlled. Qualified DDC users shall request through _____."

If the report has been furnished to the Office of Technical Services, Department of Commerce, for sale to the public, indicate this fact and enter the price, if known.

11. **SUPPLEMENTARY NOTES:** Use for additional explanatory notes.

12. **SPONSORING MILITARY ACTIVITY:** Enter the name of the departmental project office or laboratory sponsoring (*paying for*) the research and development. Include address.

13. **ABSTRACT:** Enter an abstract giving a brief and factual summary of the document indicative of the report, even though it may also appear elsewhere in the body of the technical report. If additional space is required, a continuation sheet shall be attached.

It is highly desirable that the abstract of classified reports be unclassified. Each paragraph of the abstract shall end with an indication of the military security classification of the information in the paragraph, represented as (TS), (S), (C), or (U).

There is no limitation on the length of the abstract. However, the suggested length is from 150 to 225 words.

14. **KEY WORDS:** Key words are technically meaningful terms or short phrases that characterize a report and may be used as index entries for cataloging the report. Key words must be selected so that no security classification is required. Identifiers, such as equipment model designation, trade name, military project code name, geographic location, may be used as key words but will be followed by an indication of technical context. The assignment of links, rules, and weights is optional.